High-field THz generation and nonlinear THz spectroscopy

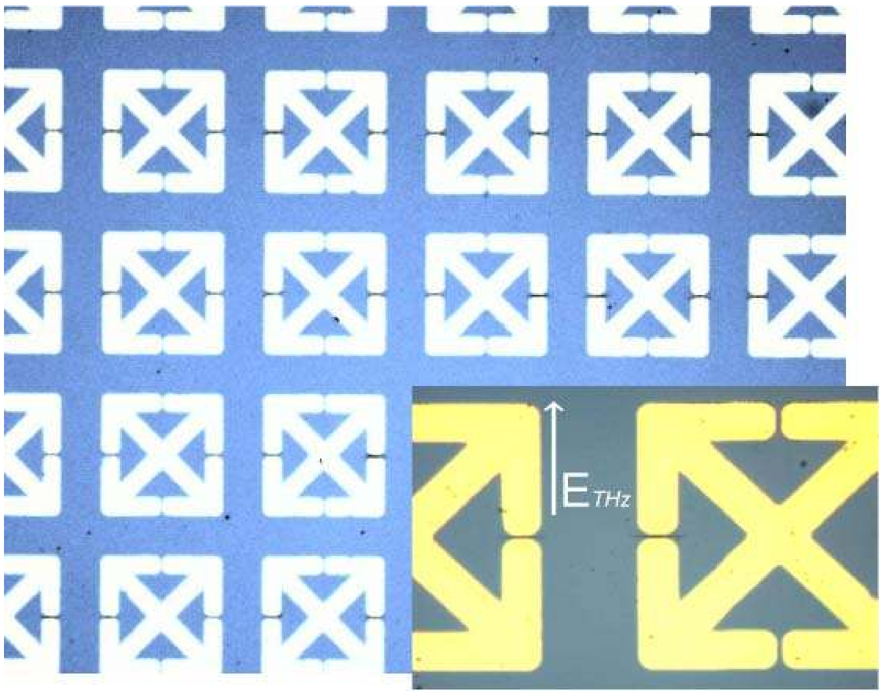

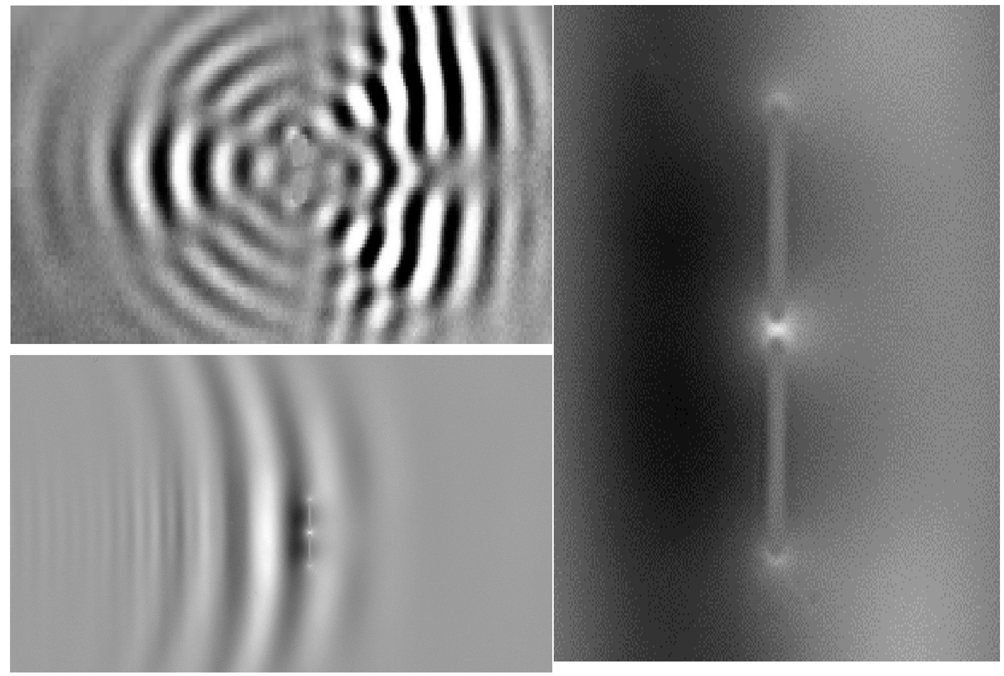

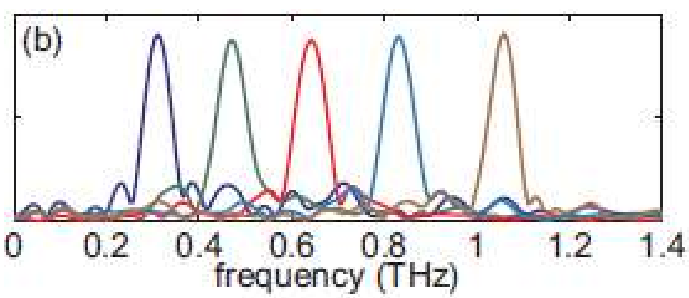

Keith A. Nelson
Department of Chemistry
MIT

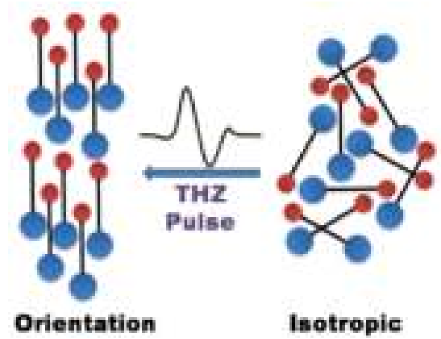

Broad objectives

Controlling charges and dipoles (electric & magnetic)

Measuring dynamical events involving their motions

Coherent control over collective & local structure & dynamics

Collective dynamics

Crystalline phase transitions

Accelerating carriers

Driving polar lattice vibrations

Driving low-frequency electronic resonances

Ferroelectric $KNbO_3$ crystal

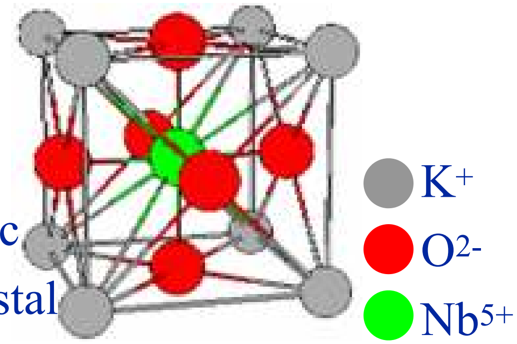

Ionic & polar liquids, glasses, polymers…

Driving orientation, local modes, liquid rearrangements

Driving motions of charges & chemical change

Atomic & molecular transitions, charge transfer

Rydberg transitions, ionization

Driving molecular rotations & alignment

Theoretical calculations: Domain switching

MD simulations of THz-driven FE domain switching: $PbTiO_3$

w/ Andrew Rappe & Tingting Qi, U Penn

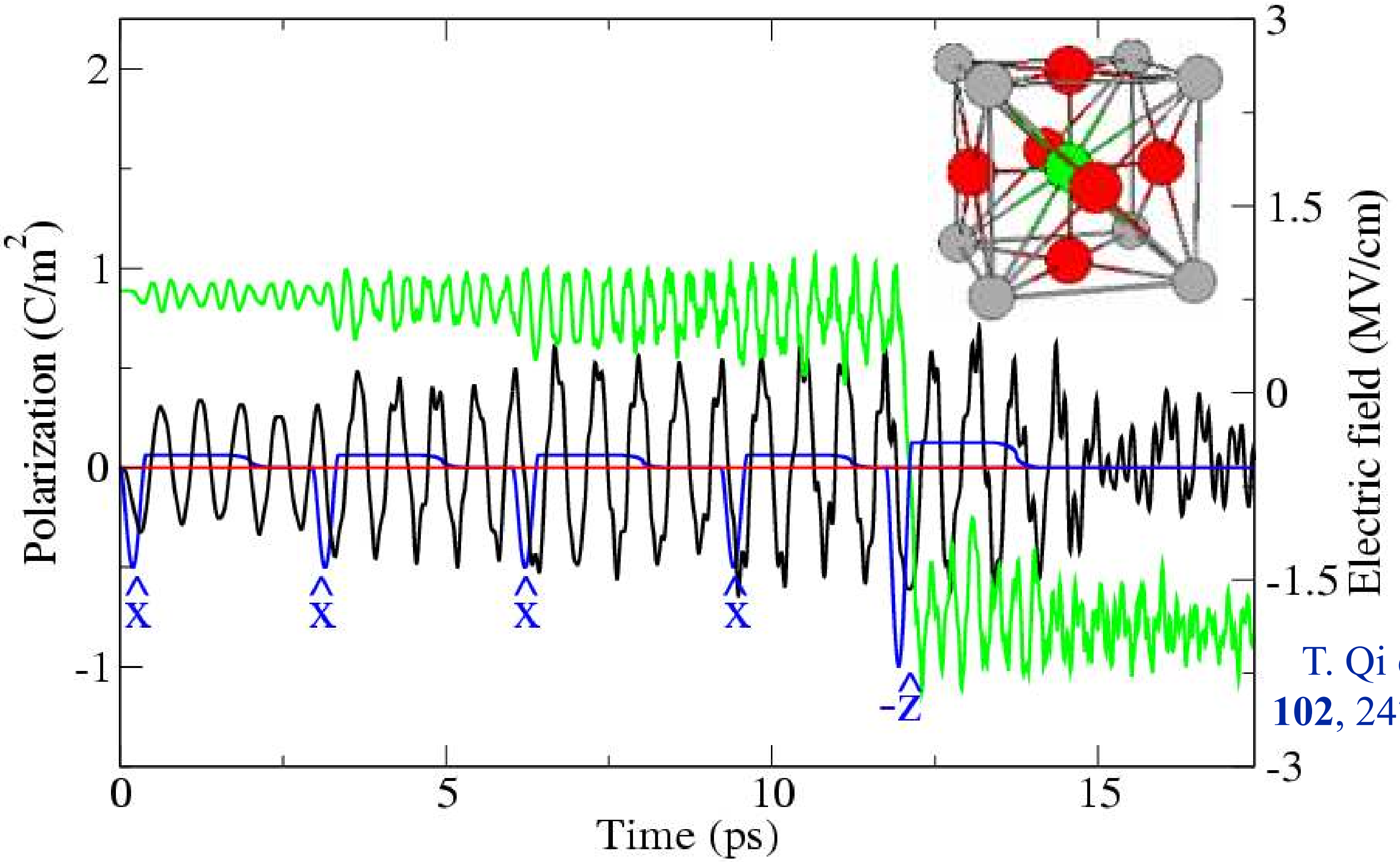

T. Qi et al., *PRL* **102**, 247603 (2009)

THz fields drive increasing amplitudes until switching occurs!

Collective coherent control

Outline

Sources for high THz pulse energy

Common tabletop methods

- Nonlinear optical crystals, optical rectification
  - THz "polaritonics"
  - **Tilted optical pulse front pumping**
- Plasmas, THz-IR generation

Non-tabletop methods

- Synchrotron sources
- E-beam fringe fields at LCLS

Nonlinear spectroscopy

Nonlinear vibrational & electronic responses in solids

- Driving phonons & electrons

Nonlinear responses in liquids & gases

- Driving molecular orientation through polarizabilities & dipoles

Prospects

Credits

Thomas Feurer
Joshua Vaughan
Nikolay Stoyanov
David Ward
Eric Statz

Janos Hebling (Pecs U)
Mattias Hoffmann
Ka-Lo Yeh
Harold Hwang

Richard Averitt (Boston U)
Mengkun Liu
Robert Field (MIT)
Yan Zhou

Christopher Werley
Nate Brandt
Qiang Wu (Tianjin U)
Kung-Hsuan Lin
Zhao Chen
Xibin Zhou
Bradford Perkins
Christopher Tait
Stephanie Teo

Thanks for slides from:

Andrei Tokmakoff, MIT
Gwyn Williams, Jefferson Lab
Antoinette Taylor, LANL
X.-C. Zhang, RPI
Koichiro Tanaka, Kyoto U
Aaron Lindenberg, Stanford
Christoph Hauri, Paul Scherer Inst

Tabletop THz generation

From photoconductive antennae

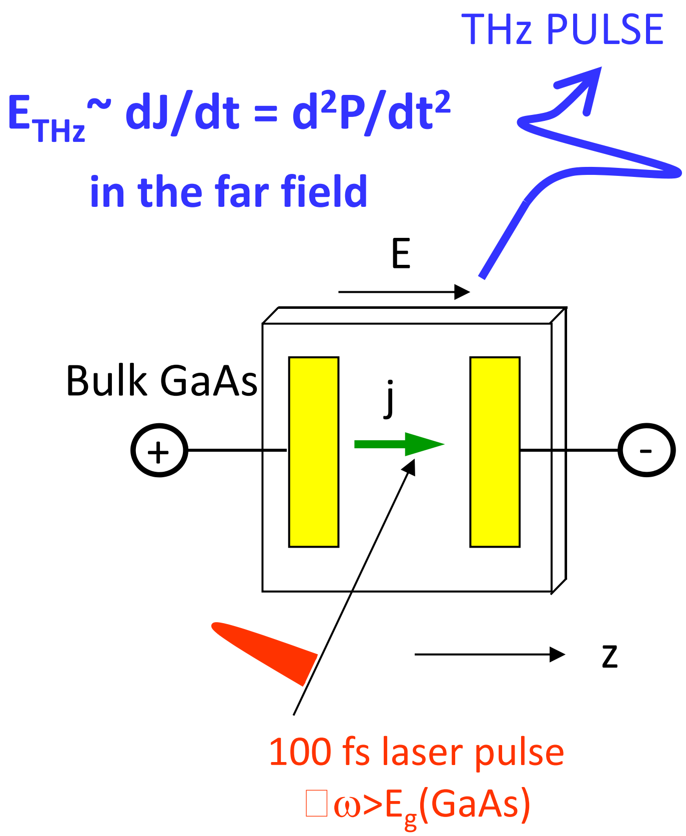

Electron acceleration produces THz emission

From nonlinear crystals

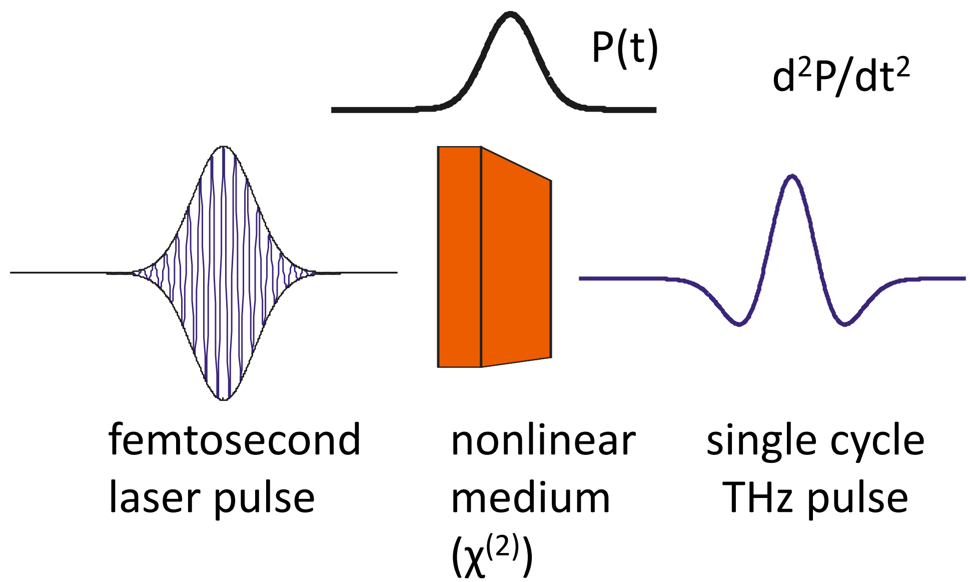

Difference-frequency mixing produces THz emission

Collinear or non-collinear velocity matching...

Optical rectification in organic crystals

Recent results from Hauri Group (EPFL/PSI, Switzerland)

APL 99, 161116 (2011) Opt. Lett. 37, 899 (2012)

- e.g. DAST (4-N,N-dimethylamino-4'-N'methyl stilbazolium tosylate), OH1, DSTMS,…
- strong optical $\chi^{(2)}$ nonlinearity
- low (IR, THz) absorption
- high damage threshold (100 GW/cm^2)
- good phase matching
- pump wavelength: 1.2-1.5 μm
- high conversion efficiencies (≈2 %)
- good focusability

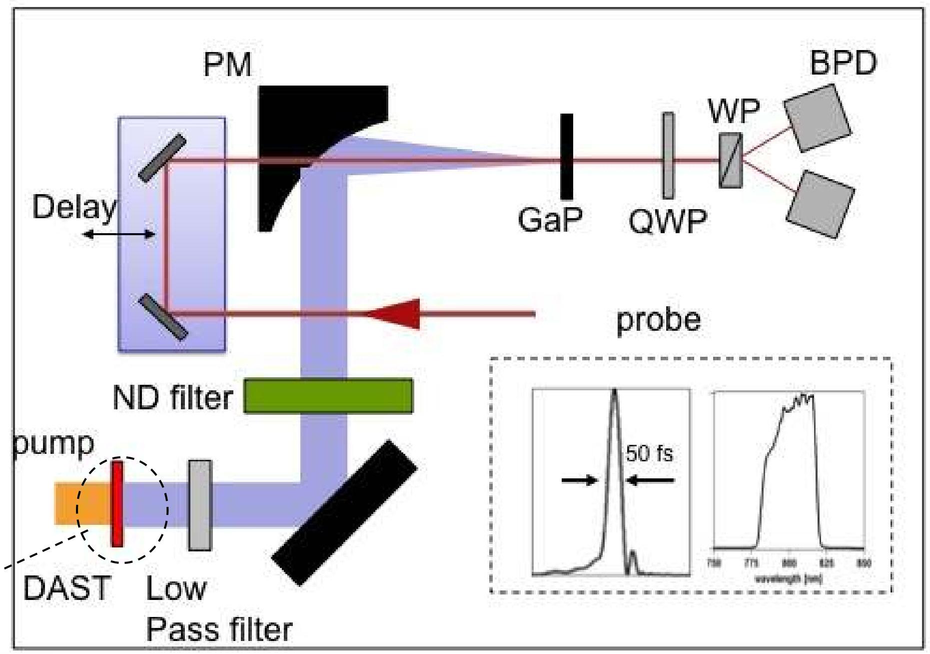

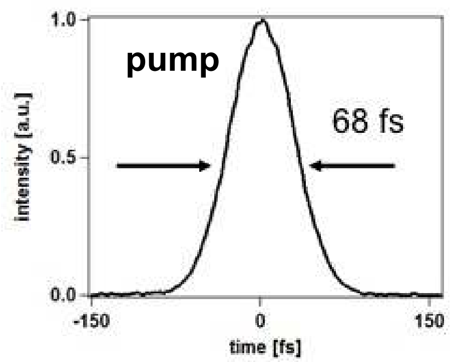

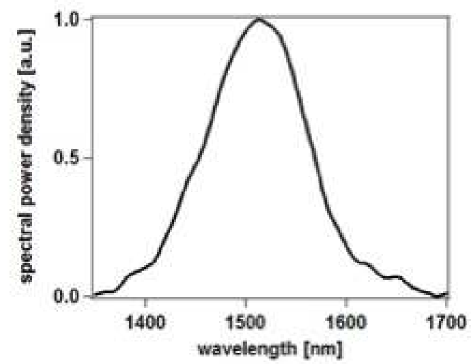

Optical rectification in organic crystals

Recent results from Hauri Group (EPFL/PSI, Switzerland)

APL 99, 161116 (2011) Opt. Lett. 37, 899 (2012)

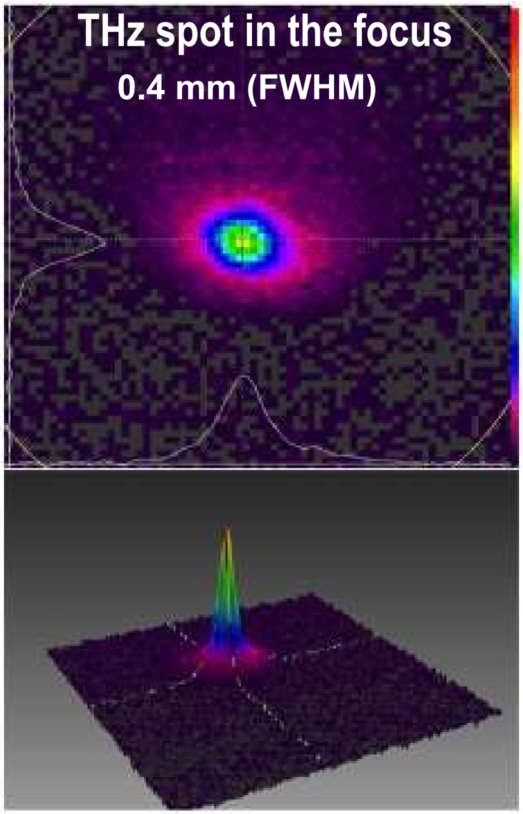

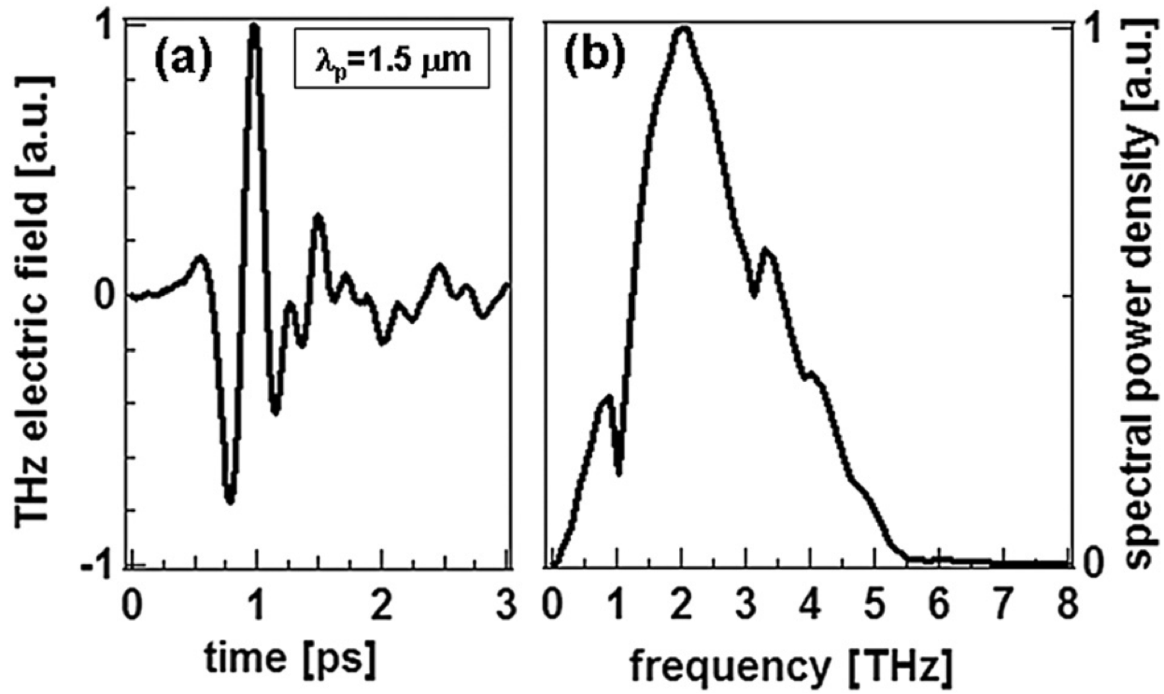

- up to 1.6 MV/cm (0.5 Tesla)
- up to 20 μJ pulse energy
- single-cycle pulses
- CEP stabilized
- excellently suited for high-field laser-matter interaction, like THz-induced magnetic switching (paper submitted)

All-Air THz Photonics

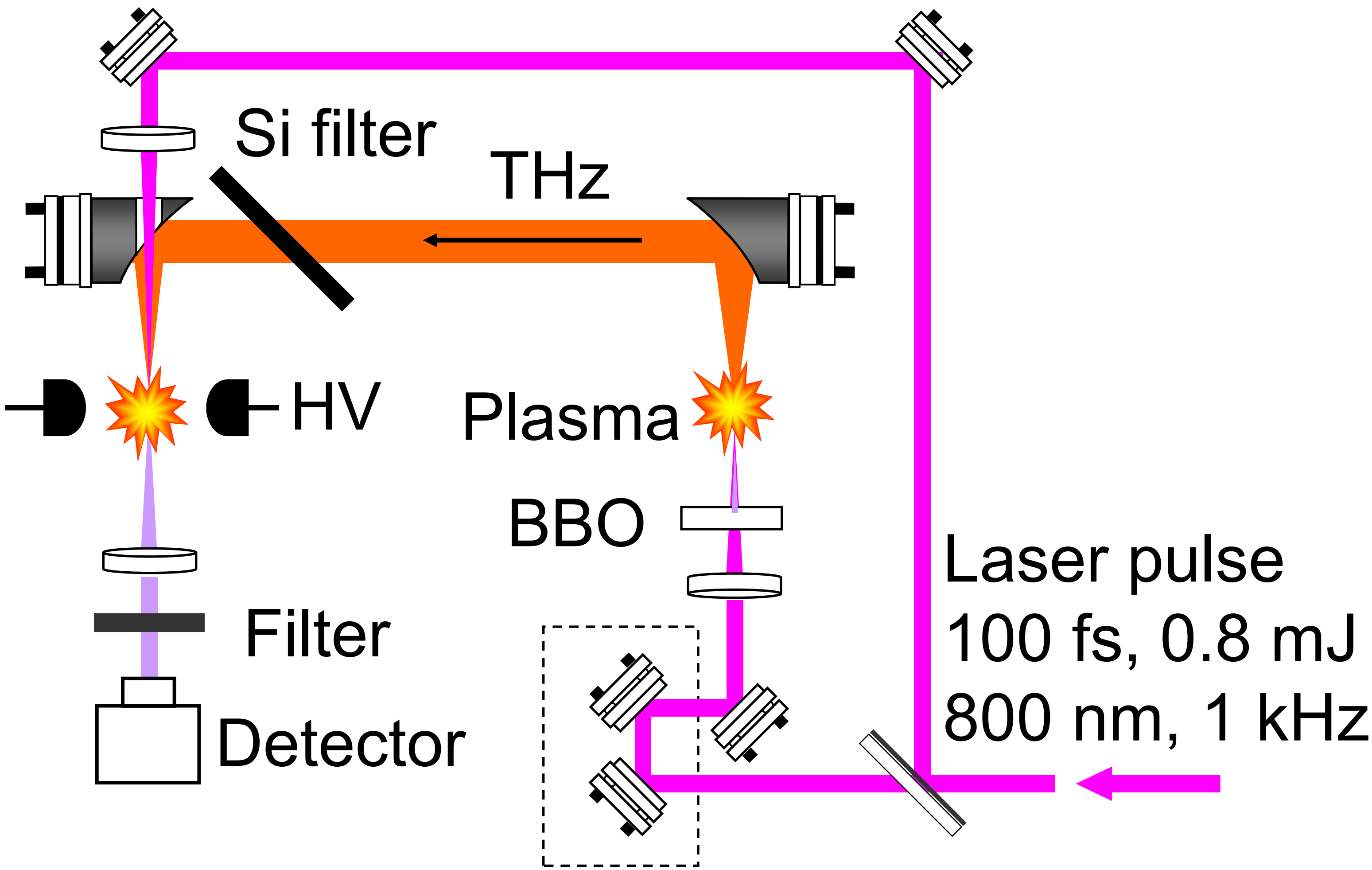

J. Dai, et al., *PRL* **97**, 103903 (2006).

THz generation mechanism:

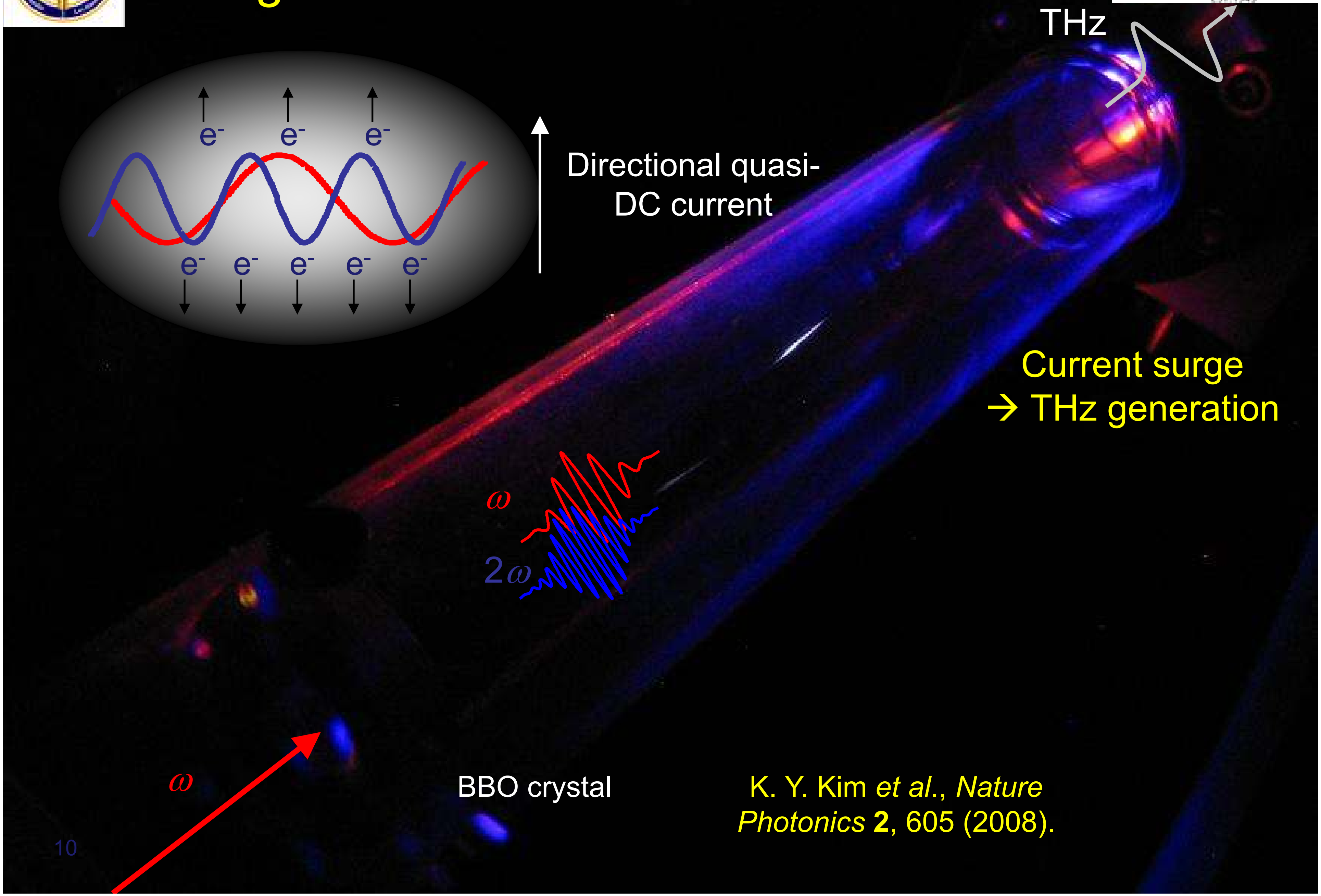

K. Y. Kim *et al.*, *Nature Photonics* **2**, 605 (2008).

P.B. Andersen & A. Tokmakoff,
Opt. Lett. **35**, 1962 (2010)

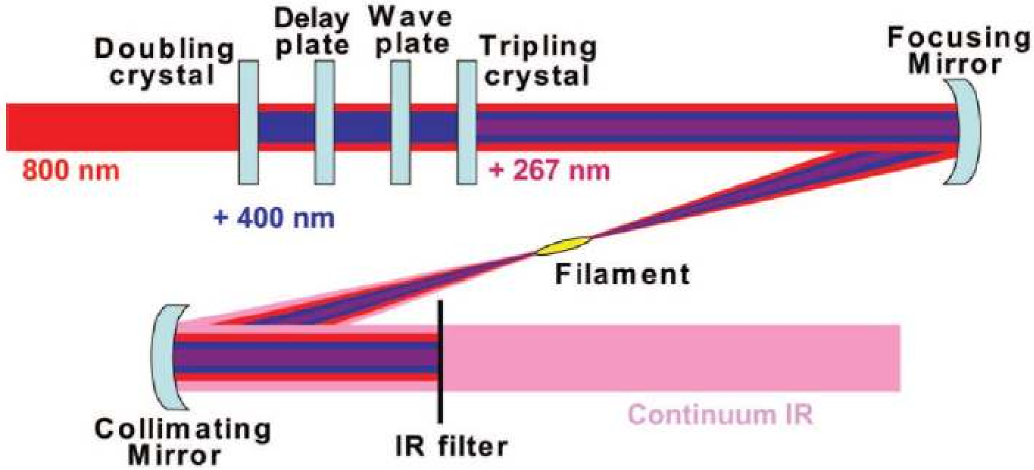

Cross-correlation
with 45 fs 3 μm in InSb

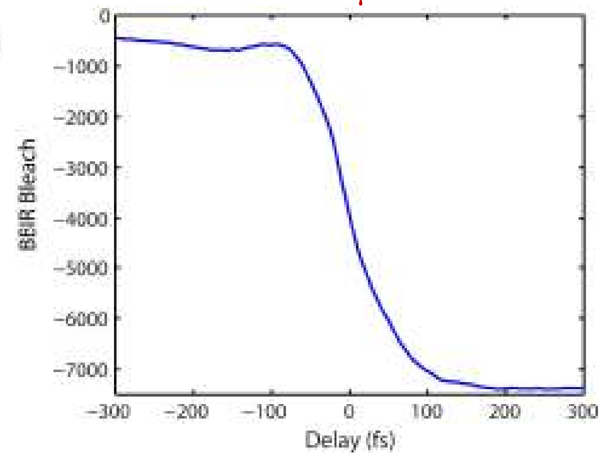

Pulse duration < 100 fs

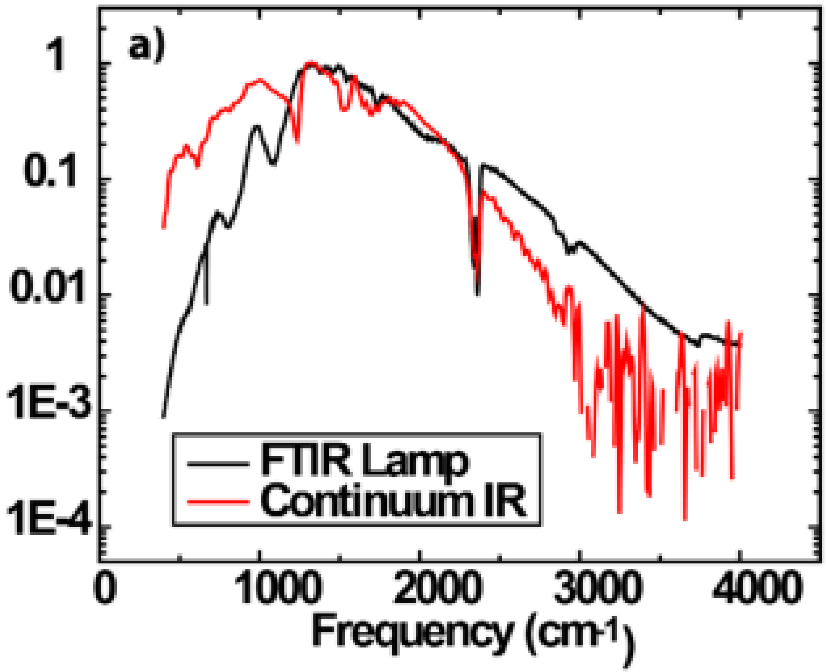

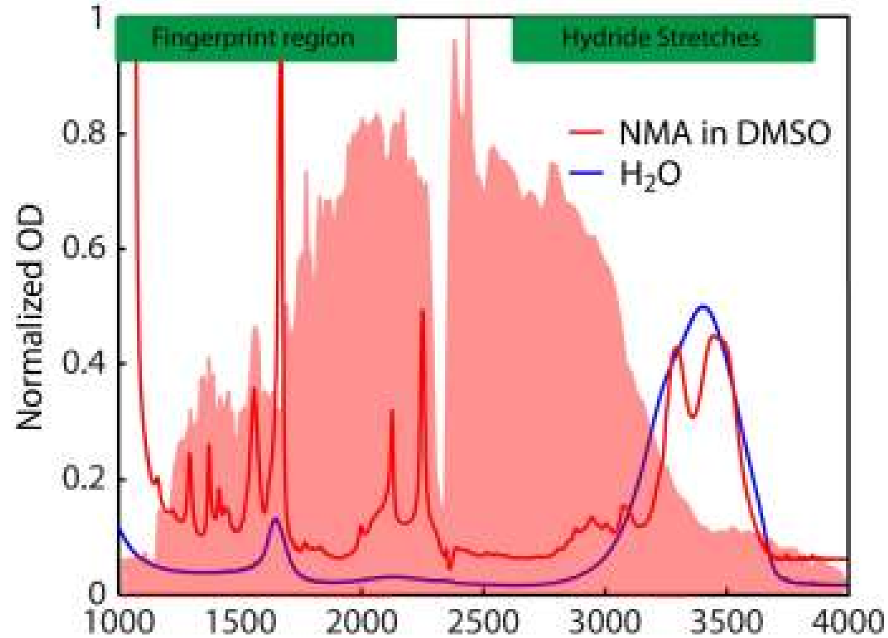

TOKMAKOFFGROUP

THz generation at large facilities

From electron accelerator

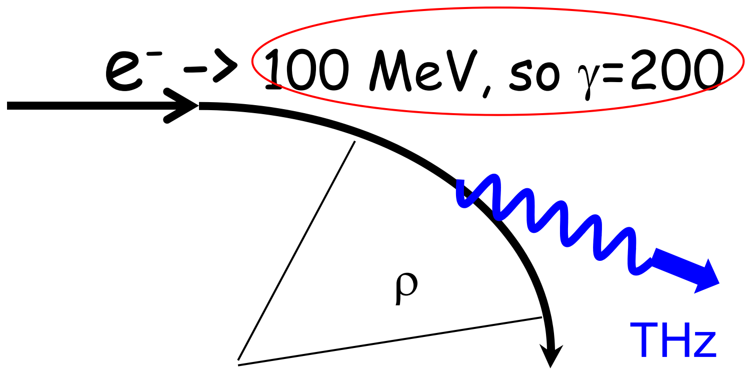

Electron acceleration produces THz emission

Gwyn Williams, Jefferson Lab

Carr et al., *Nature* **420**, 153 (2002)

From electron beam near field

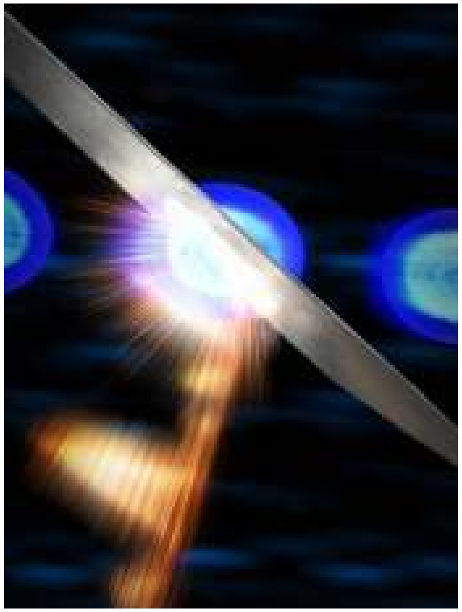

Reflection directs THz into far field

Aaron Lindenberg, Stanford/LCLS

Daranciang et al., *APL* 99, 141117 (2011)

Optical rectification: velocity matching

Conventional NLO crystal

Collinear velocity matching

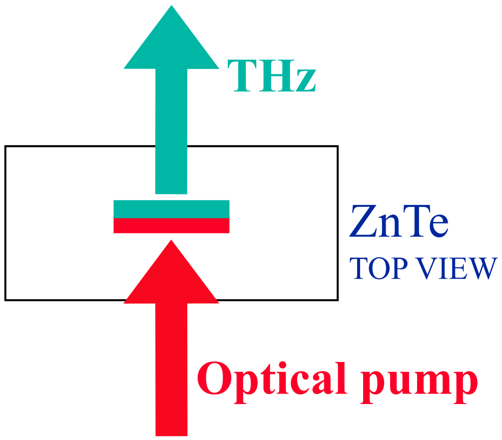

$$n_{vis}^{gr} = n_{THz}$$

$$v_{vis}^{gr} = v_{THz}^{ph}$$

Equal refractive index values

$\Rightarrow$ Equal velocities

Optical & THz pulses copropagate through crystal

ZnTe, GaP, GaSe, etc.

High-dielectric NLO crystal

$n_{THz} >> n_{vis}^{gr}$, $v_{THz}^{ph} << v_{vis}^{gr}$

Collinear velocity matching is not possible

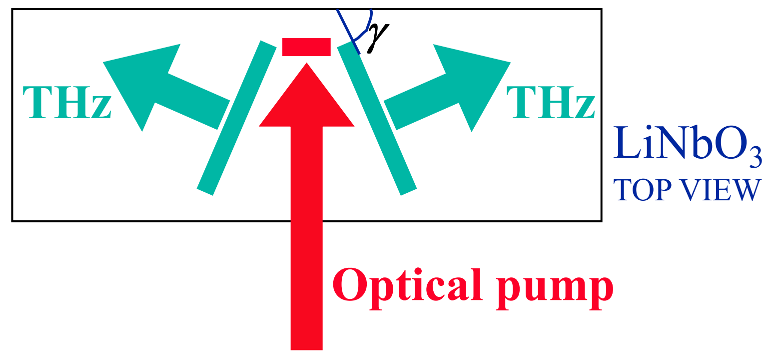

Cerenkov condition: $$\cos\gamma = n_{vis}^{gr} / n_{THz}$$

$$v_{vis}^{gr} \cos\gamma = v_{THz}^{ph}$$

THz velocity << optical velocity

THz pulses propagate *mostly laterally* through crystal

So $LiNbO_3$ can’t velocity match collinearly

But it has a very high figure of merit!

THz phonon-polariton generation in $LiNbO_3$ slabs

- The large index mismatch between THz and optical light leads to Cherenkov radiation: the THz propagates mostly perpendicular to optical pulse

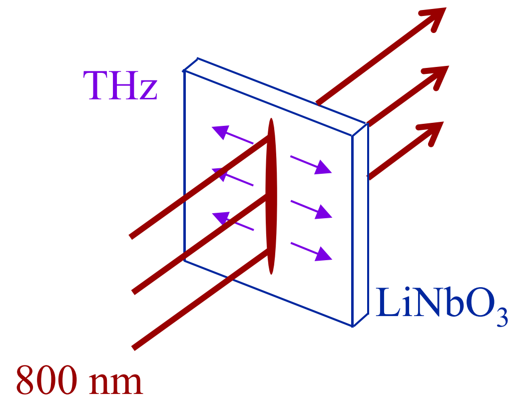

- Optical Intensity envelope → THz E-field waveform

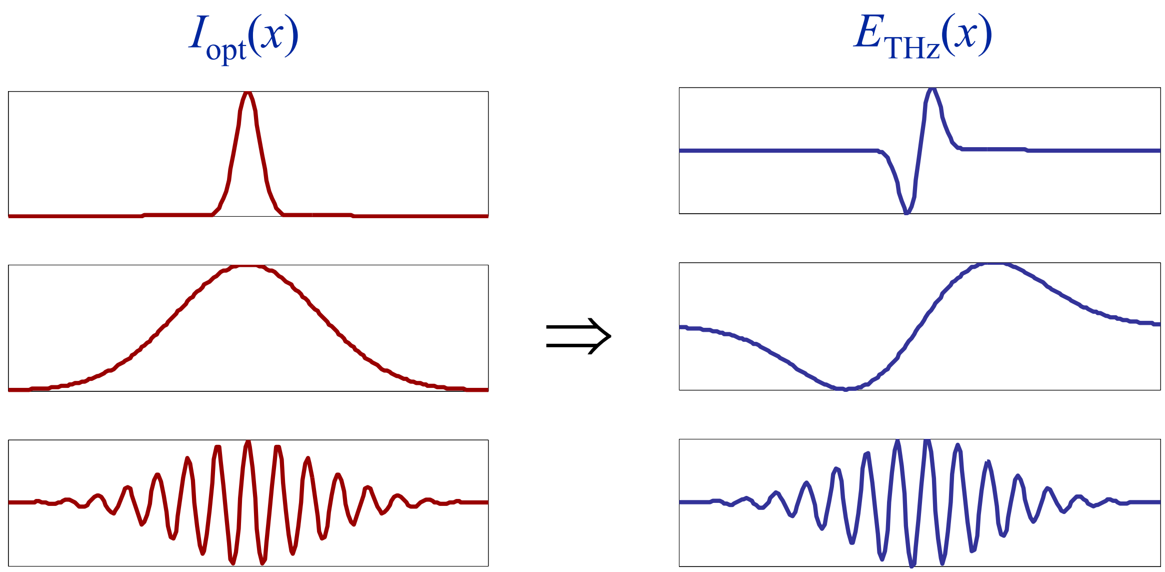

High EO constants in ferroelectric crystals

It's the ions!!

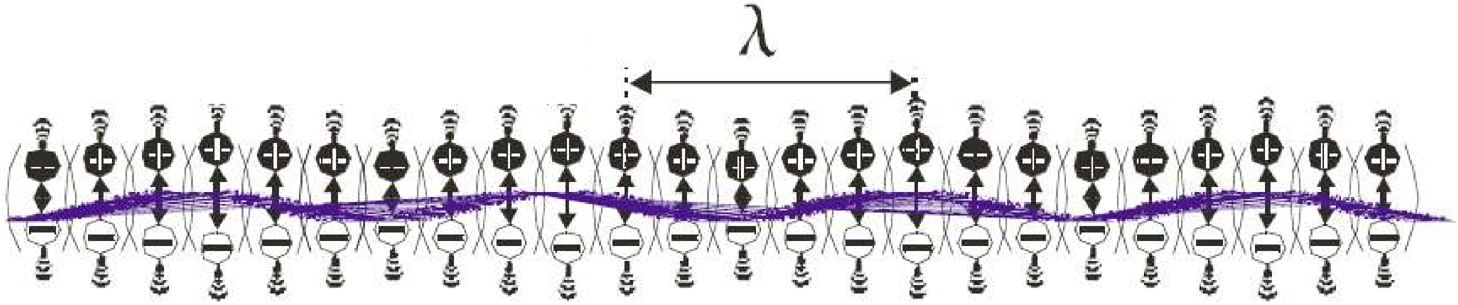

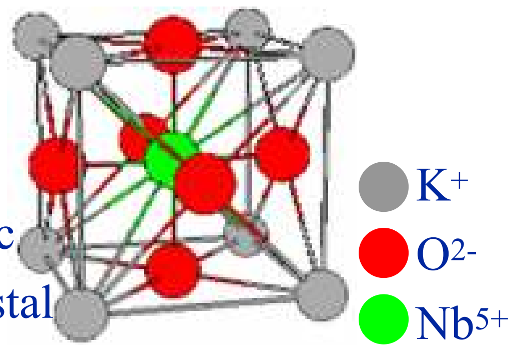

Ferroelectric $KNbO_3$ crystal

Polar lattice vibrational mode
"Soft" mode in FE phase transitions
$\Rightarrow$ high ε

Fs pulses drive lattice through impulsive stimulated Raman scattering

THz phonon coordinate   THz Field

Laser Field

$$\begin{cases} \ddot{\vec{\mathbf{Q}}} + \Gamma\dot{\vec{\mathbf{Q}}} + w_{TO}^2\vec{\mathbf{Q}} = b_{12}\vec{\mathbf{E}} + \boxed{\frac{1}{2}\varepsilon_0\sqrt{\frac{N}{M}}\left(\frac{\partial\alpha}{\partial\vec{w}}\right)\left|\vec{E}(t)\right|^2} \\ \left(\nabla^2\vec{\mathbf{A}} - \frac{1}{c_0^2/\varepsilon_\infty}\ddot{\vec{\mathbf{A}}}\right) = -\mu_0 b_{21}\dot{\vec{\mathbf{Q}}} + \cancel{\boxed{F}} \end{cases}$$

electronic nonlinearity – neglected!

F_{ISRS}

THz optic phonon-polariton modes in FE crystals

Coupled lattice vibrational/electromagnetic modes
~ 0.1-10 THz frequencies, 5-500 μm wavelengths in FE crystals
Polaritons move through host crystal at light-like speeds

Four-wave mixing data

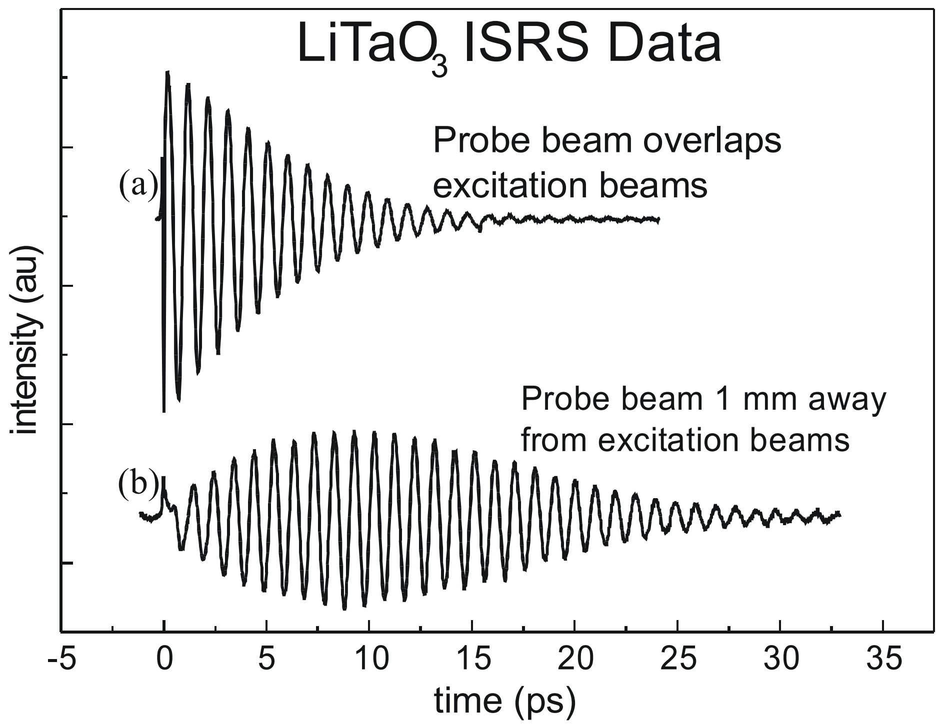

FWM results with many wavevectors

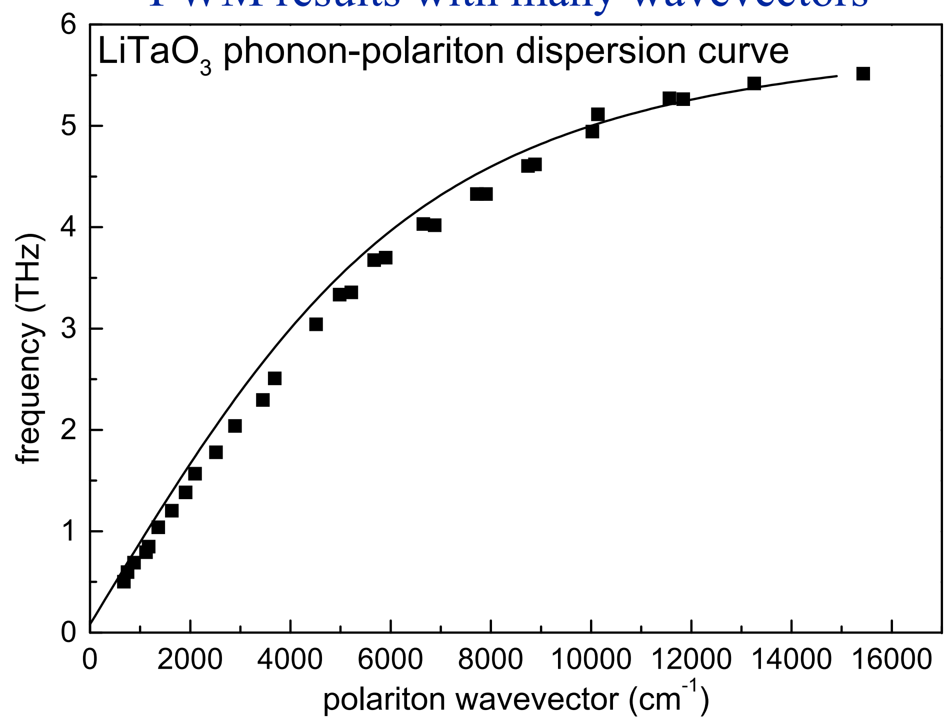

Polaritons can be used as THz signals
Terahertz "Polaritonics" platform possible

Direct x-ray probing of polariton lattice displacements

Fs x-ray pulse used for time-resolved diffraction

Derived from LBL synchrotron source

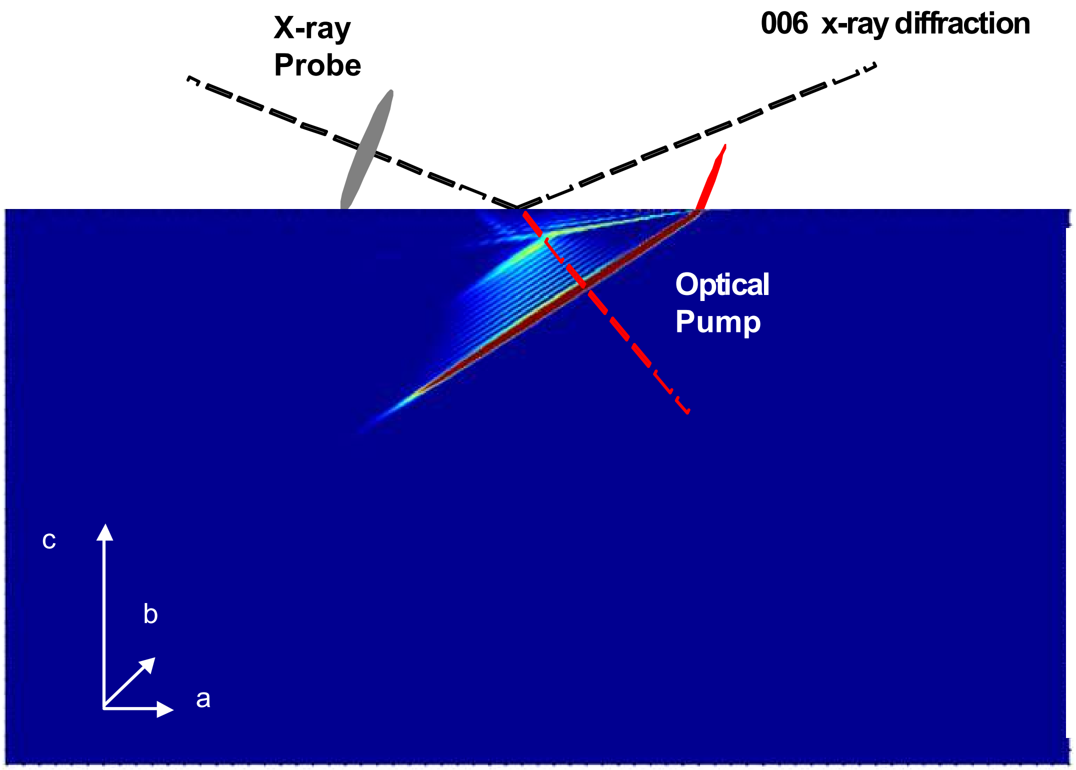

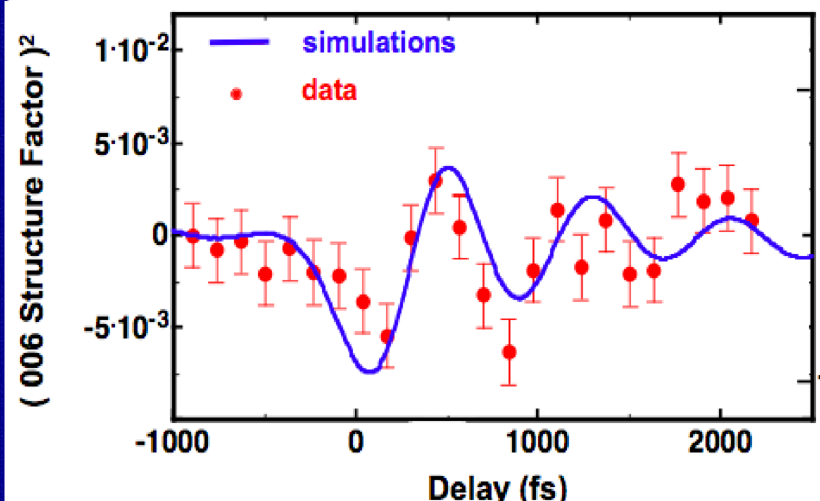

Nature **442, 664 (2006)**

Collaborators: A. Cavalleri, S. Wall, C. Simpson, M.Rini, R.W. Schoenlein

Fs x-rays achievable through tabletop laser system

Polaritons & polariton-induced structural change may be monitored

THz polariton imaging

T. Feurer et al., Annu. Rev. Mater. Res. **37**, 317 (2007)

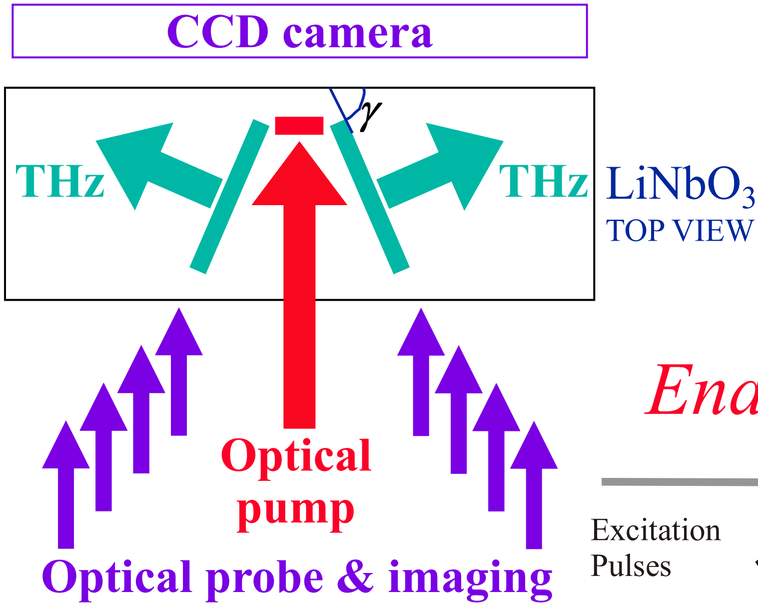

Lateral propagation makes THz wave accessible to further optical inputs

Enables real-space polariton imaging

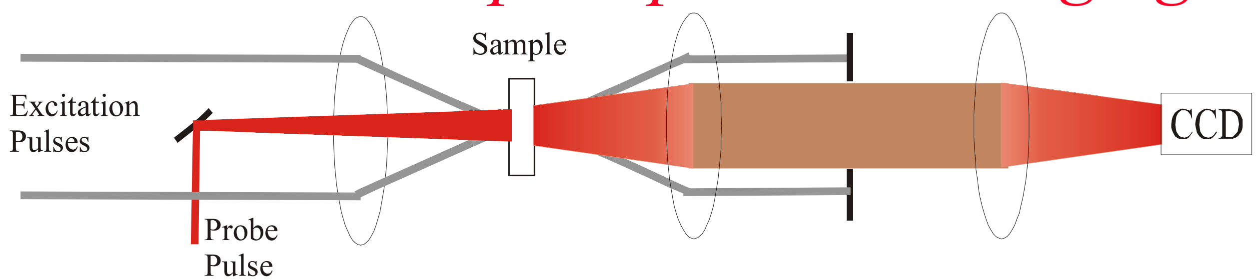

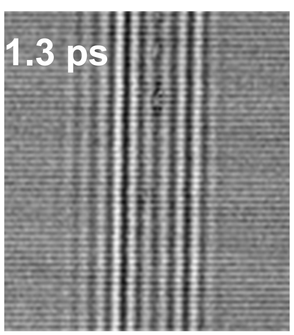

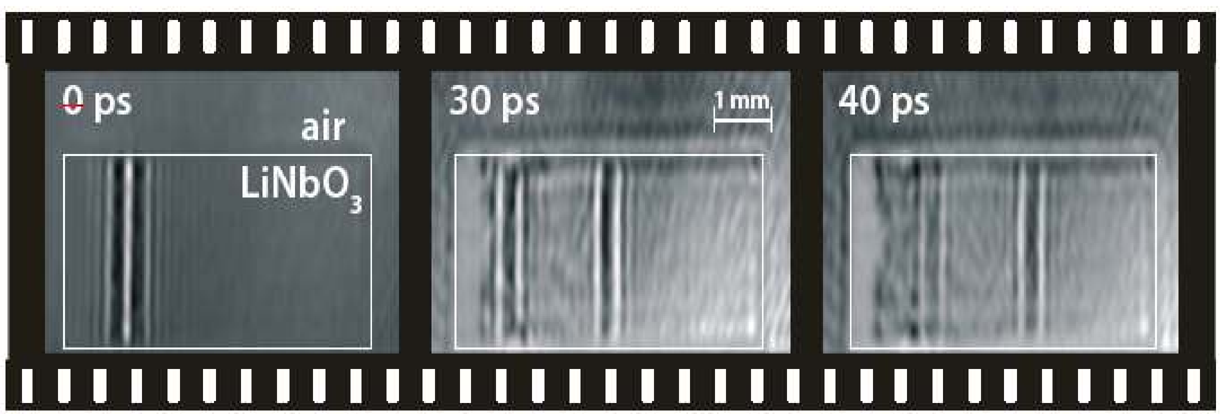

Complete temporal and spatial evolution monitored

Spatiotemporal polariton imaging & control
The movies

Samples: $LiTaO_3$, $LiNbO_3$ crystals   Polariton speed ≈ $c/6$ = 50 μm/ps
Length scale ~ 1-2 mm, Temporal range ~ 20-40 ps

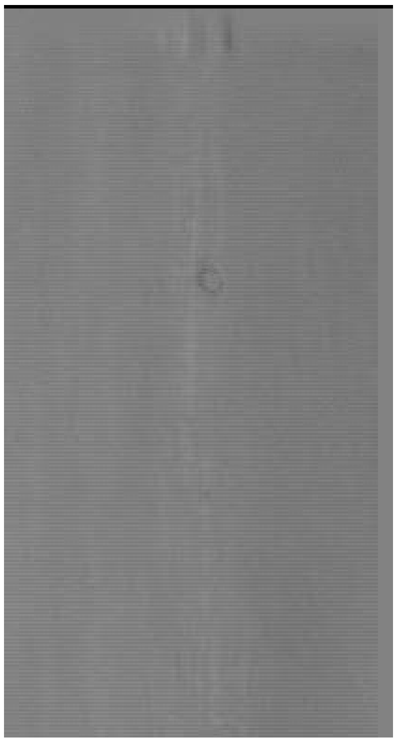

Crossed beams

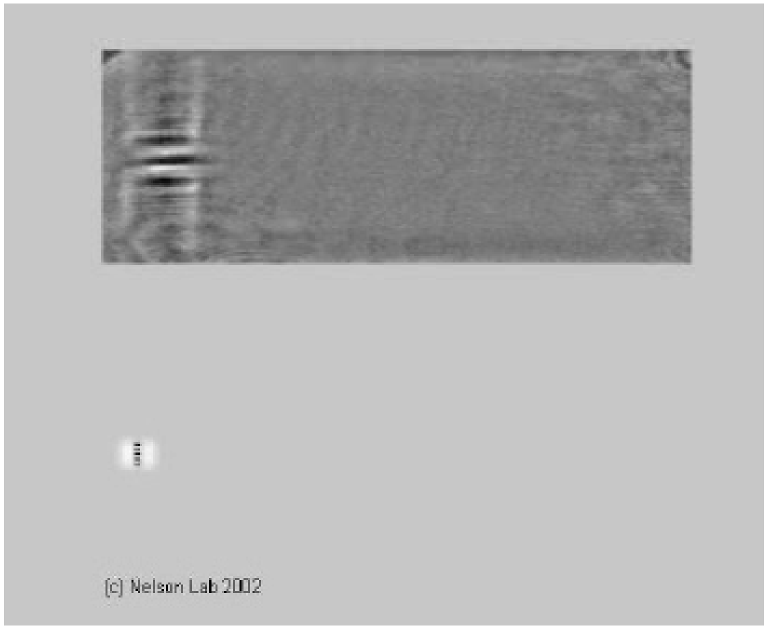

Round spot

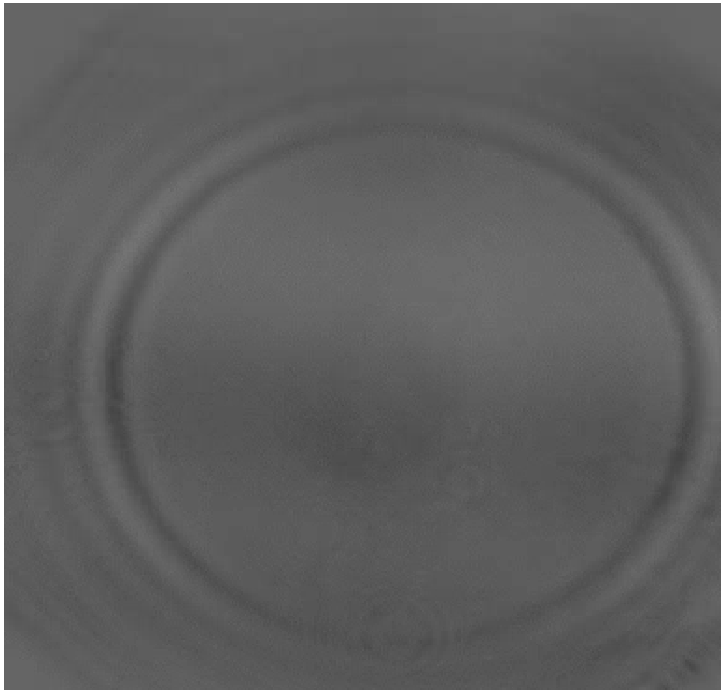

Ring of light

Spatiotemporal polariton imaging & control
The movies

Samples: $LiTaO_3$, $LiNbO_3$ crystals   Polariton speed ≈ $c/6$ = 50 μm/ps
Length scale ~ 1-2 mm, Temporal range ~ 20-40 ps

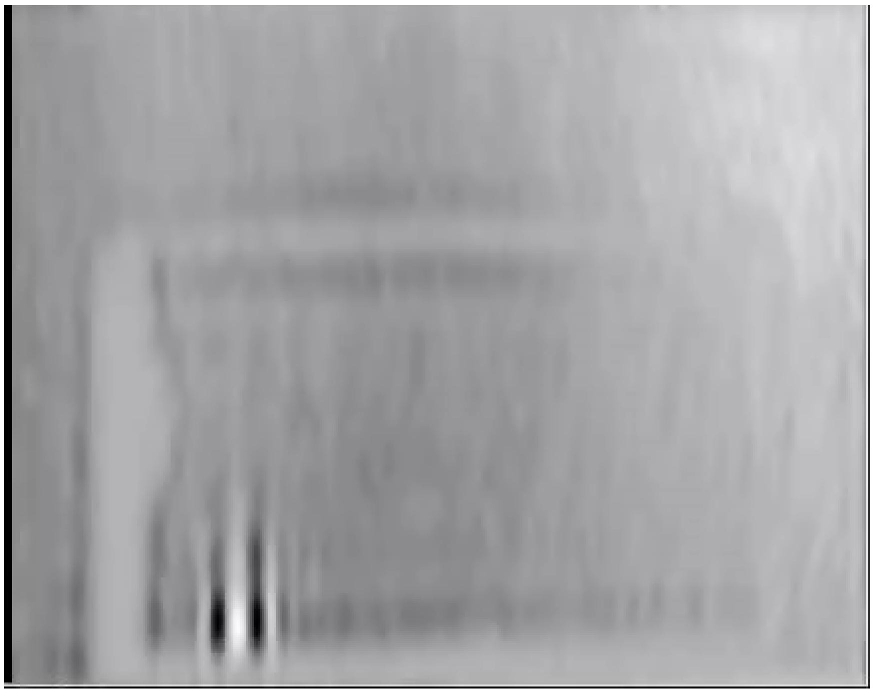

Line source
Single crystal

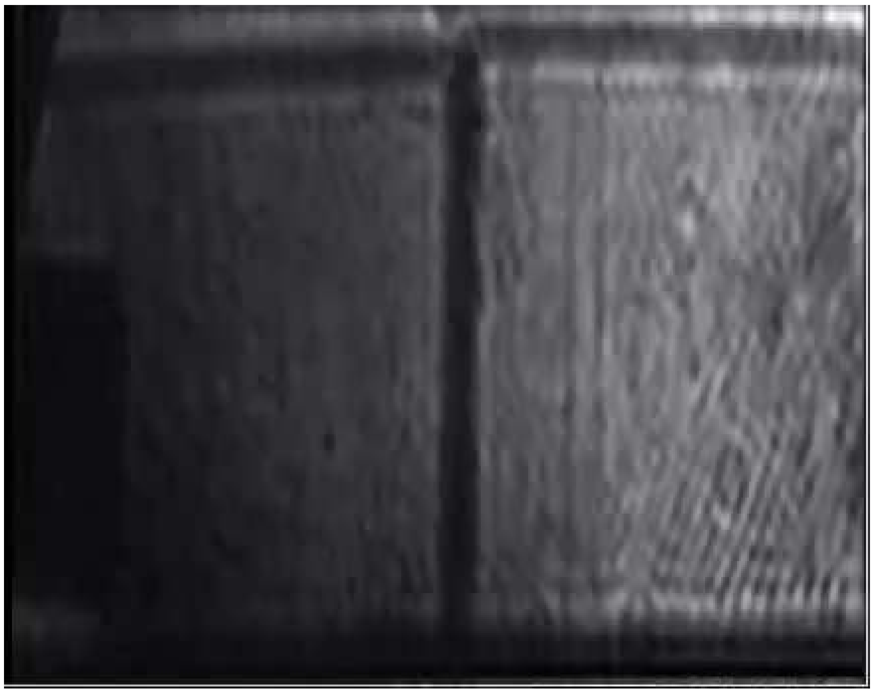

Line source
Two crystals

Phase-contrast THz polariton imaging

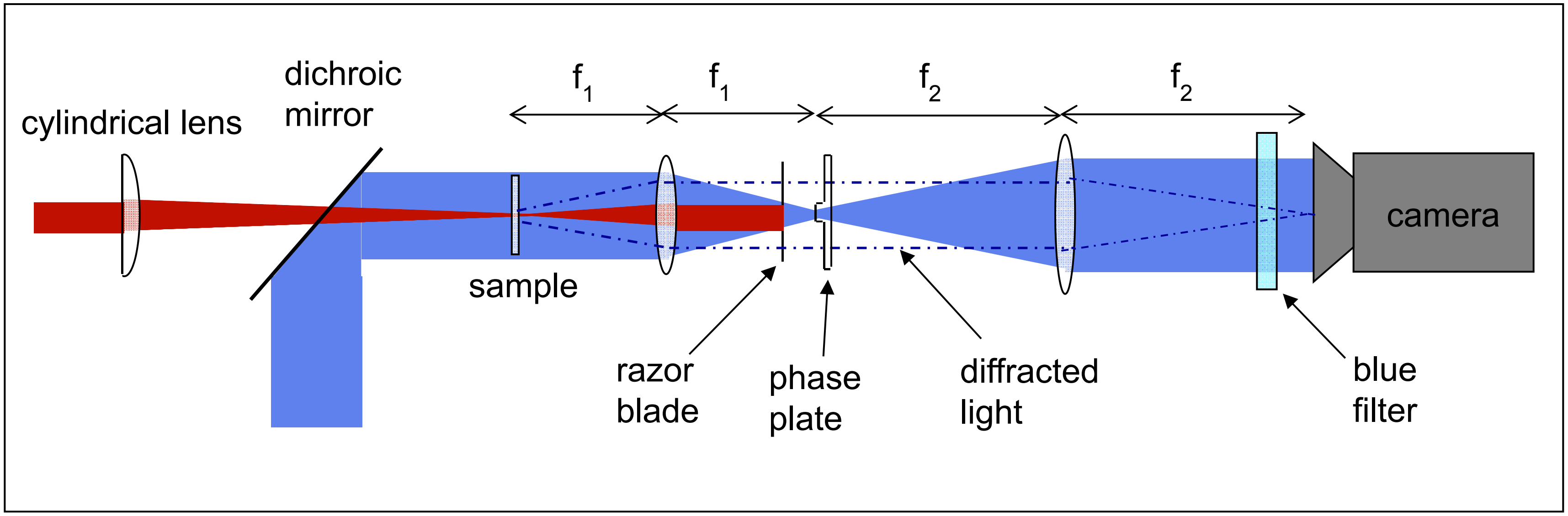

phase plate

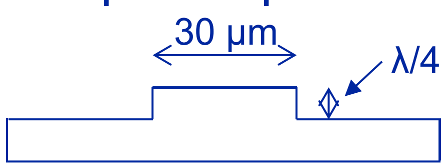

High sensitivity
In focus
Quantitative

C.Werley et al., *JOSA B* (in press)

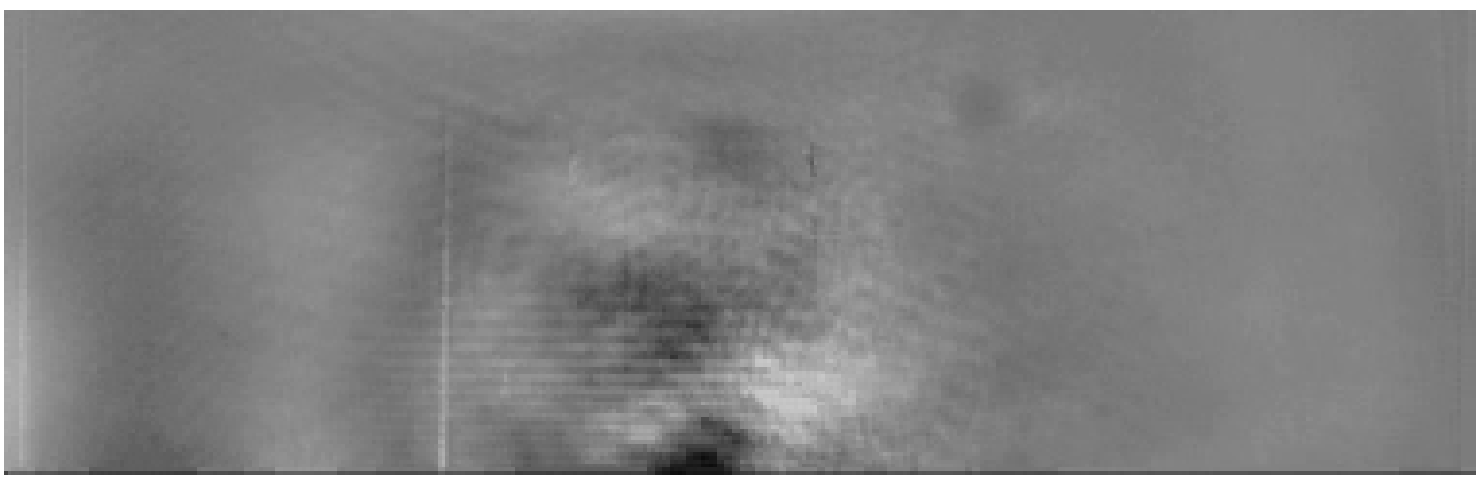

Polaritonic structures & devices

Integrated THz functionalities

Polaritonic waveguide splitter, interferometer, resonator, 90º bend

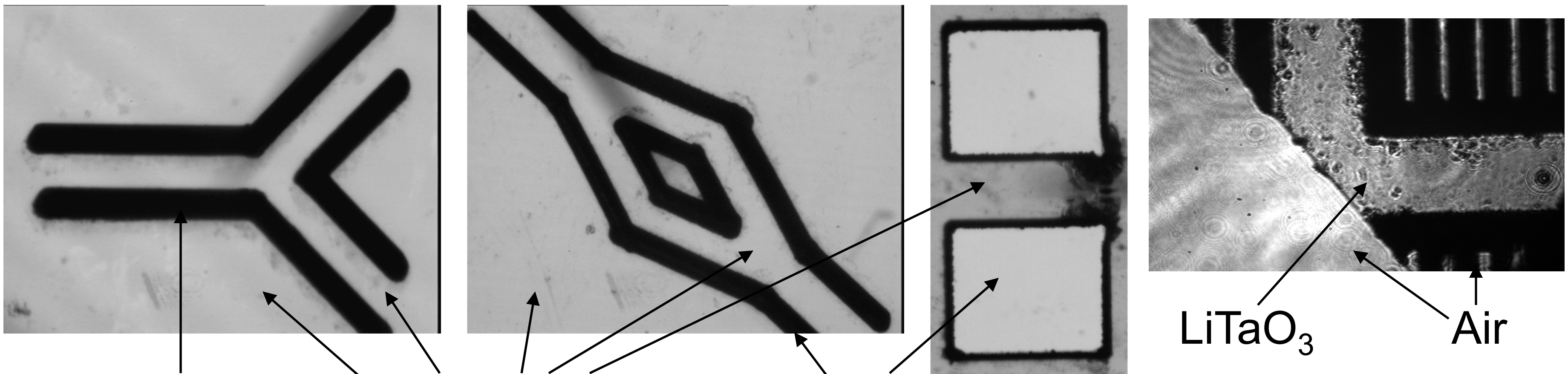

All $LiNbO_3$ channels are 200-300 μm wide

Nature Materials **1**, 95 (2002)

Polaritonic grating

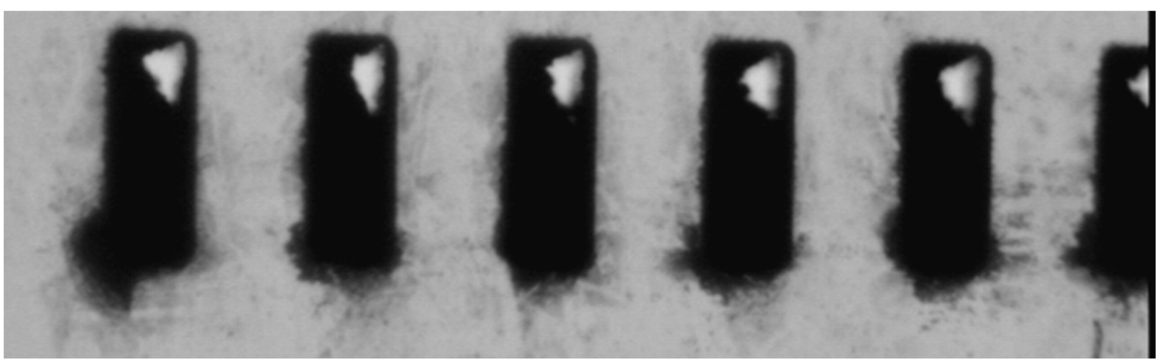

5 mm x 4 mm crystal, 250 μm thick

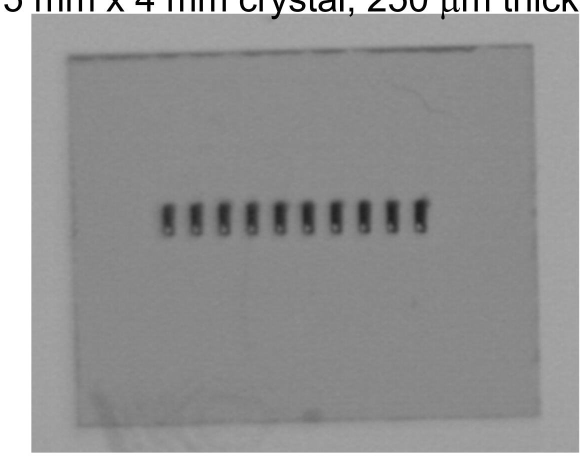

Polaritonic structures & devices

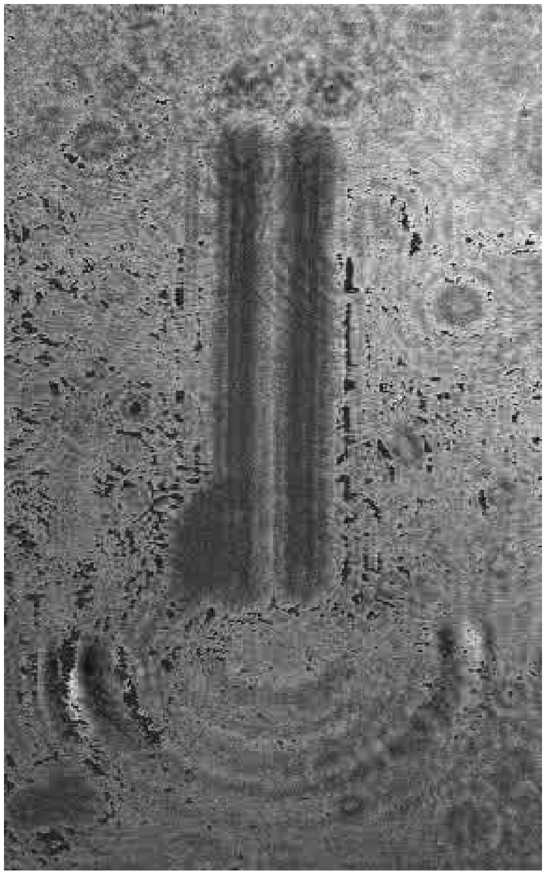

Waveguide

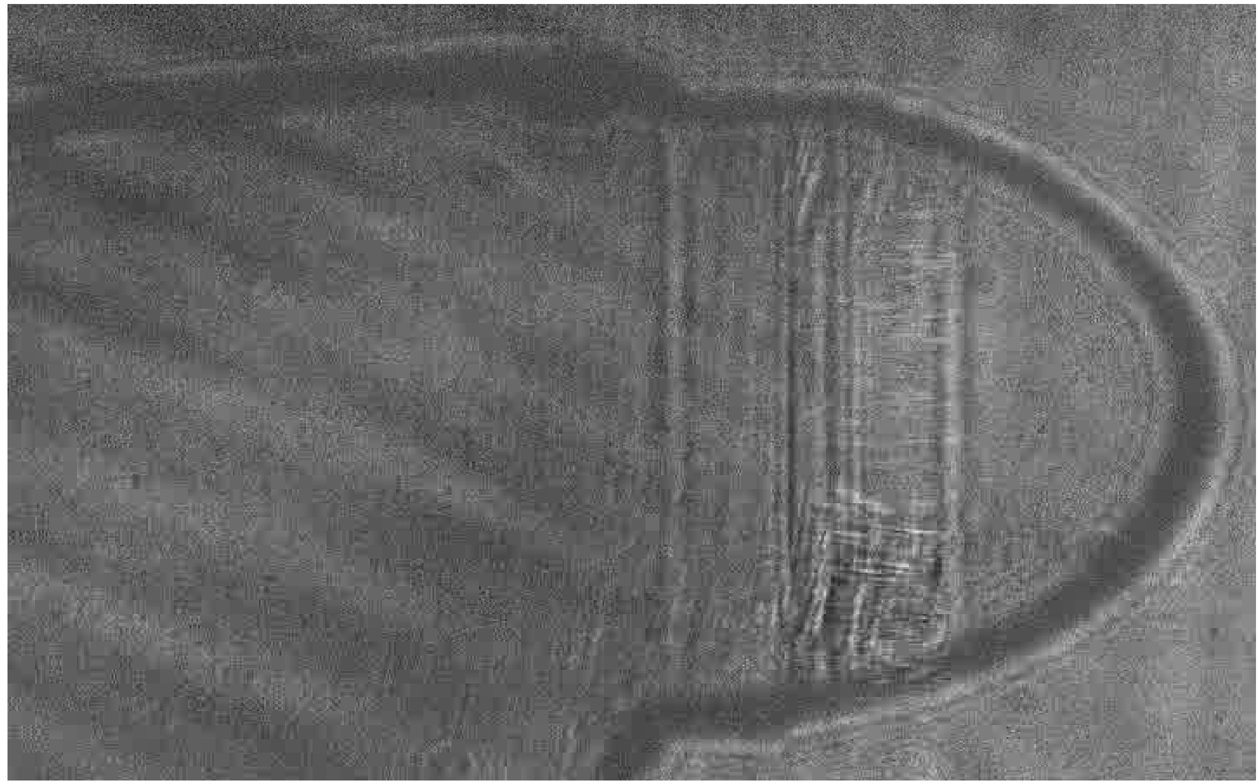

Focusing reflector

The polaritonics toolset

T. Feurer et al., Annu. Rev. Mater. Res. **37**, 317 (2007)

Spatiotemporal polariton imaging

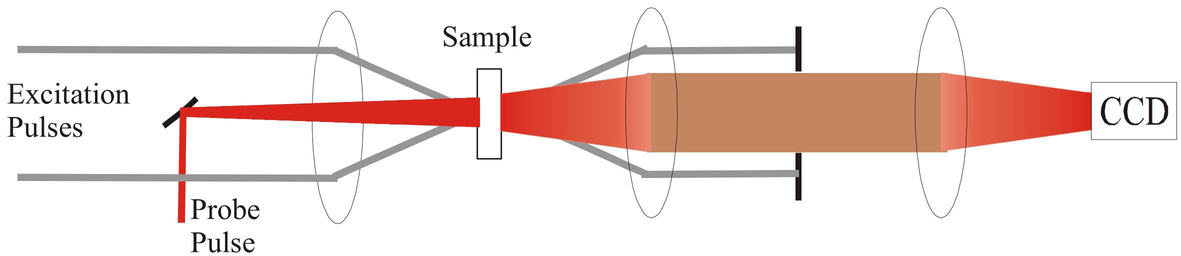

THz "movies" yield complete spatial & temporal evolution

Spatiotemporal THz coherent control

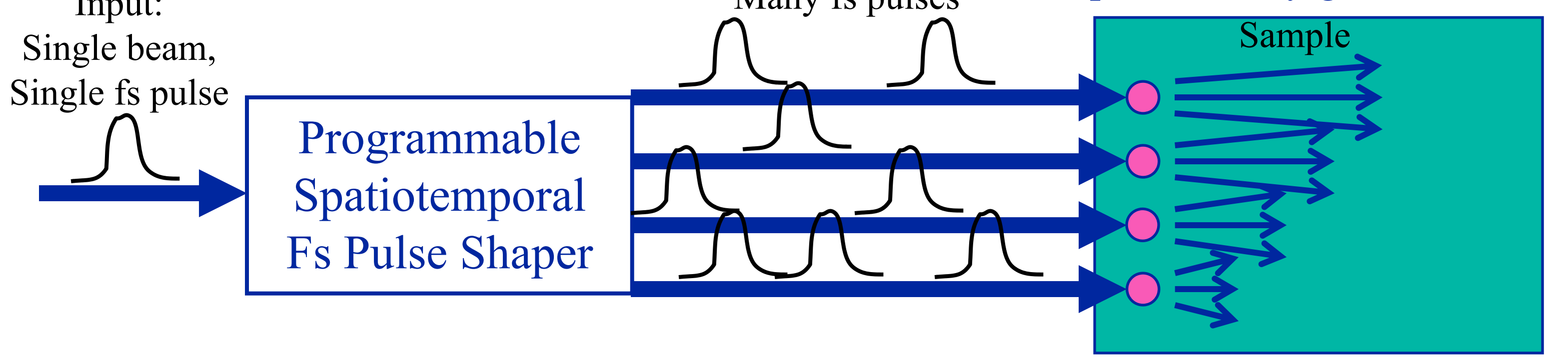

Integrated THz functional elements

fabricated by fs laser machining

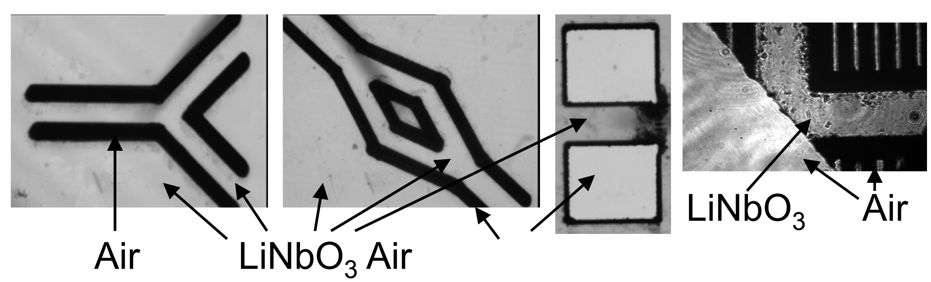

Spatiotemporal polariton coherent control

Through spatiotemporal fs pulse shaping

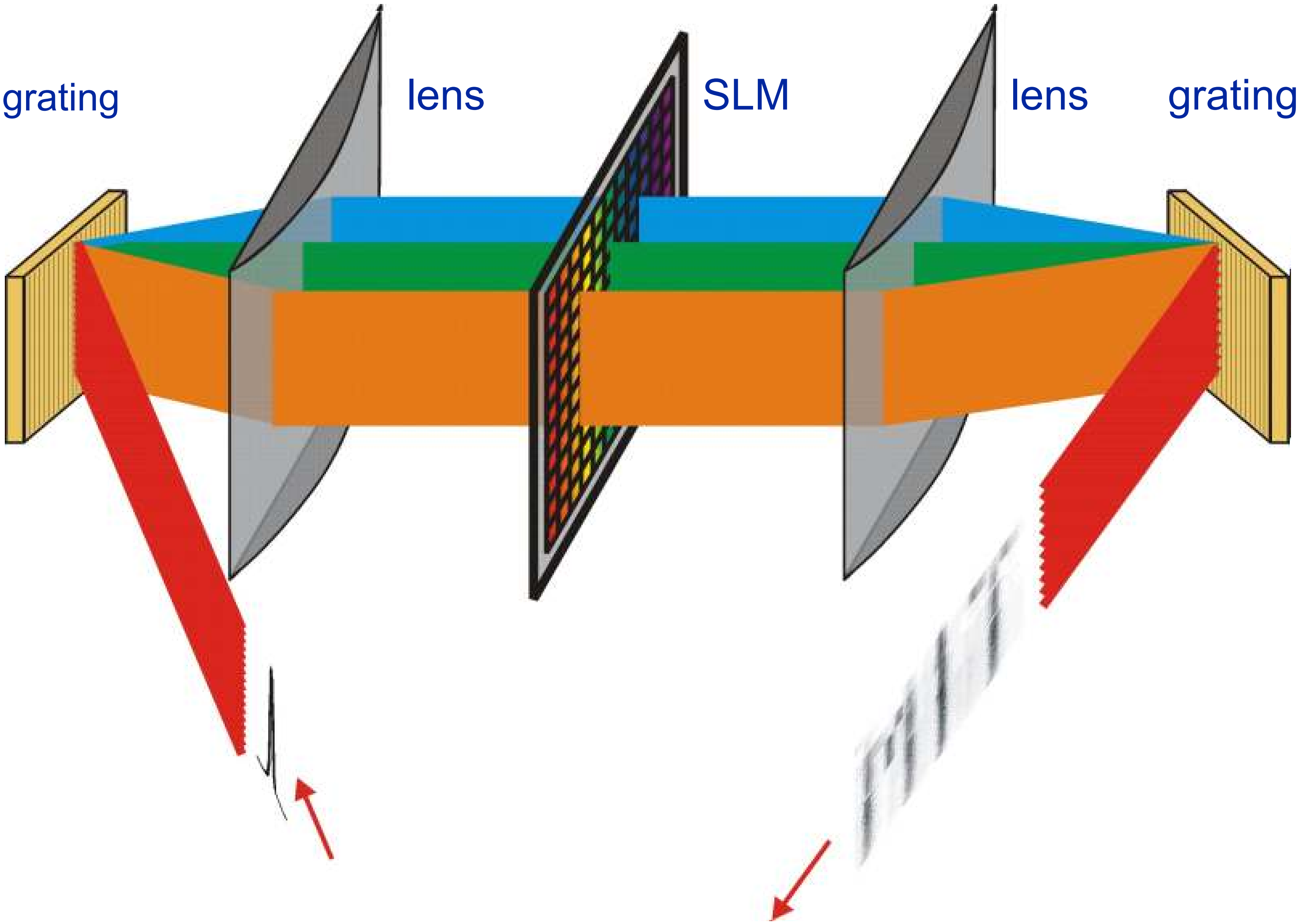

Spatiotemporal polariton coherent control

Timed/phased array generation

4 spots
Tilt down

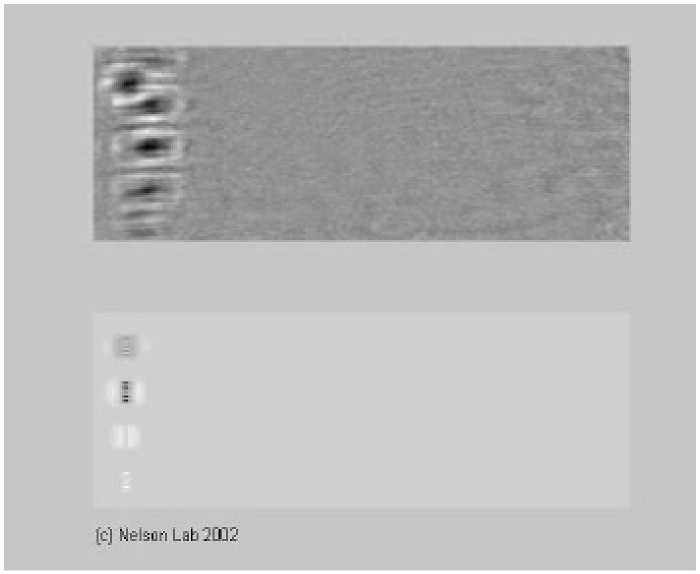

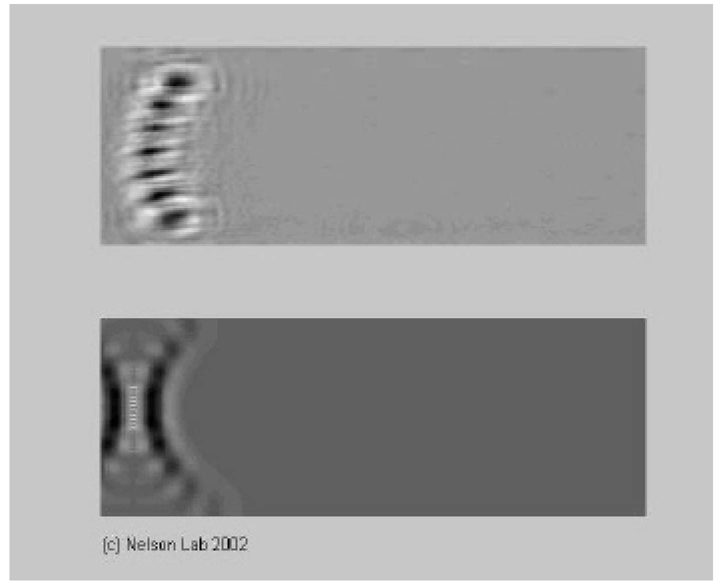

8 spots
Focus

40 spots
Tilt up

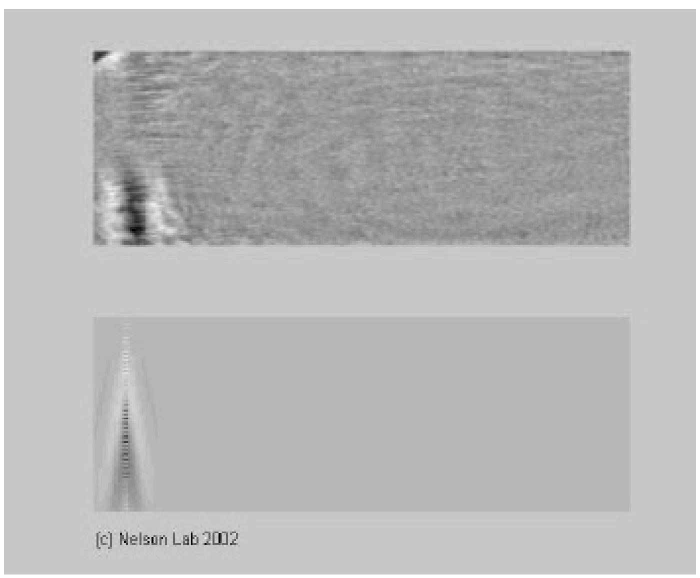

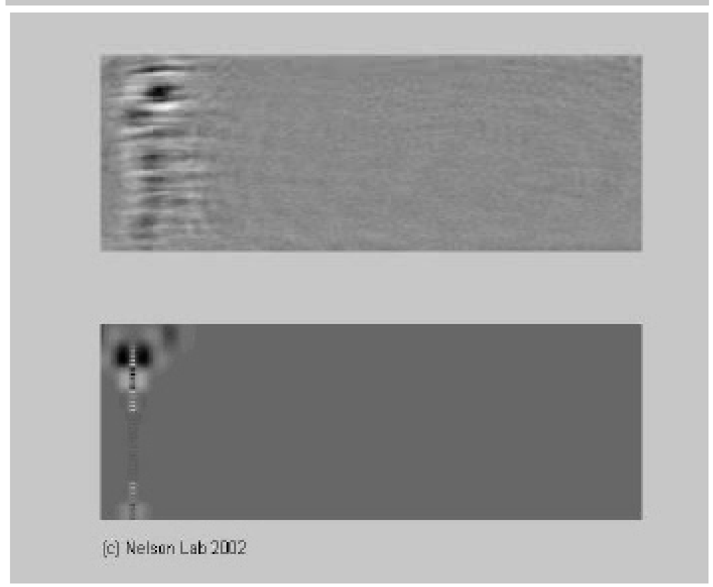

8 spots
Focus
Tilt down

Spatiotemporal polariton coherent control

Coherent THz amplification

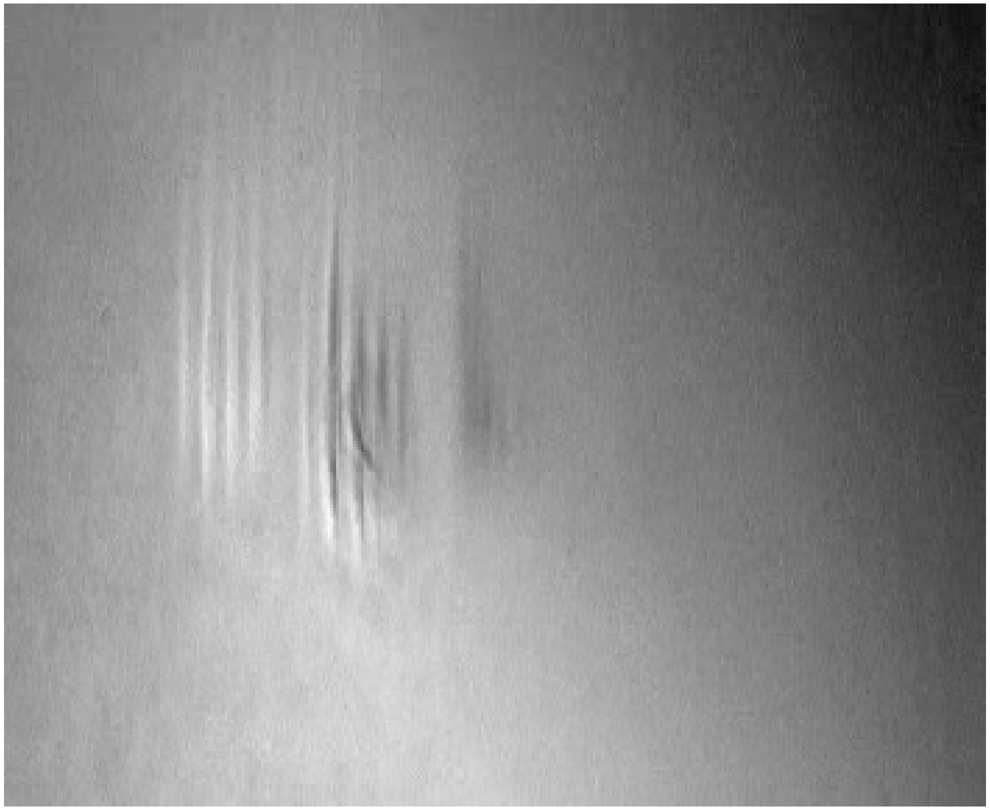

Horizontal array
Cylindrically focused "line" sources
Linear temporal sweep

T. Feurer et al., *Science* **299**, 374 (2003)

Large THz pulse energies

Spatiotemporal control over THz field

With reconfigurable spatiotemporal fs pulse shaping

With non-reconfigurable echelon structure

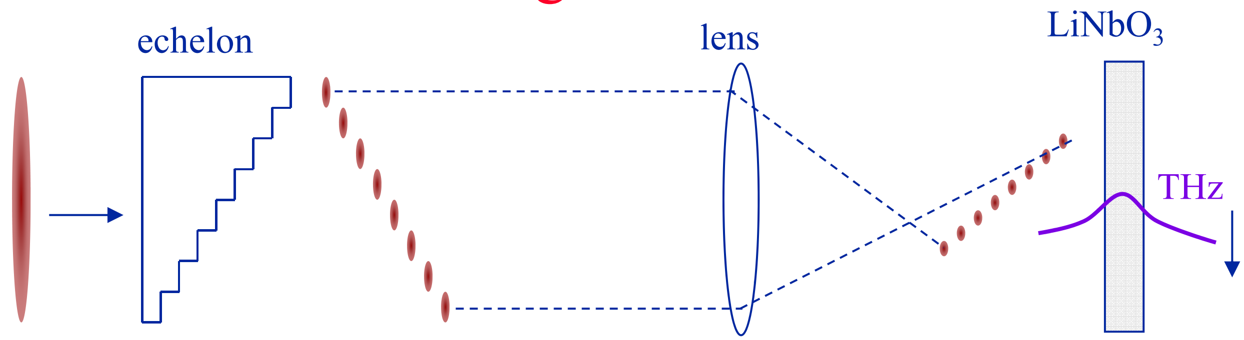

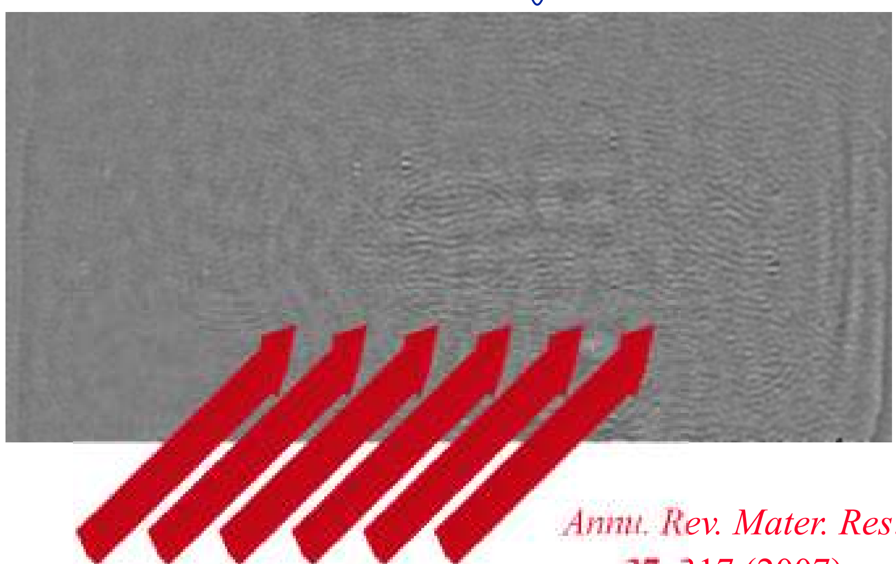

Annu. Rev. Mater. Res. **37**, 317 (2007)

THz wave coherent amplification

Tilted pulse front: Simple, compact setup

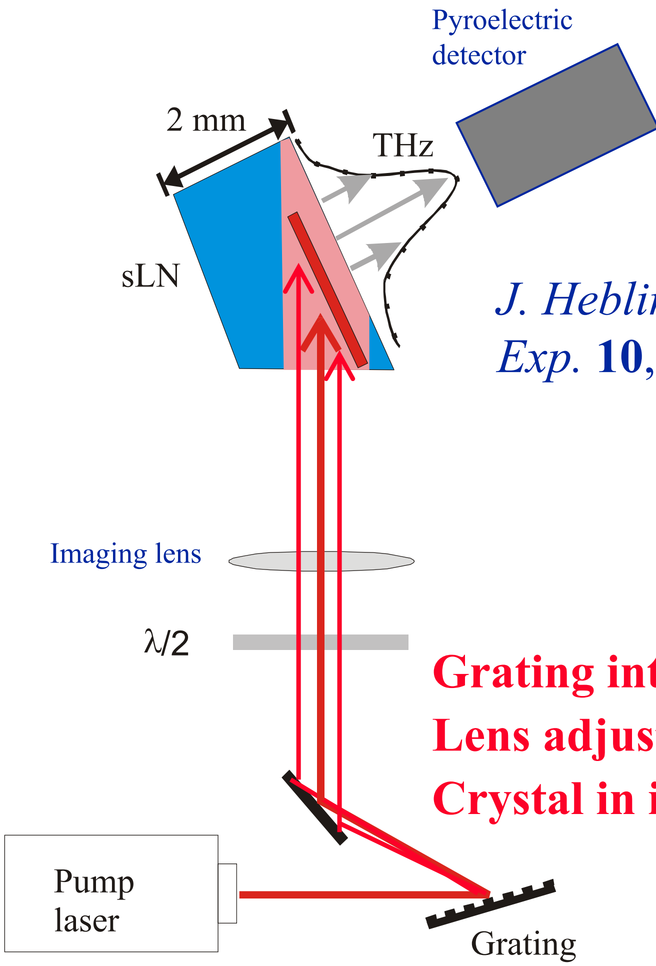

J. Hebling et al., Opt. Exp. **10**, 1161 (2002)

Grating introduces tilt
Lens adjusts tile angle
Crystal in image plane

$LiNbO_3$ prism

Works well at Hz-KHz-MHz rep rates

Higher THz pulse energies

10 Hz

THz Pulse Energy:

50 μJ

Average power: 100 μW

Terahertz peak intensity

10 MW/cm^2

Field strength: 750 kV/cm

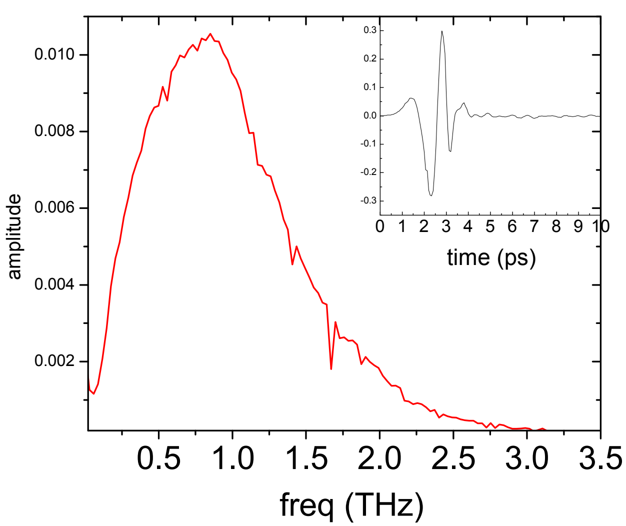

J. Hebling et al. *APL* **90** 171121 (2007)

1 kHz

THz Pulse Energy: 7 μJ

THz Av. Power: > 2.5 mW

Peak power: 2.5 MW

Energy efficiency: 4 x 10^{-4}

Photon efficiency: 15 %

Field strength: 150 kV/cm

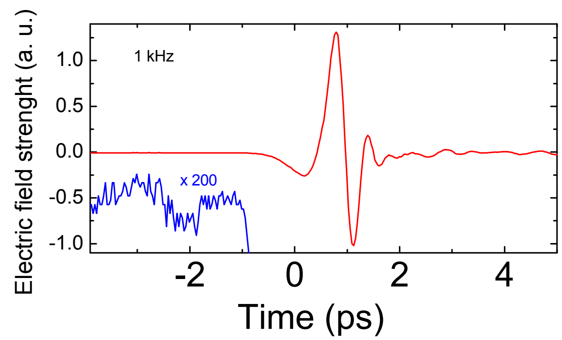

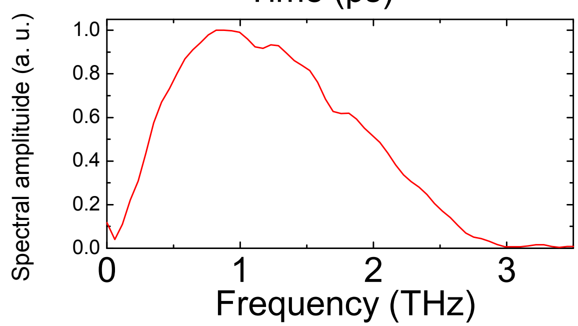

Yeh et al., *Opt. Commun.* **13,** *3567* (2008)

1 MHz

THz Av. Power: > 0.25 mW

THz Pulse Energy: > 2.5 nJ

Pump: Yb fiber laser/amp

Energy efficiency: 1.8 x 10^{-5}

Photon efficiency: ½ %

Suitable for practical applications

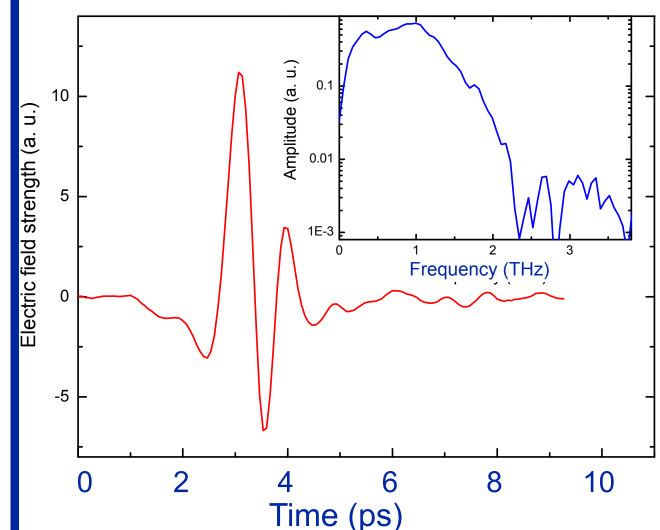

M. Hoffmann et al., *APL* **93**, 141107 (2008)

THz multiple-cycle waveform generation

Chirp-and-delay optical pump yields tunable THz frequency

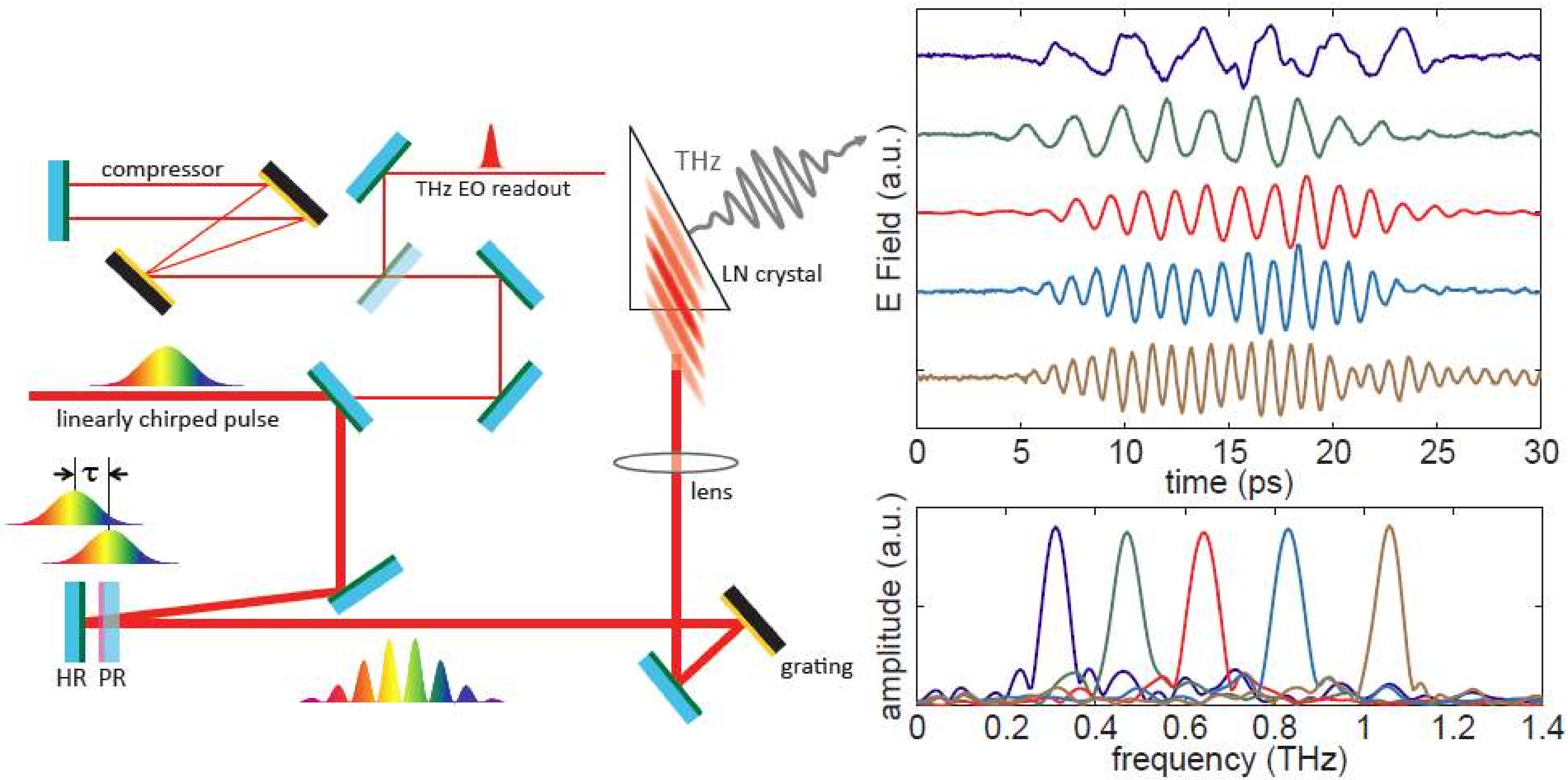

Multi-μJ multiple-cycle pulse energies

Z. Chen, X. Zhou, C.A. Werley, KAN, *Appl. Phys. Lett*. **99**, 071102 (2011)

THz beam profile

Beam profile with pyroelectric camera (Spiricon Pyrocam III)
Focusing with an aspheric lens
100 mm pixel size
2.5 mJ THz pulse energy, 1 kHz rep rate

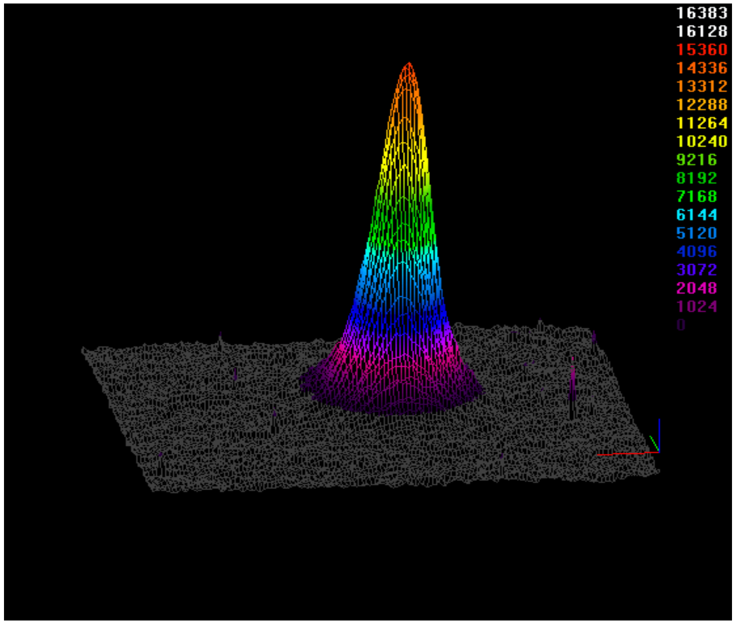

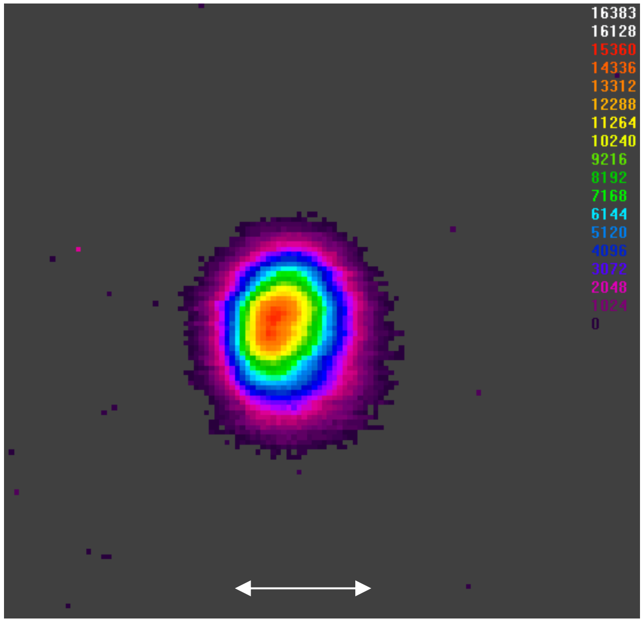

Excellent for imaging, spectroscopy, other applications

Improved focusing

Cherenkov THz wave generation in $LiNbO_3$

H. Hirori, K. Tanaka *et al.*, Appl. Phys. Lett., 98, 091106, 2011 .

E_{THz} ~ 1.2 MV/cm B_{THz} ~ 0.4 Tesla

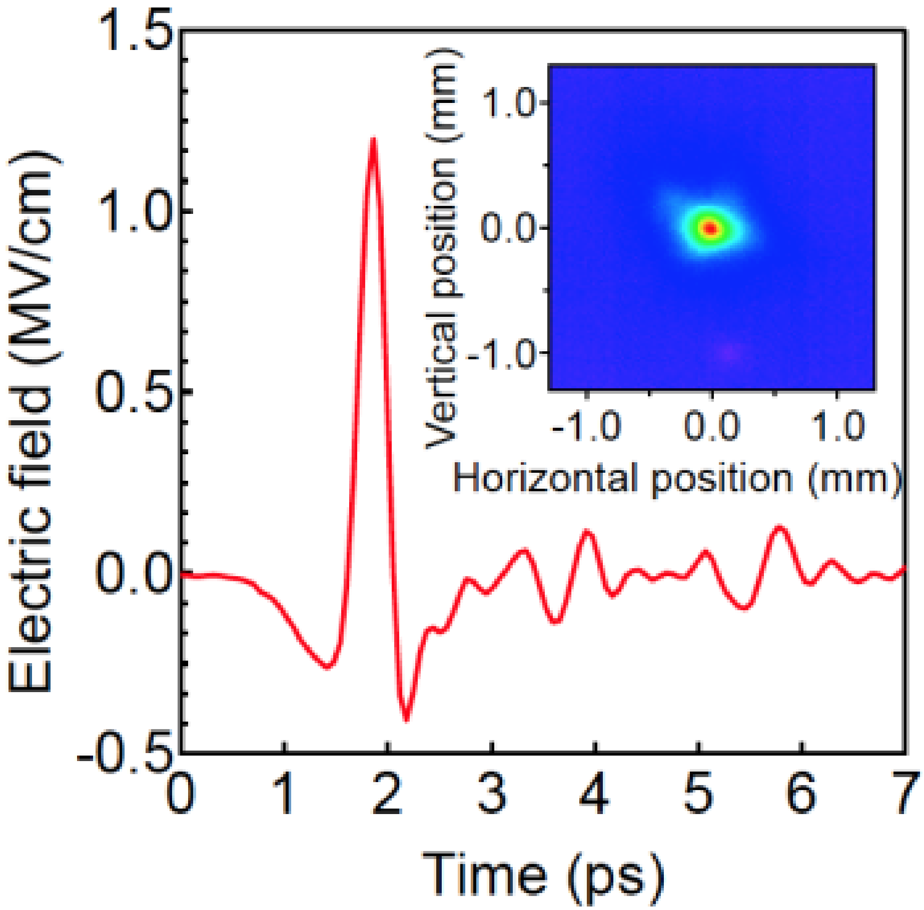

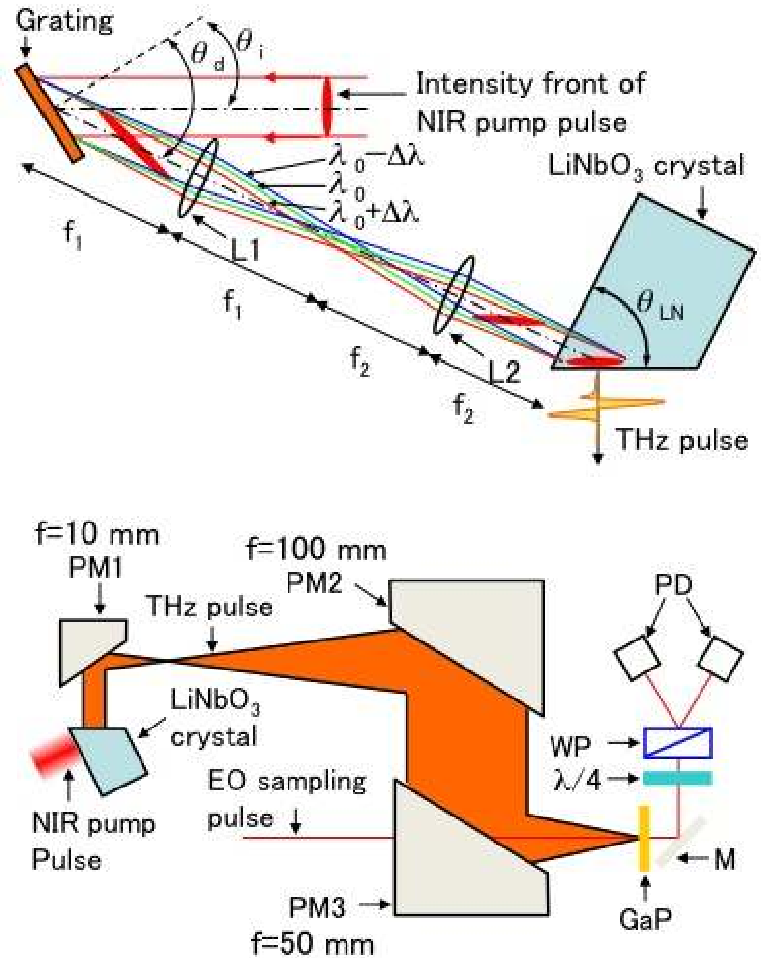

Nonlinear THz spectroscopy

Microjoule level pulses ⇒ THz nonlinear spectroscopy

THz nonlinear spectroscopy measurements conducted

- **Nonlinear THz transmission, self-phase modulation**
- **THz-induced ionization, fluorescence**
- **THz pump – optical probe**
- **THz pump – THz probe**

Nonlinear vibrational & electronic responses studied

- **Solid-state vibrational & electronic responses**
- **Phase transitions, chemical reactions**
- **Liquid-state molecular alignment**
- **Gas-phase molecular orientation, ionization**

THz Transmission Spectrometer

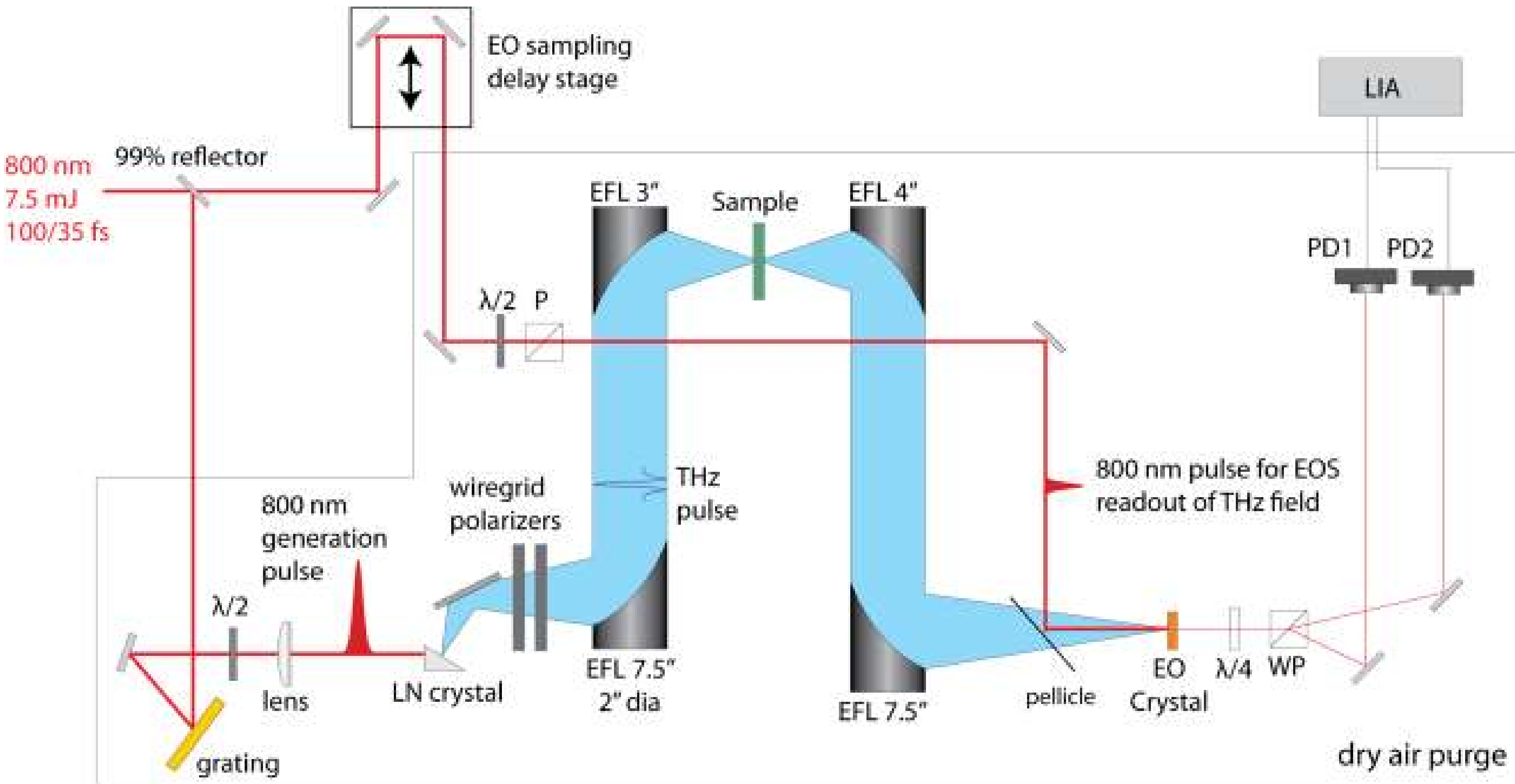

THz Pump – THz Probe Capabilities

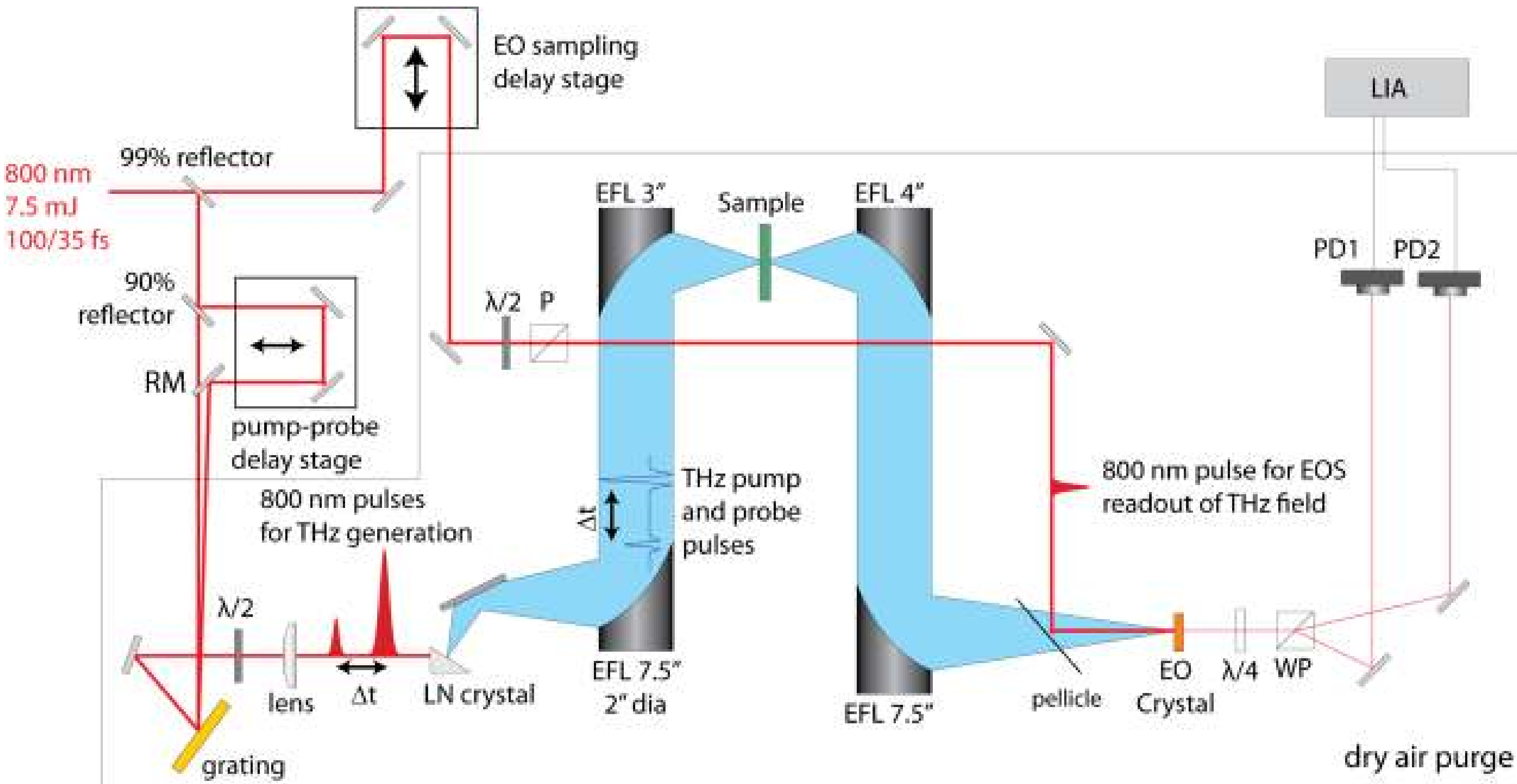

Also THz pump – Optical probe
Measure optical birefringence, SHG,…

THz pump-probe nonlinear spectroscopy

Collinear pump & probe pulses

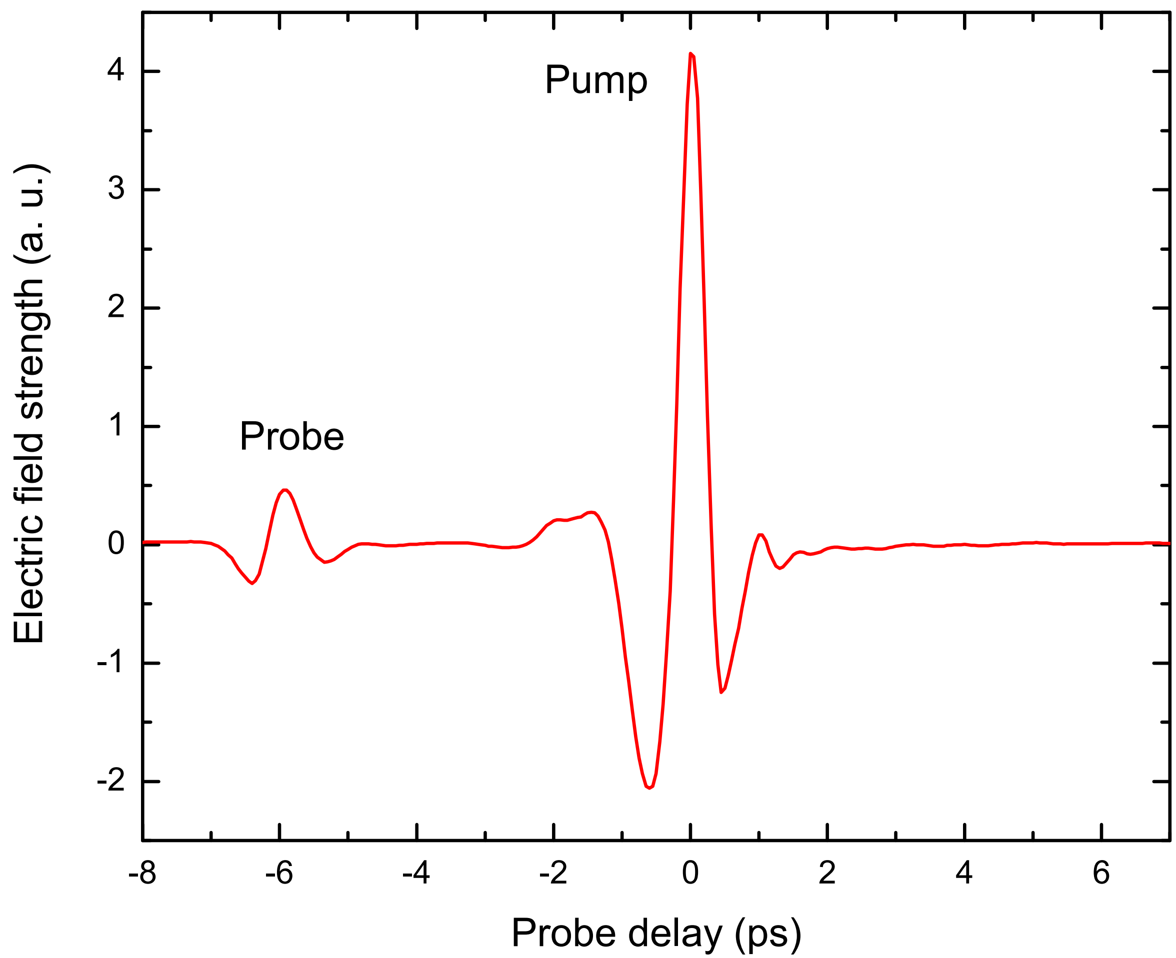

EO readout of transmitted pump & probe fields

Nonlinear THz spectroscopy

Crossed THz pump beams induce anharmonic lattice vibrations

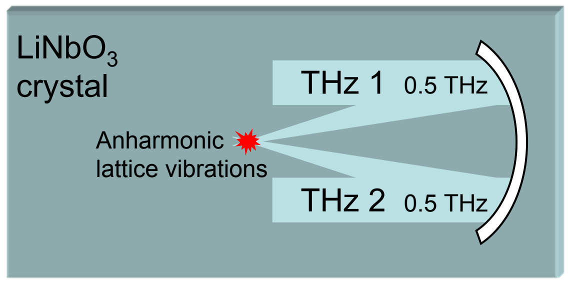

J. Hebling et al., *IEEE J. Sel. Top. QE* **14**, 345 (2008)

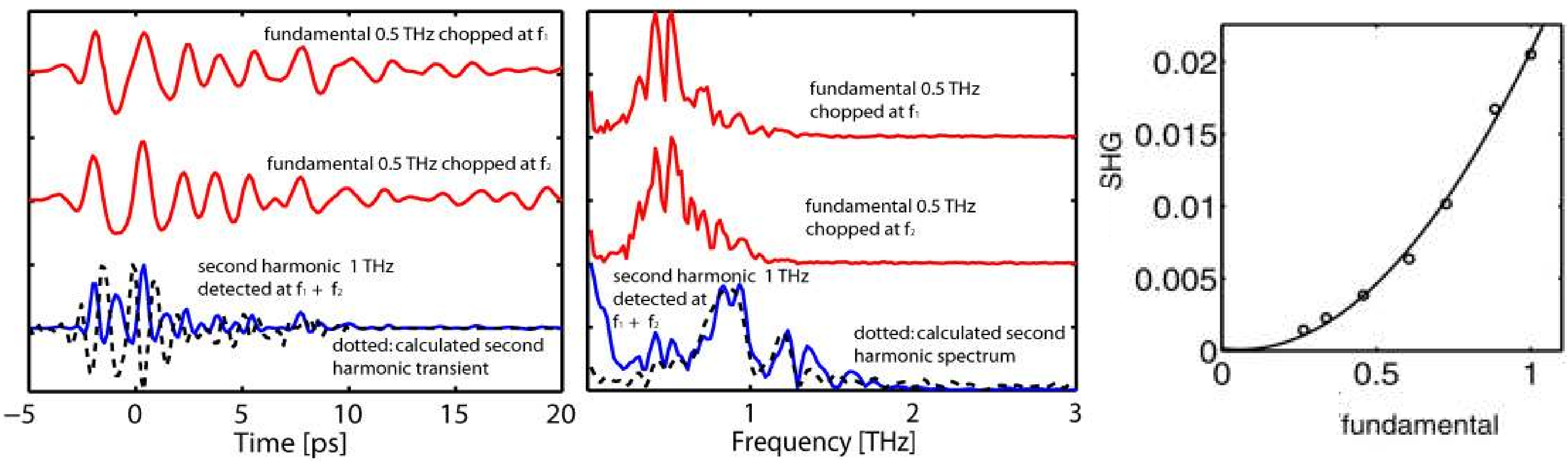

Start toward collective coherent control

Excitation of the soft-mode in $SrTiO_3$

I. Katayama K. Tanaka *et al.*, Phys. Rev. Lett., 108, 097401 (2012)

THEORY

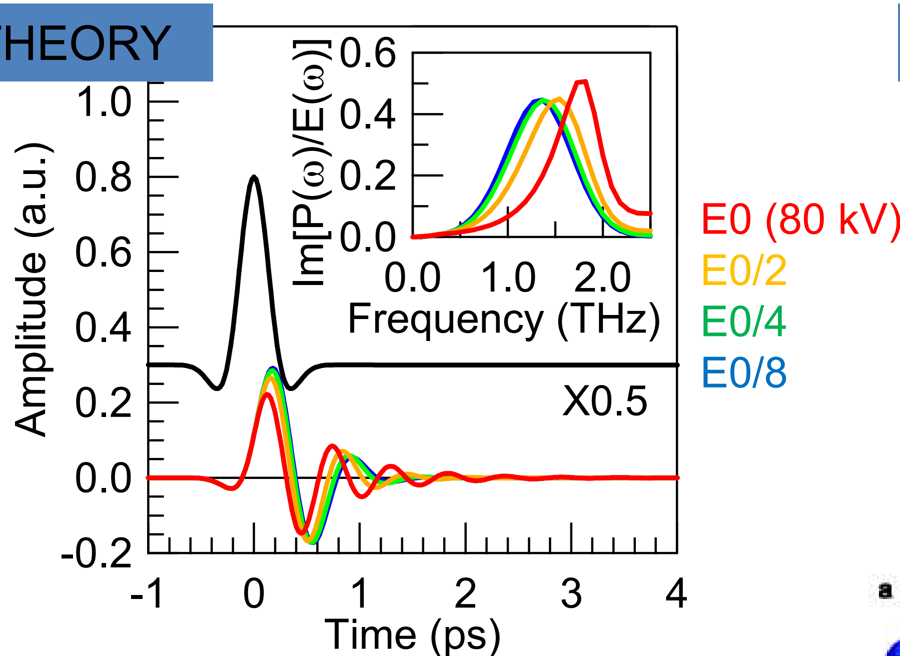

$$\frac{d^2q}{dt^2}+\Gamma\frac{dq}{dt}+\omega_0^2q+aq^3=AE(t)$$

EXPERIMENT

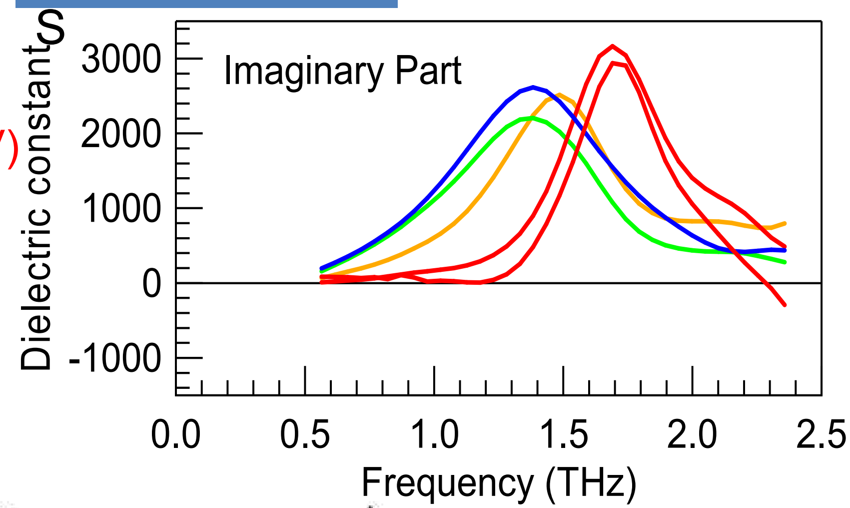

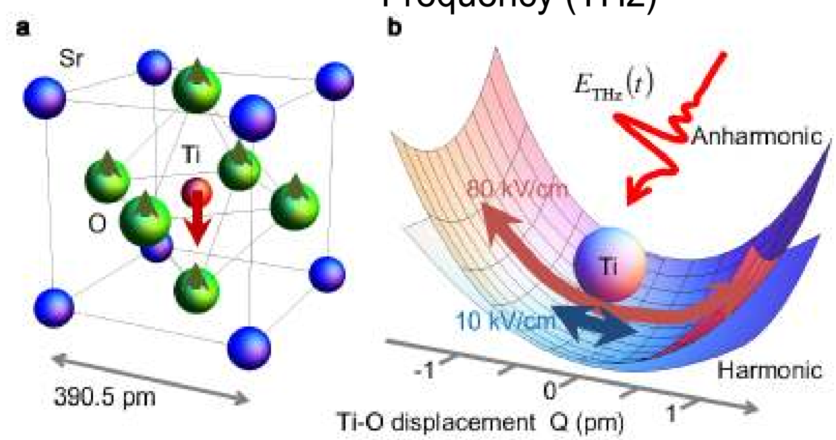

$SrTiO_3$ TFISH detects symmetry loss

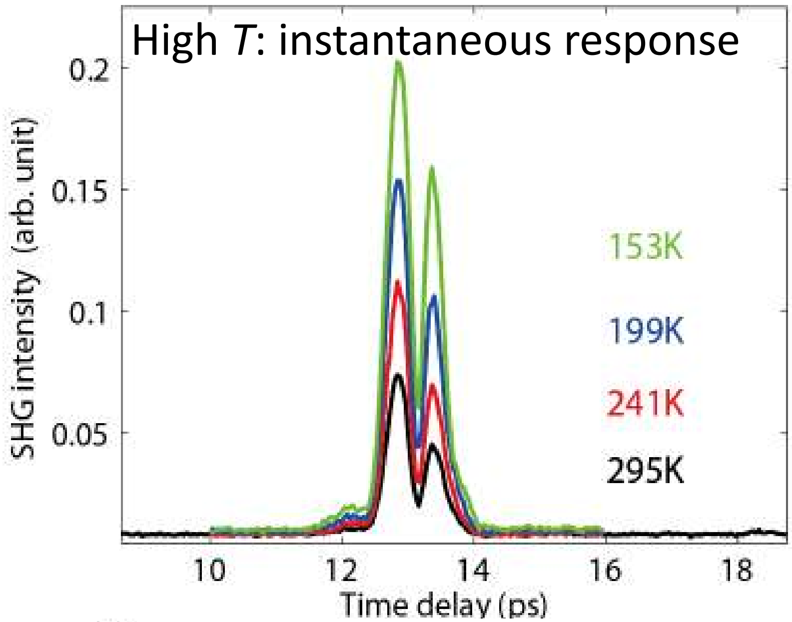

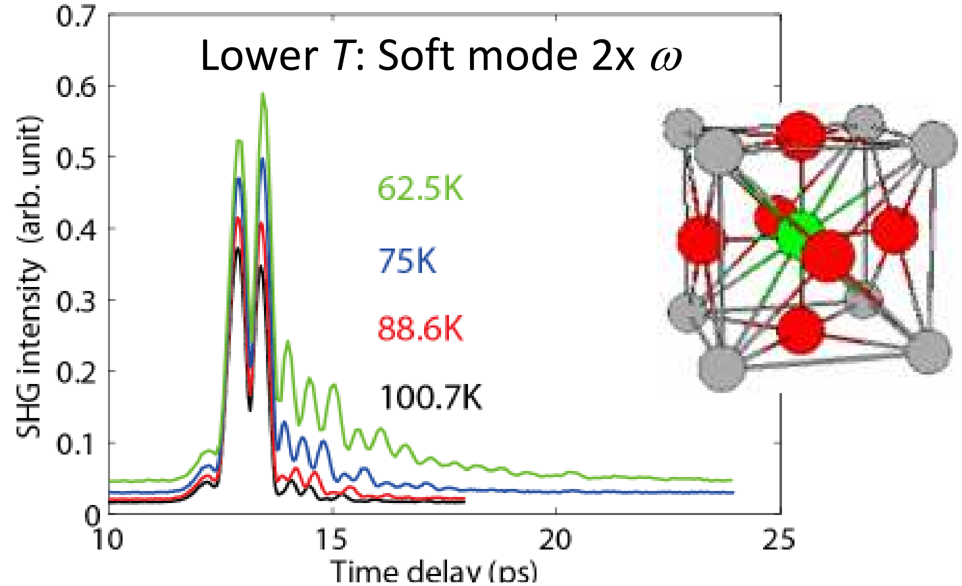

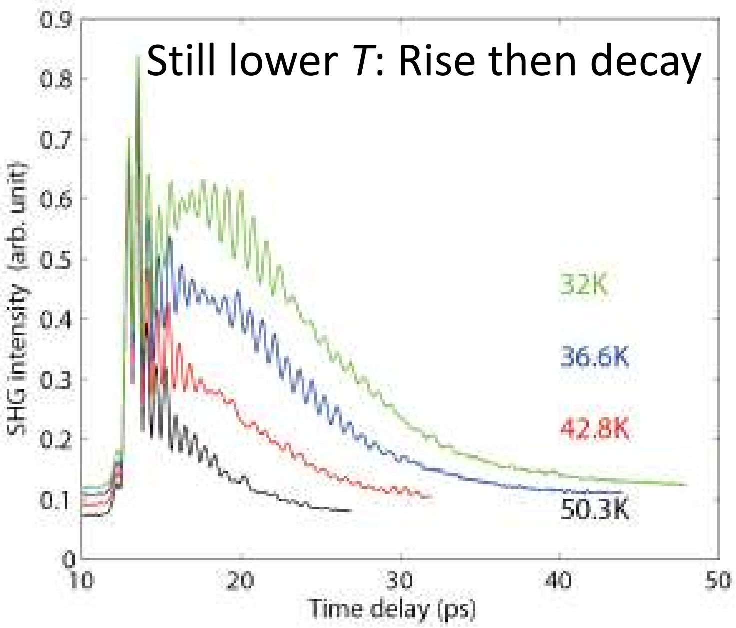

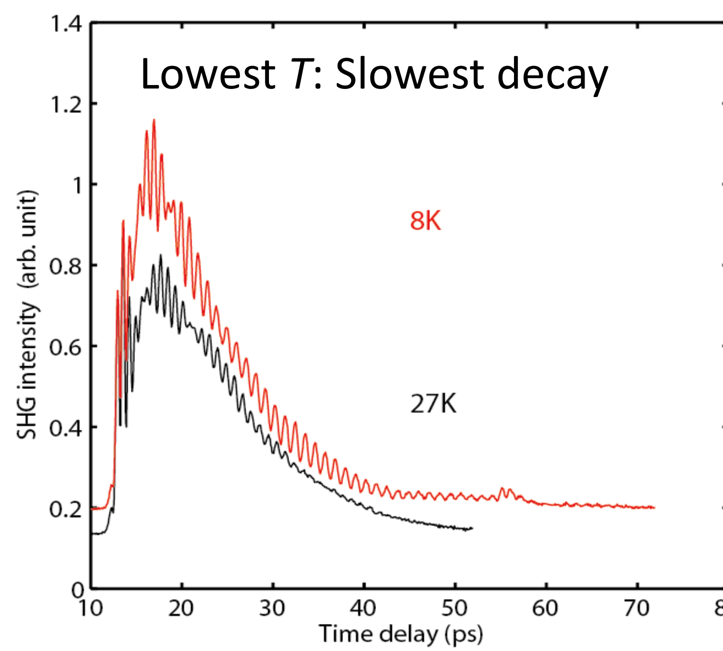

Oscillating & non-oscillating components

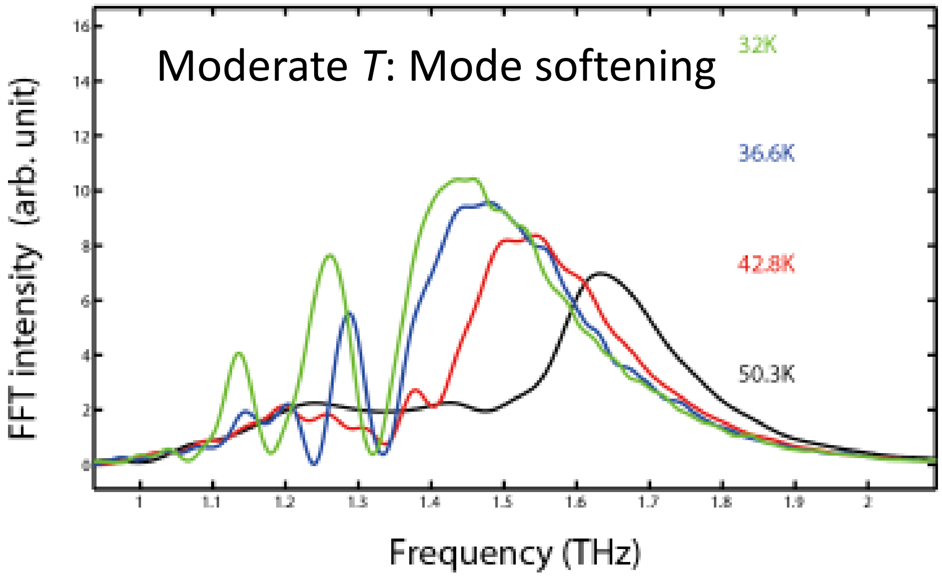

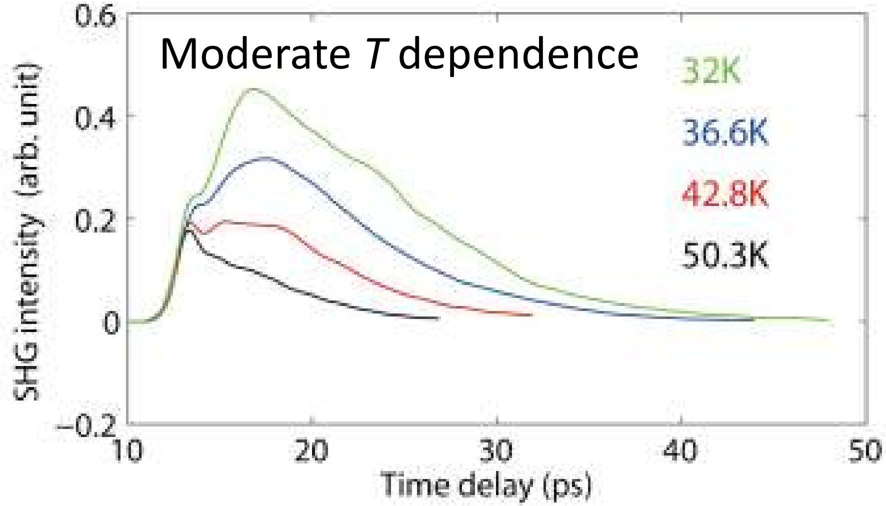

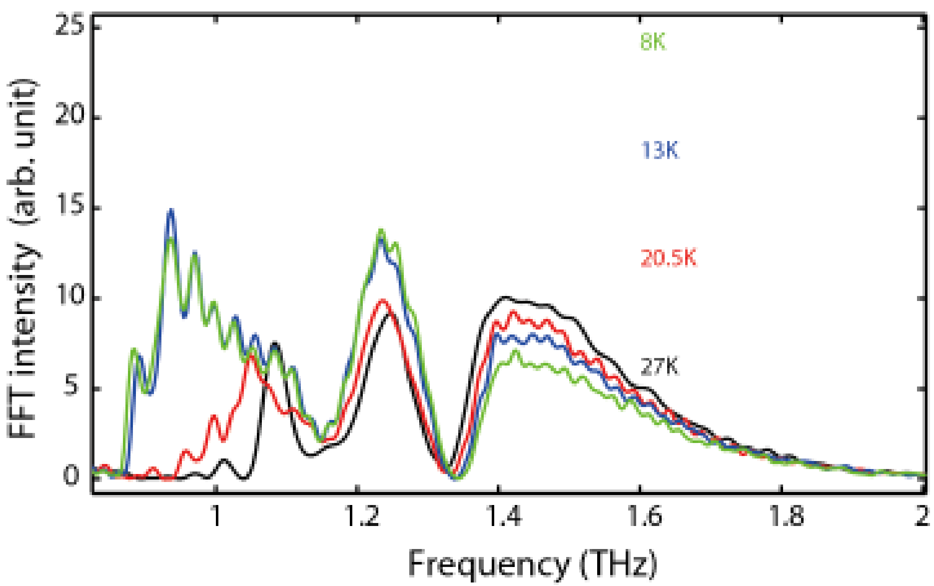

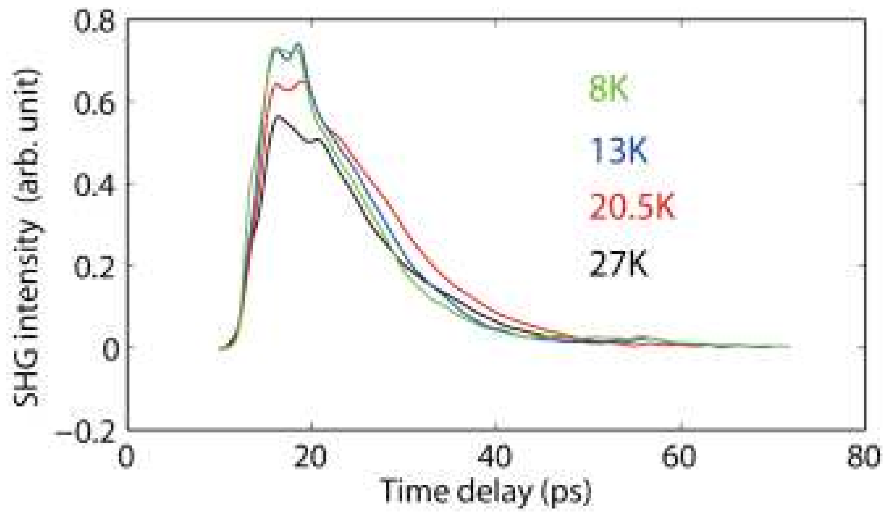

Soft mode & ***polar nanoregion response***

Spectrally integrated THz pump-probe results

Overall hot electron relaxation dynamics

Bulk Ge & GaAs crystals

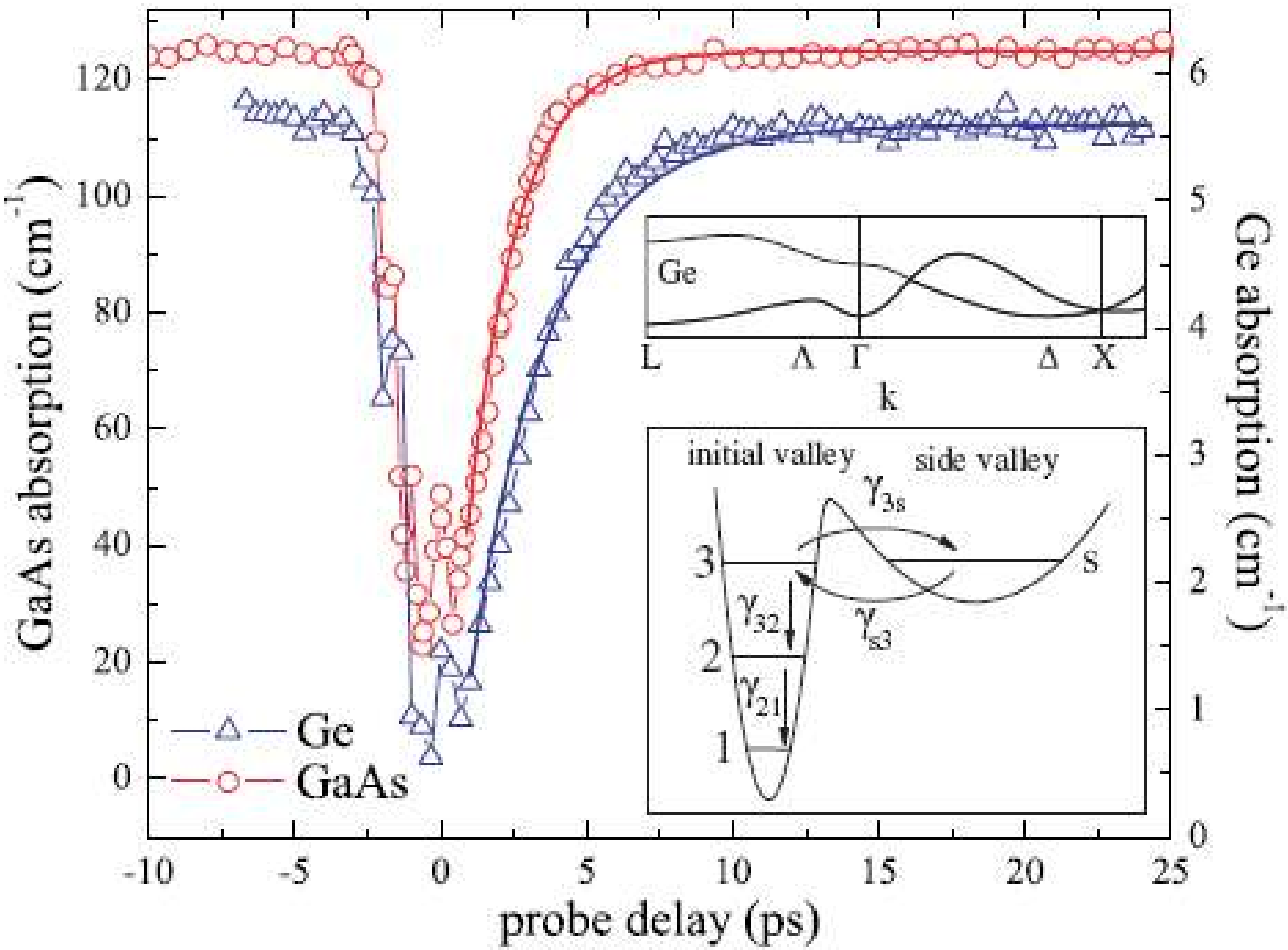

Phys. Rev. B **79**, 161201 (R) (2009)

THz-induced carriers in InSb

THz pump – THz probe electron dynamics

InSb impact ionization & THz-induced tunneling

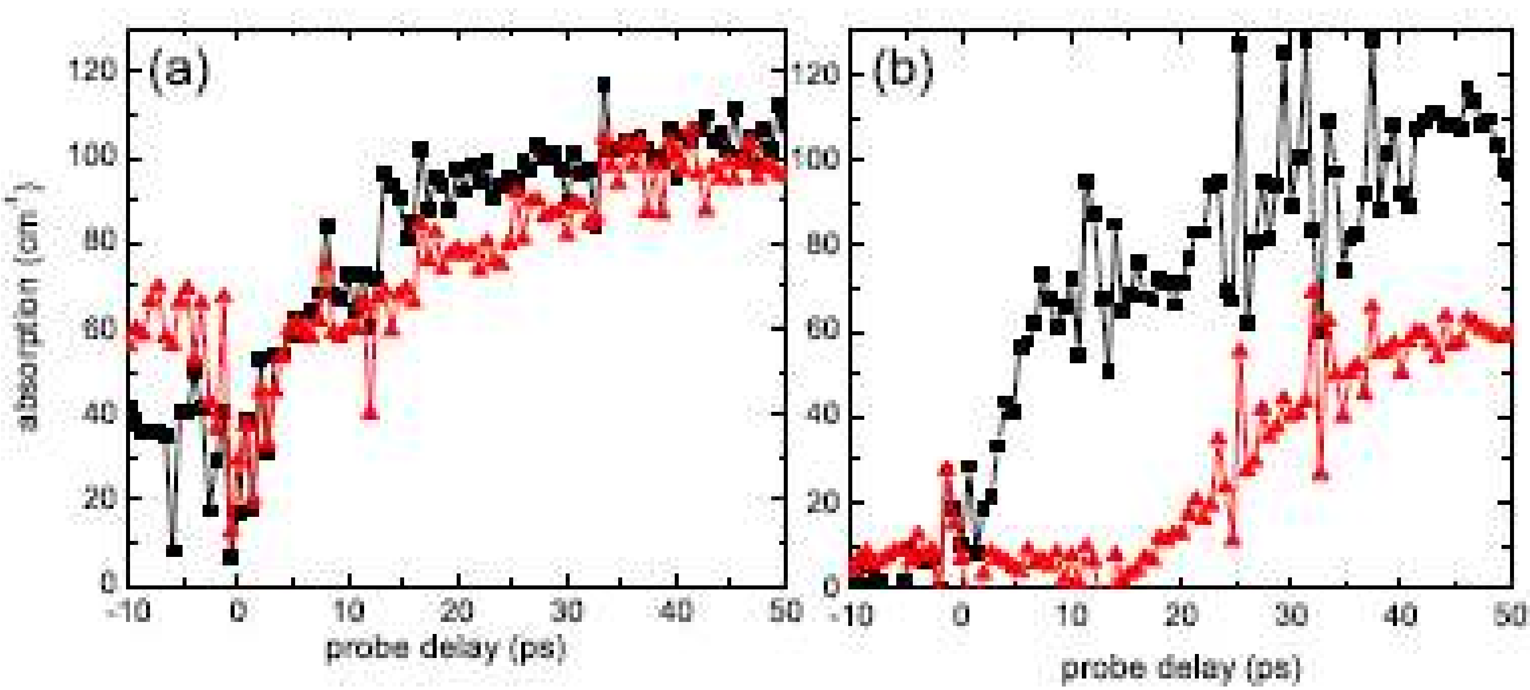

THz fields pull weakly bound electrons out of conduction band

Accelerated carriers ionize additional electrons

THz fields can release weakly bound electrons generally

THz-induced carriers in InSb

THz pump – THz probe electron & lattice dynamics

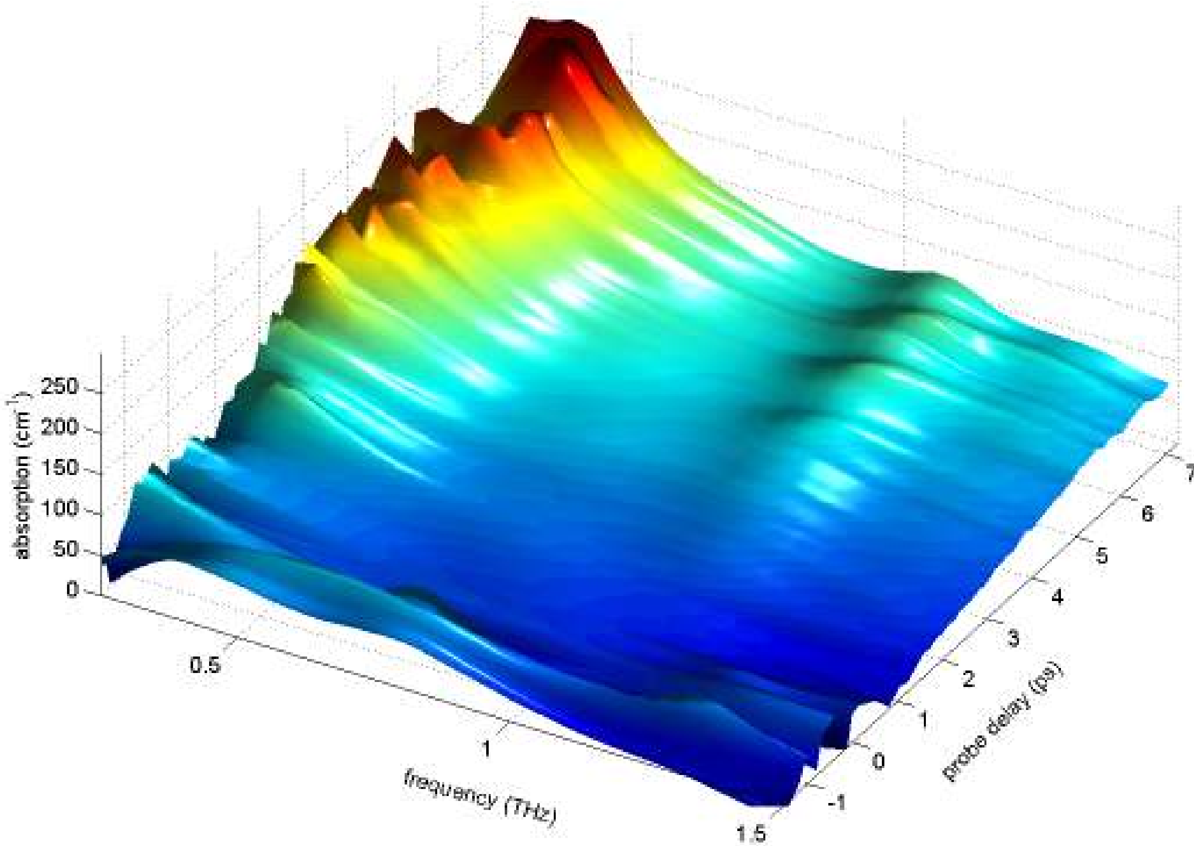

Difference phonon absorption at 1.2 THz due to carrier equilibration with lattice phonons

JOSA B **26**, A29-A34 (2009)

PRB **79**, 161201 (R) (2009)

Temporal and spectral resolution reveal buildup of carriers, relaxation into phonon manifold

Exciton ionization in ZnSe MQWs

H. Hirori, K. Tanaka *et al.*, Phys. Rev. B, 81, 081305(R), 2010

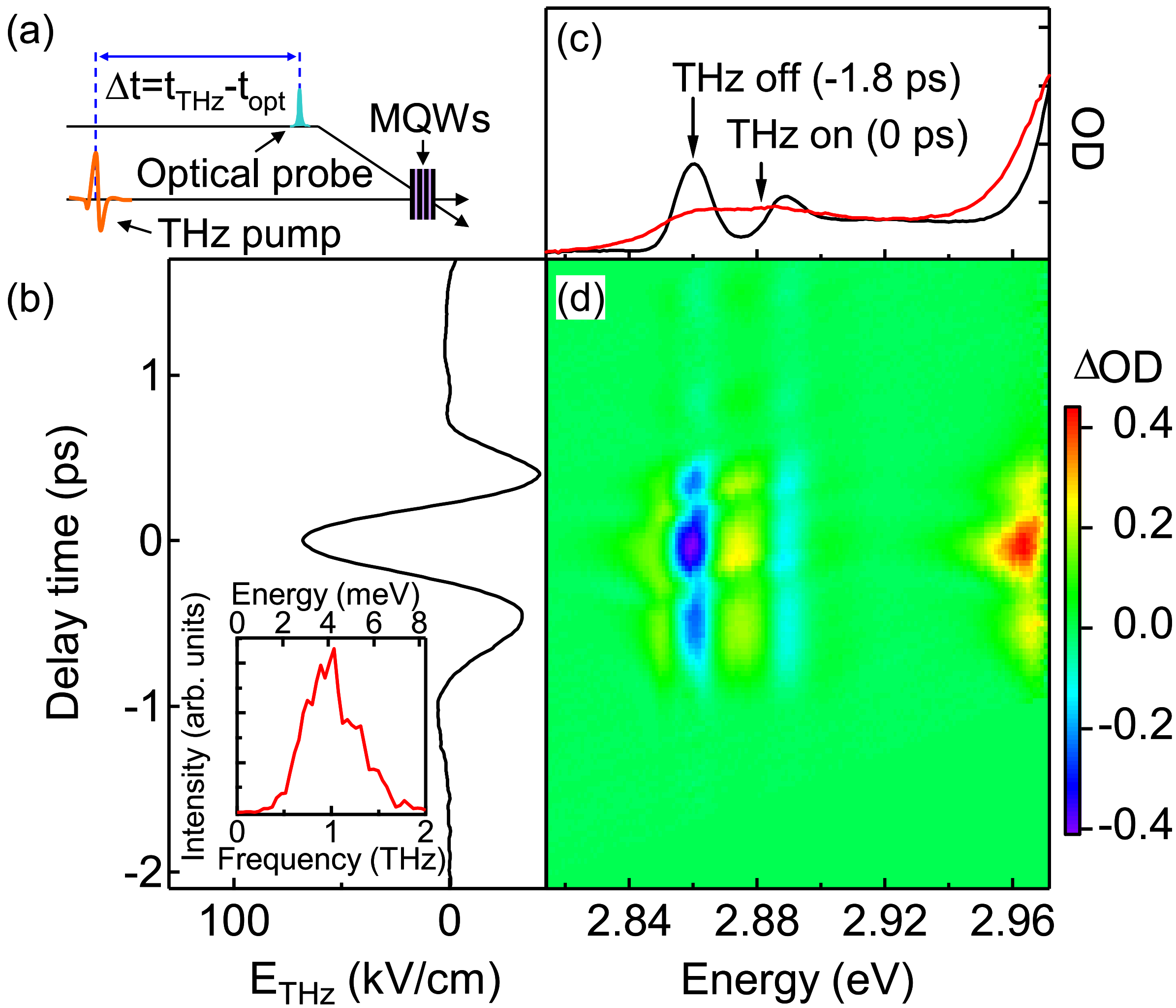

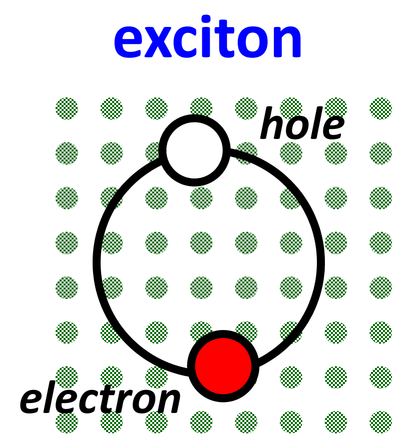

- Field ionization of excitons (instantanious)
- Dynamical Franz-Keldysh effect in band to band transition

Carrier Multiplication in GaAs MQWs

H. Hirori, K. Tanaka *et al.*, Nature Comm. 2, 594, 2011

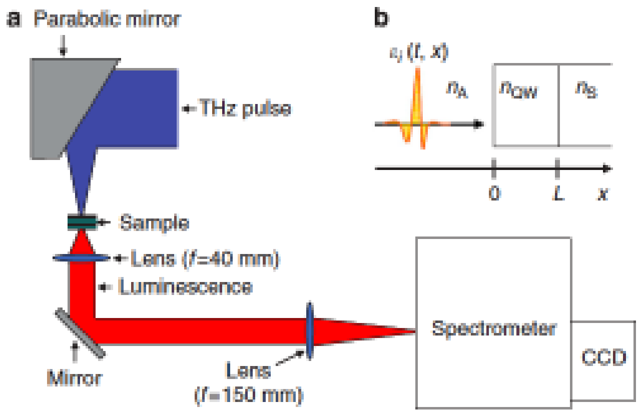

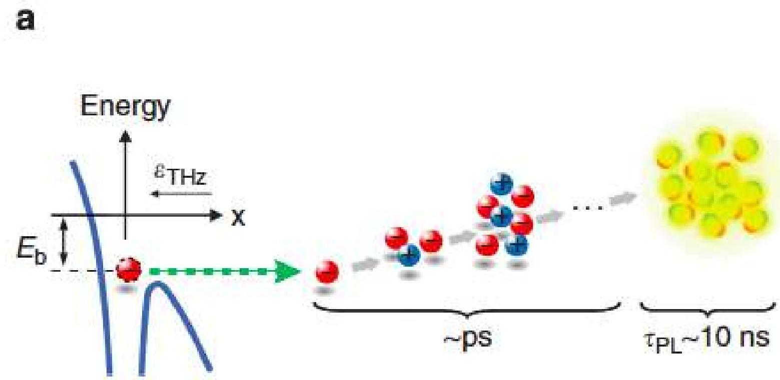

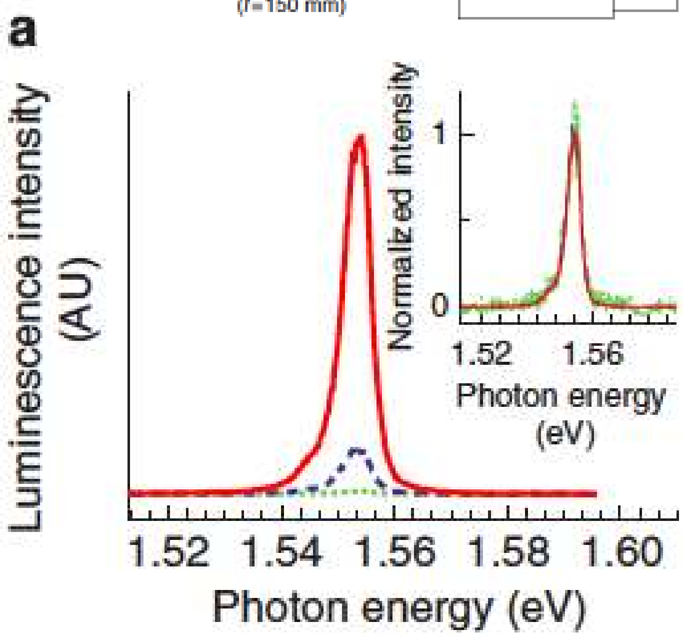

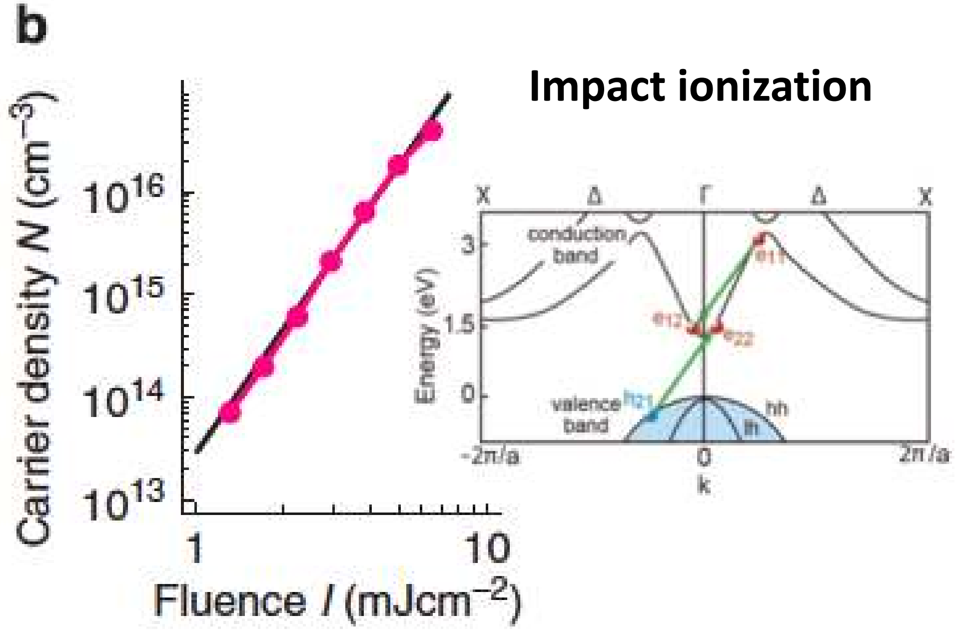

Impact ionization

Graphene

Exfoliated Graphene

- Linear electronic dispersion
- Massless (or very low mass) carriers
- High mobility ($>10^4$ $cm^2V^{-1}s^{-1}$)
- Small size (due to difficulties in exfoliation technique)
- Low intrinsic carrier concentration

CVD graphene

- Linear electronic dispersion
- Massless (or very low mass) carriers
- Limited mobility (~2500 $cm^2V^{-1}s^{-1}$)
- Large sizes (macroscopic meter size sheets!)
- Fairly high doping from etching and possibly impurities

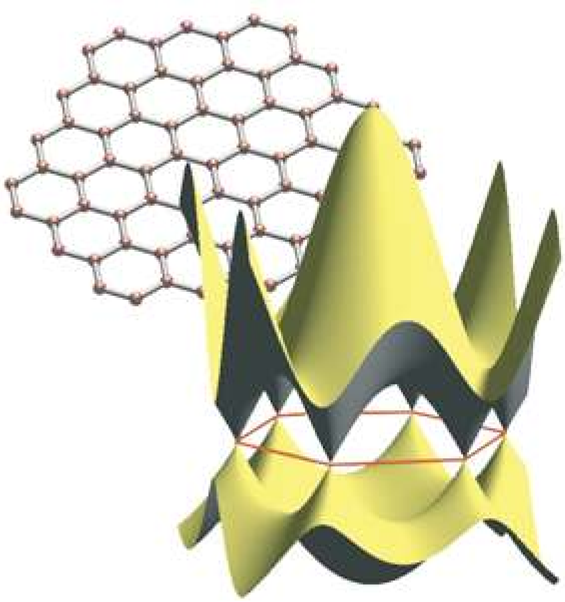

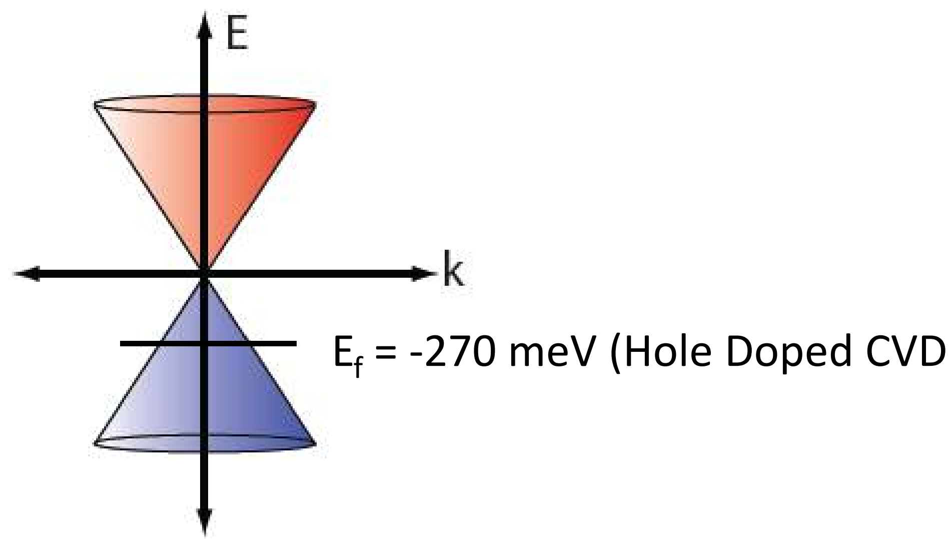

Nonlinear Transmission

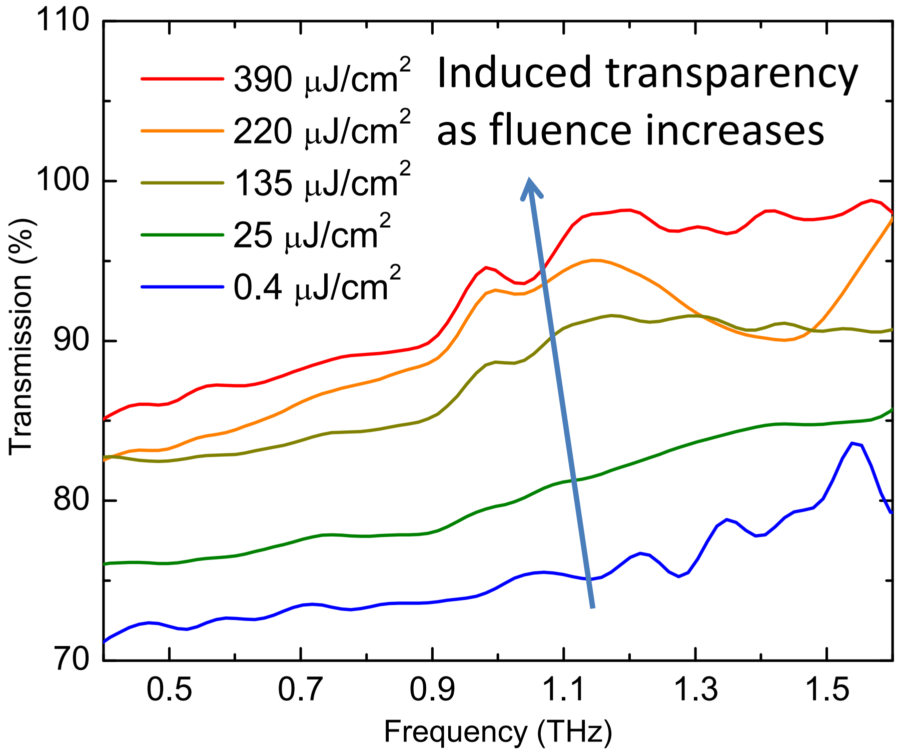

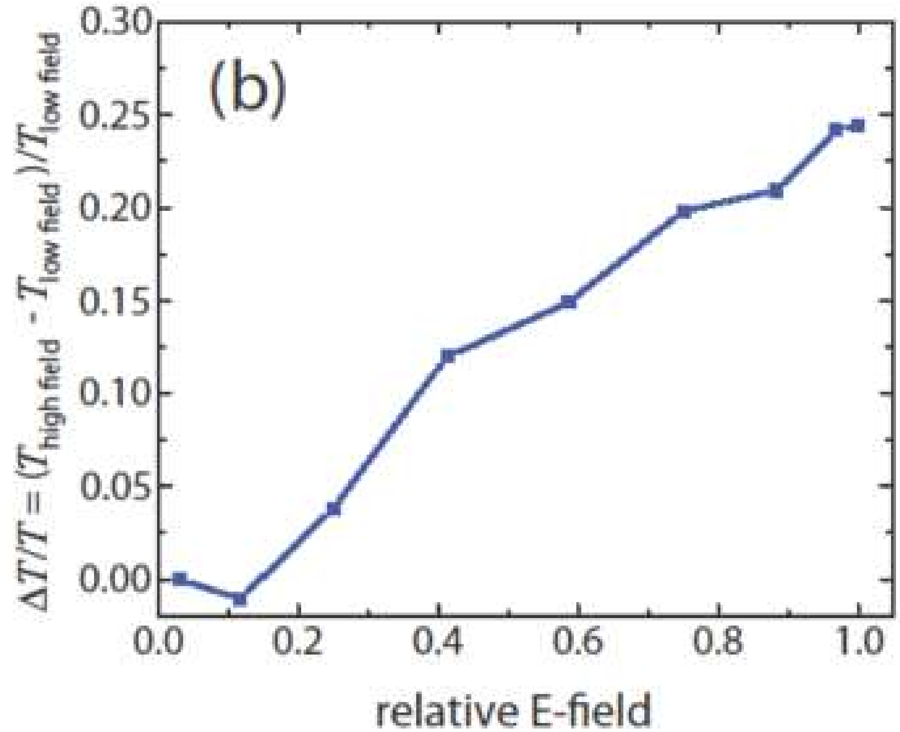

Intraband Drude conductivity

$$\frac{\sigma_1(\omega)}{\sigma_Q} = \frac{8k_B T}{\pi\hbar}\ln(e^{-E_F^\epsilon/2k_BT} + e^{E_F^\epsilon/2k_BT})\frac{1}{\omega^2\tau + 1/\tau}$$

• When Temp increases, weak effects on conductivity (increase) and transmission (decrease)

•When τ decreases, strong effects on conductivity (decreases) and transmission (increases) – Suggested by theoretical results from Bao

arXiv:1101.4985v1

Nonlinear THz Responses in CVD Graphene

Hole-doped graphene

Saturation of THz absorption

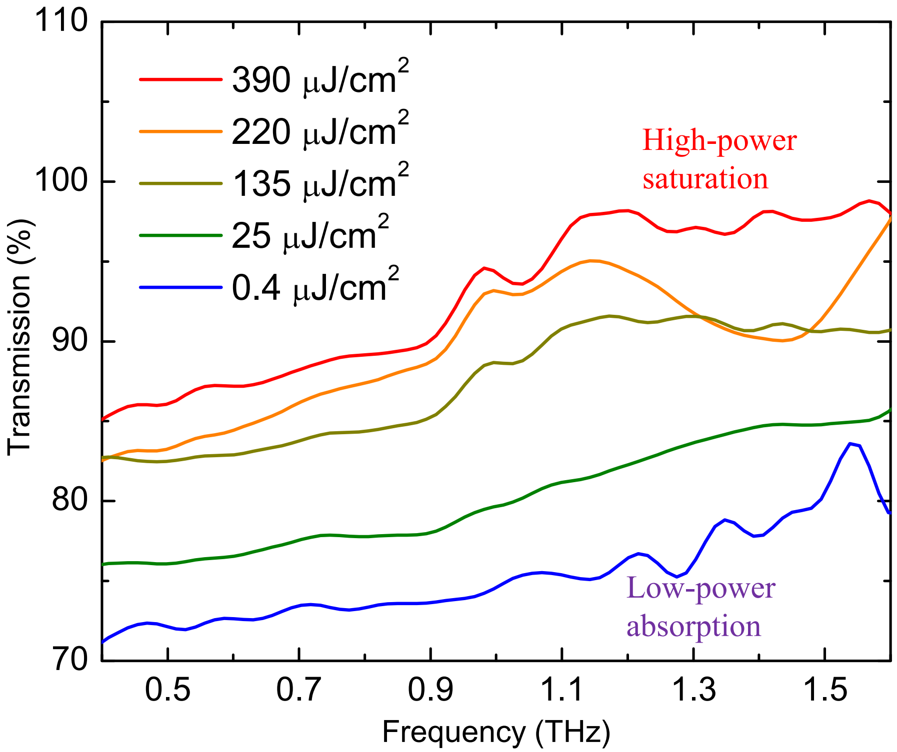

Time-dependent absorption recovery

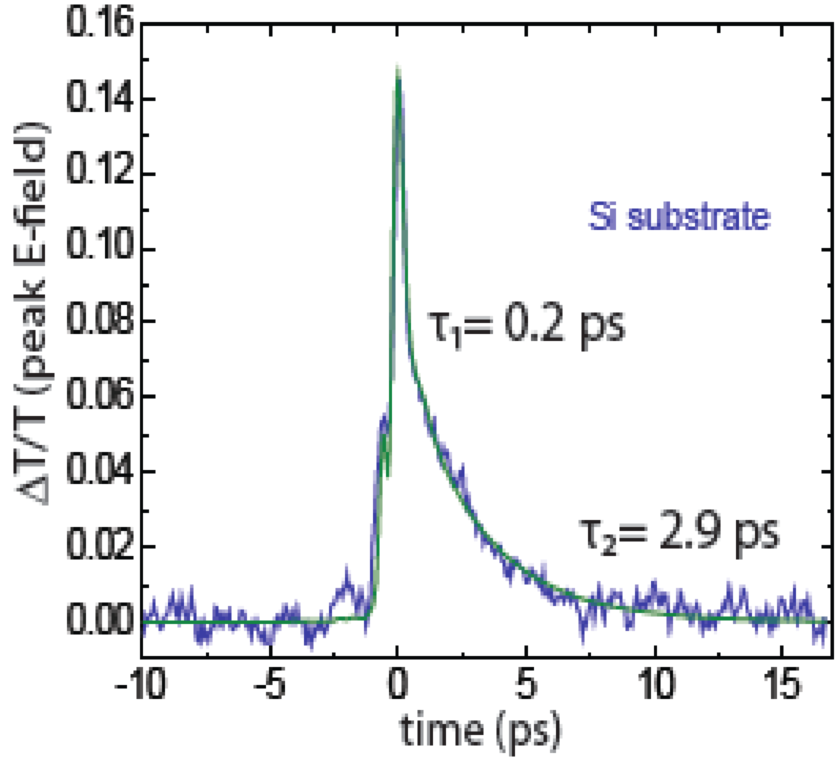

THz field drives carriers & impact ionization

arXiv:1101.4985v1 {cond-mat.mtrl.-sci] 26 Jan 2011

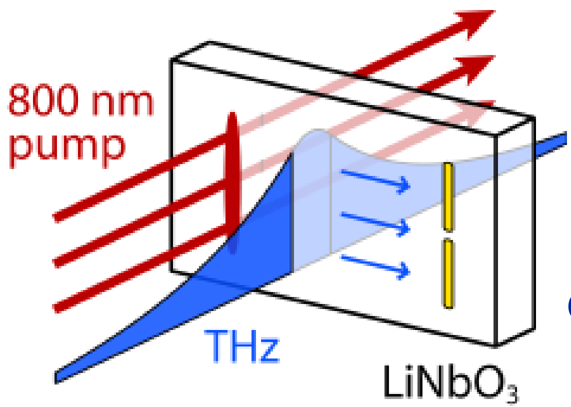

THz dipole antenna

Collaboration w/ R. Averitt group, Boston U

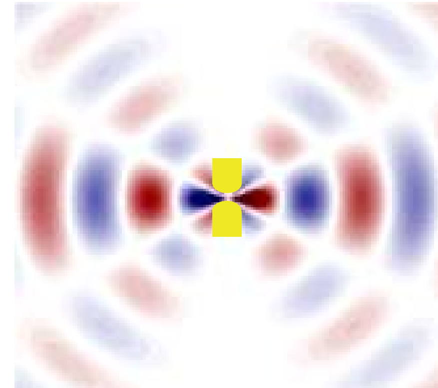

530 GHz, on resonance

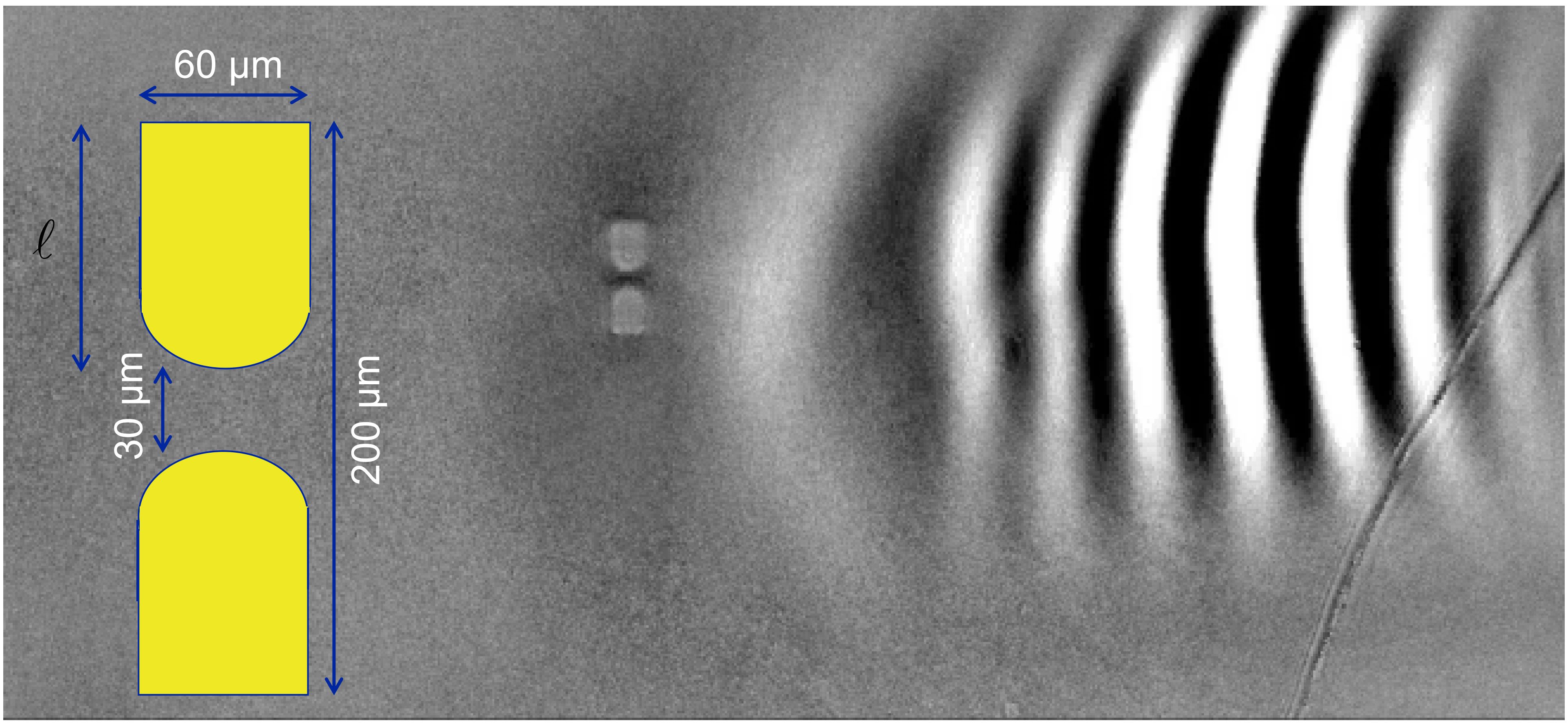

THz dipole antenna
Low-order mode
Field enhancement

C.A. Werley et al, *Optics Express* **20**, 8551-8567 (2012)

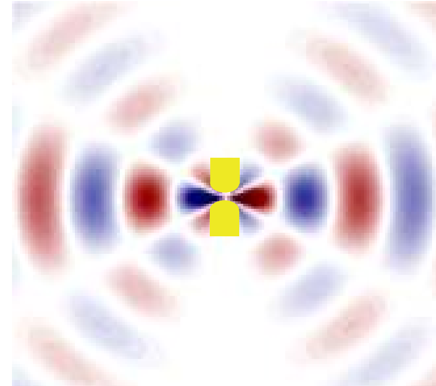

530 GHz, on resonance

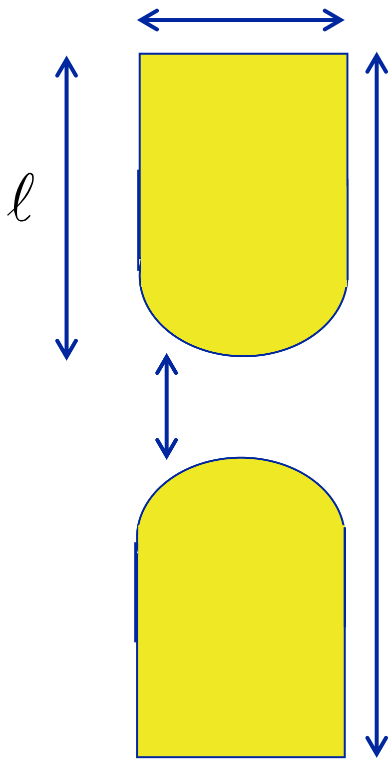

Nano-gap THz field enhancement: work by Dai-Sik Kim and by Thomas Feurer

Metamaterials: Tailored electromagnetic responses

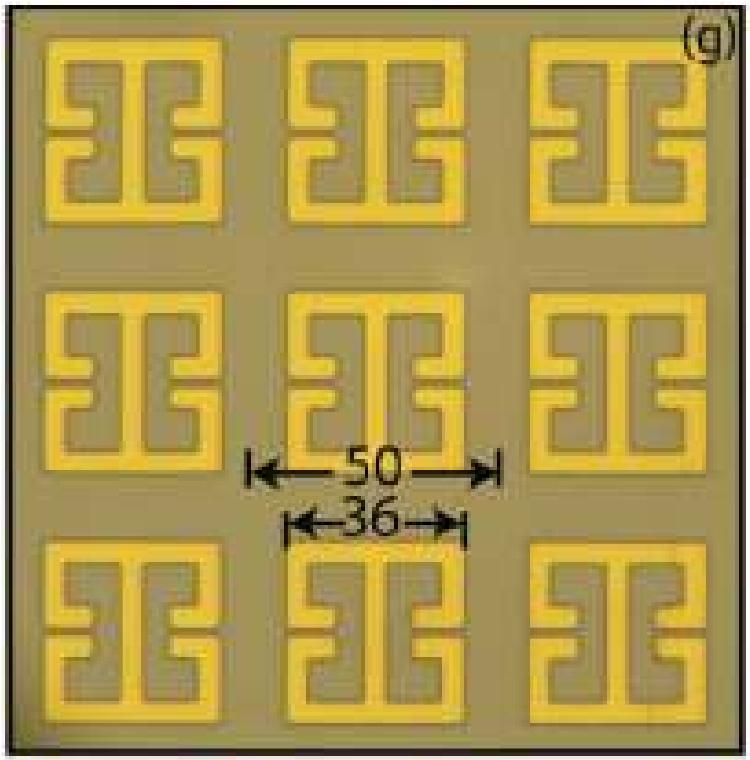

- Engineered resonant structures
- Specific EM responses
- Depends strongly on materials used

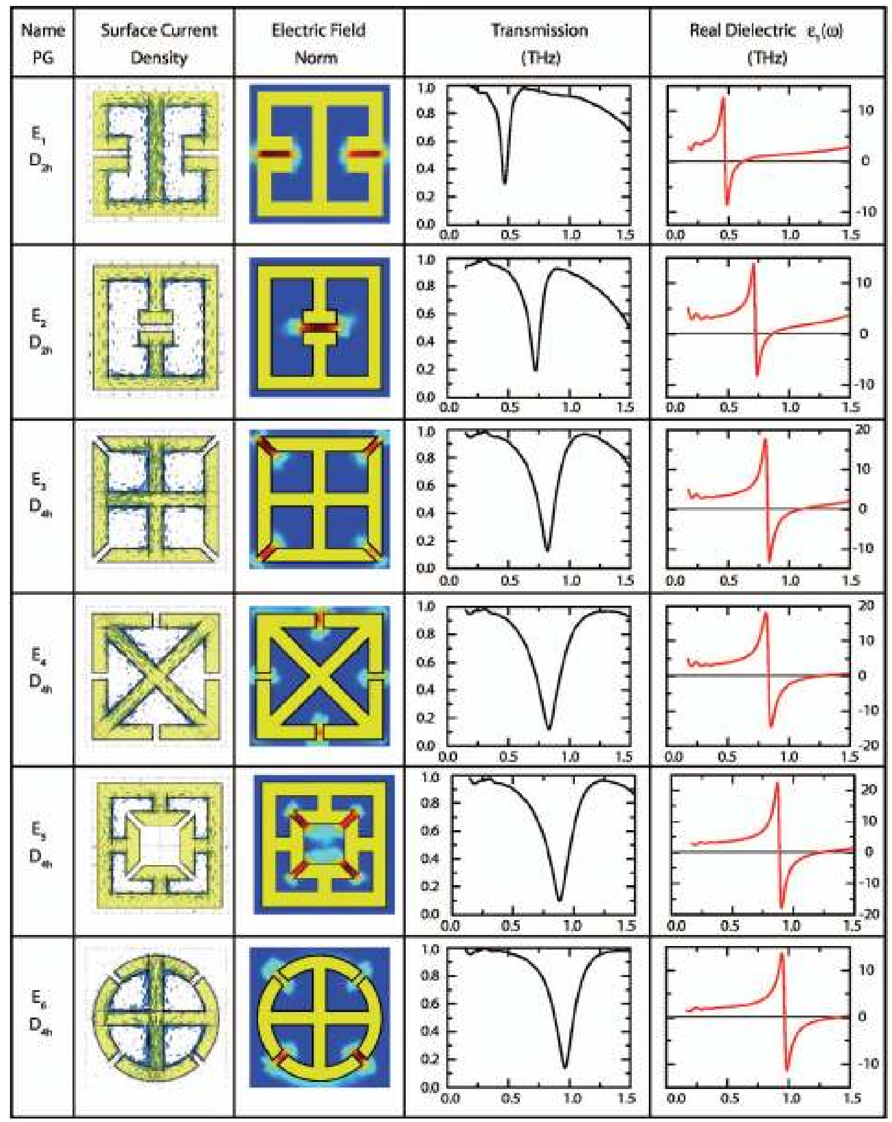

Padilla, et. al. PRB 75, 041102® (2007)

Enhancing field strength with metamaterials

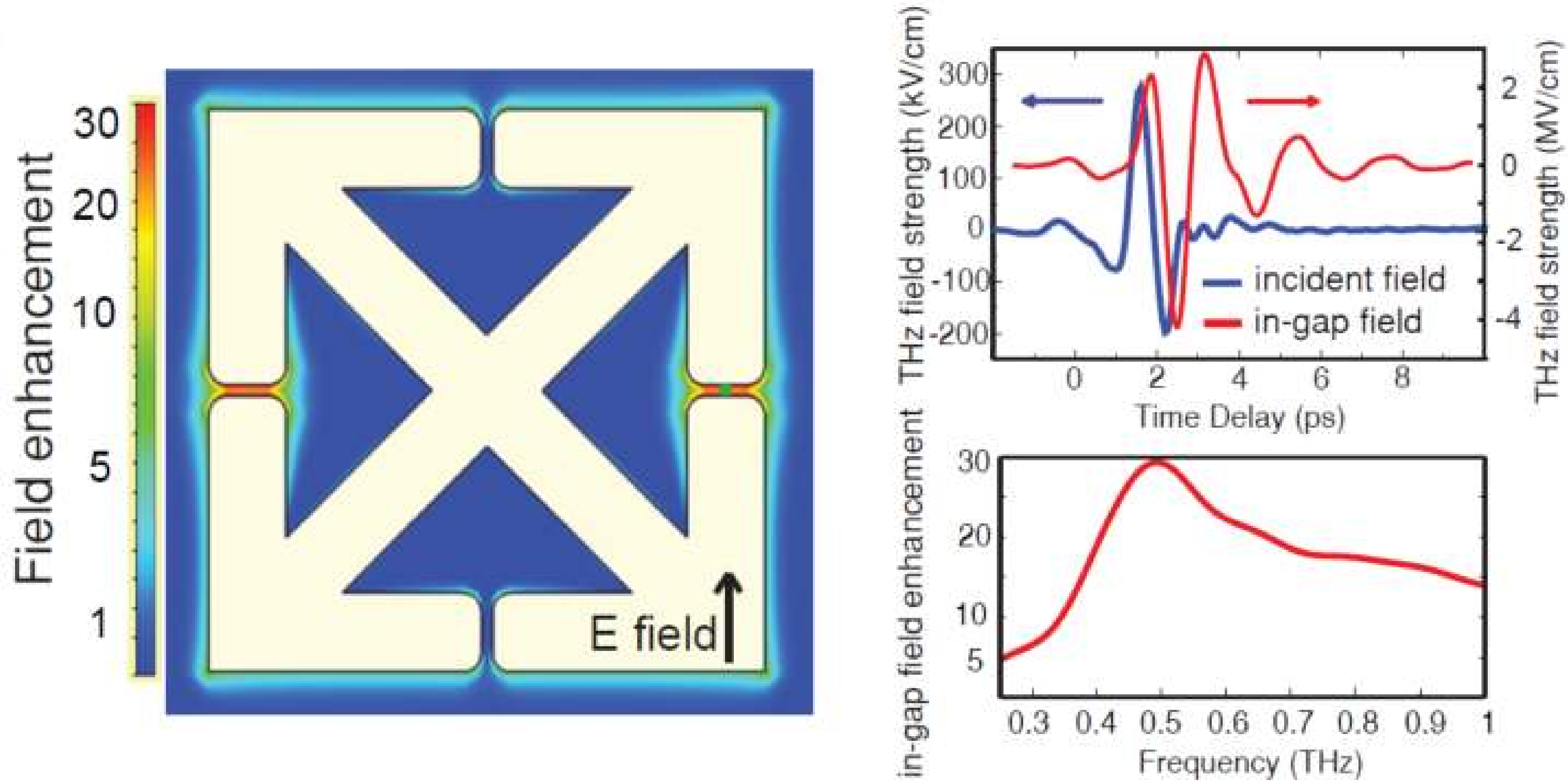

Metamaterial responses are highly sensitive to the substrate

Nonlinear metamaterial responses in n-doped GaAs: Electron acceleration at moderate fields

n_e = 1 x 10^{16} cm^{-3}
No metamaterial response *in unexcited system* due to substrate conductivity σ

THz excitation reduces σ
MM resonance appears!

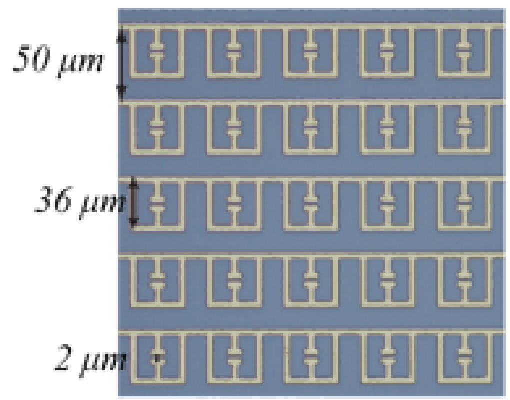

Unexcited system

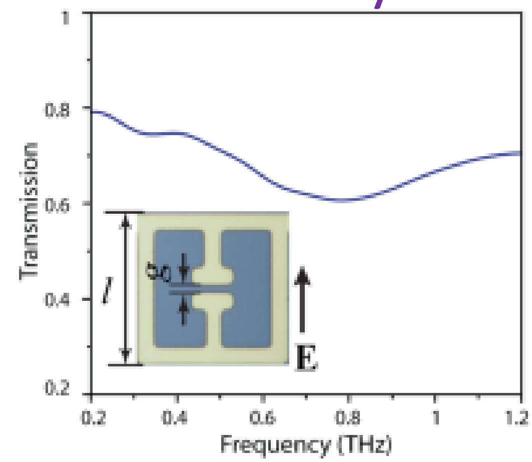

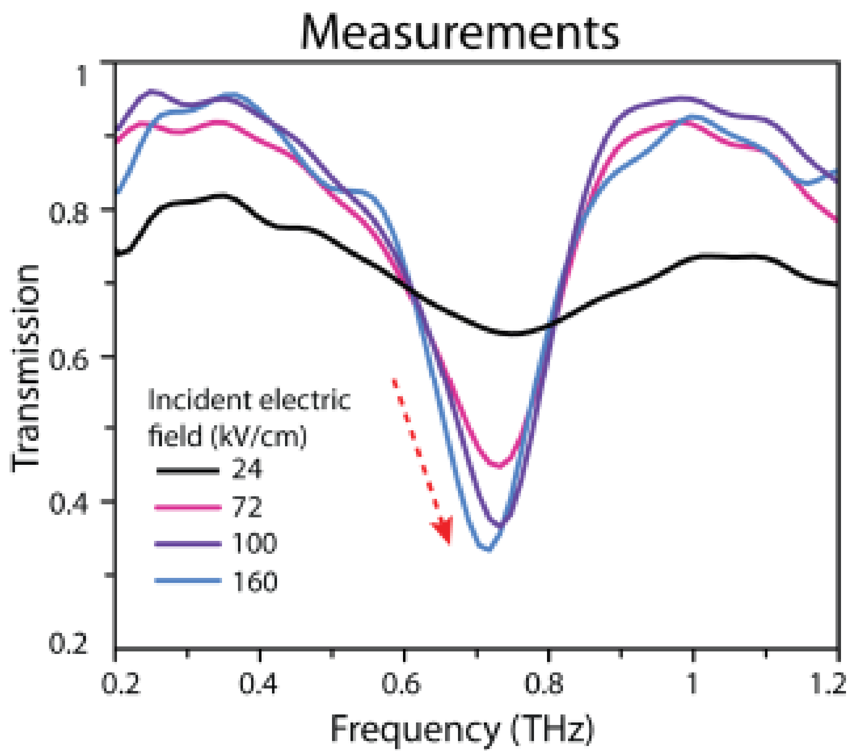

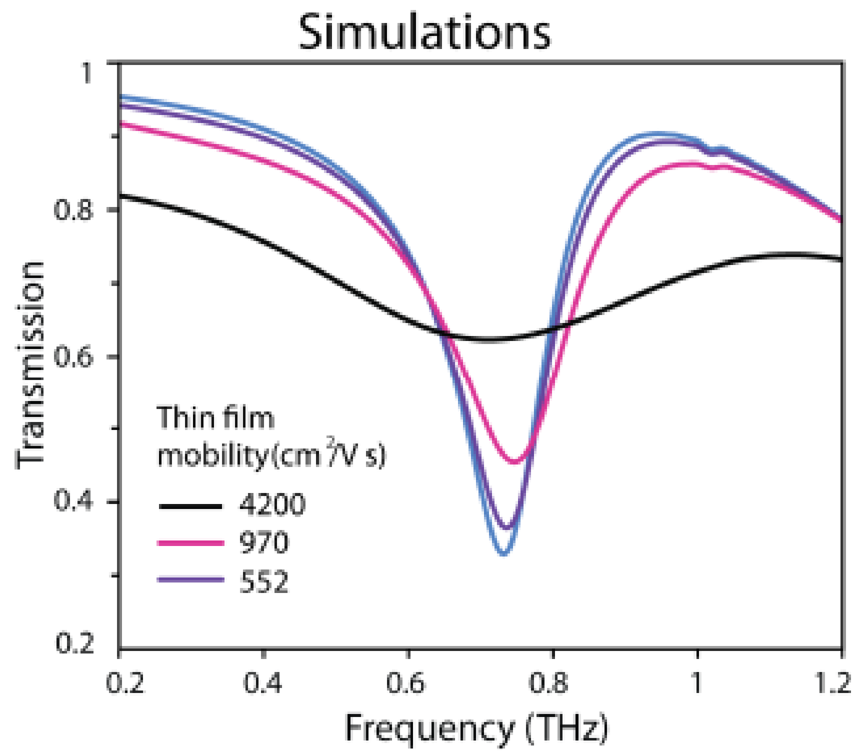

Nonlinear metamaterial responses in n-doped GaAs: Impact ionization at high fields

Strong THz field is enhanced at induced MM resonance!
MV/cm fields $\Rightarrow$ impact ionization $\Rightarrow$ increases σ
MM resonance is suppressed!

Measurements

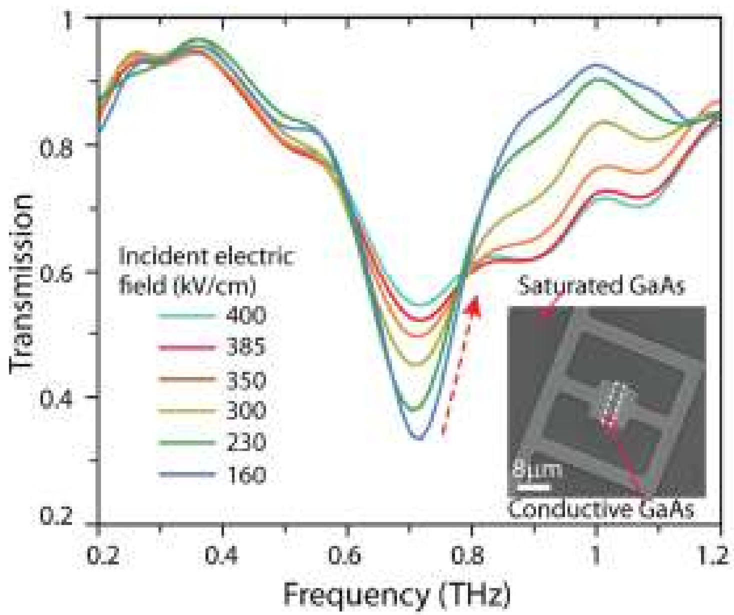

Simulations

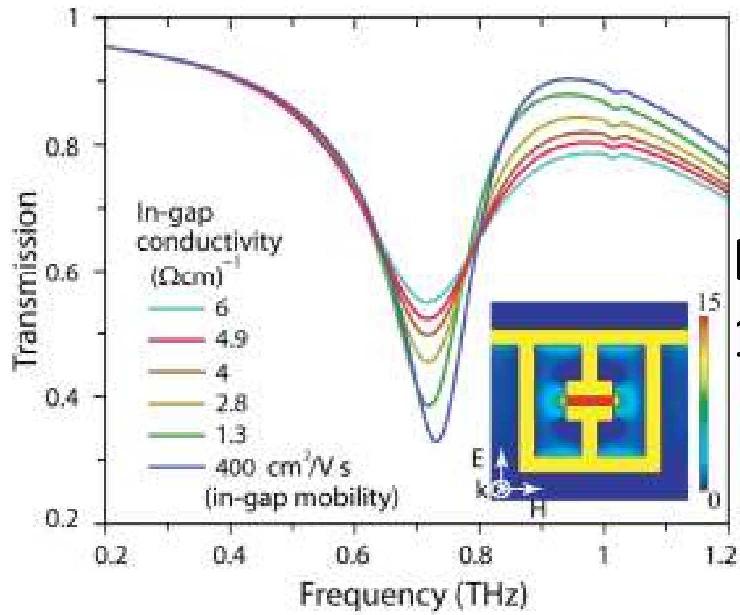

E_g = 1.4 eV
1 THz = 4 meV

Metamaterial response enhances THz field and sensitizes THz measurement

Nonlinear metamaterial responses in SI GaAs: Tunneling & impact ionization increase σ

$n_e = 2 \times 10^6\ cm^{-3}$
Metamaterial response in unexcited system due to low substrate conductivity σ

Strong THz field is enhanced
MV/cm fields $\Rightarrow$ impact ionization
$\Rightarrow$ increases σ by 10^8!
MM resonance is suppressed!

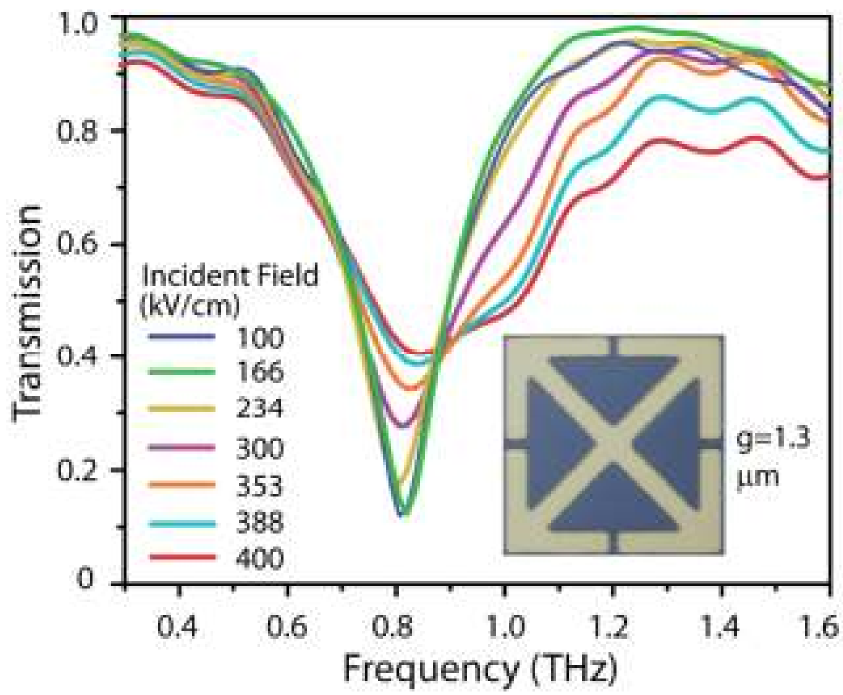

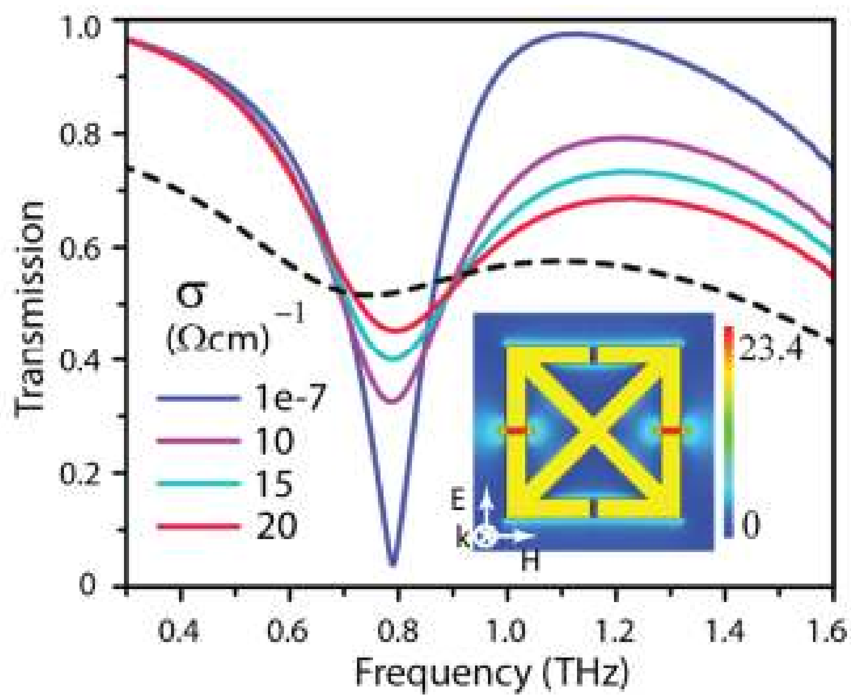

Huge conductivity change suggests THz sensing applications!

THz-induced damage in GaAs

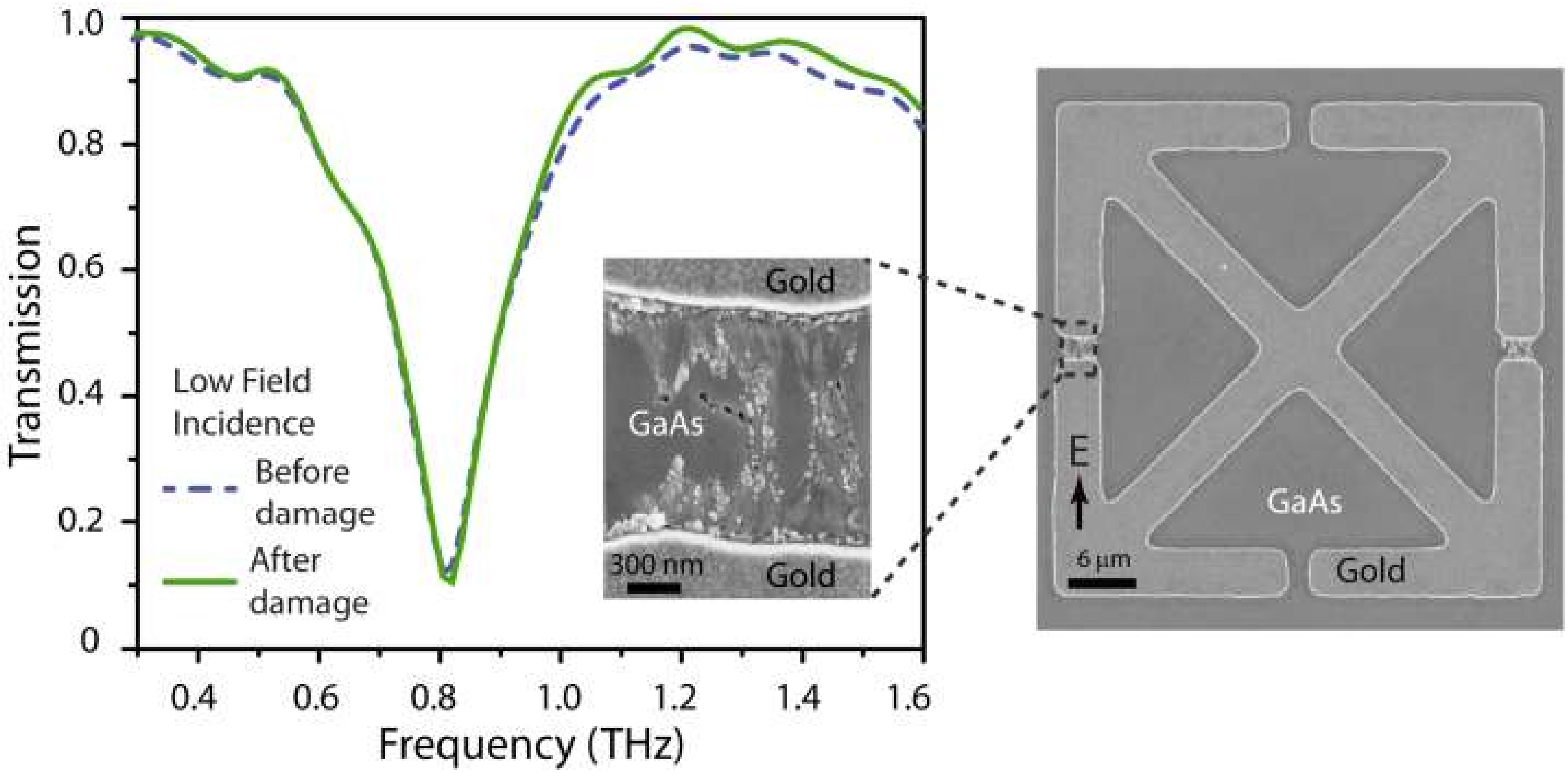

Damage along field lines

Pattern resembles dielectric breakdown

Multielement Detector on GaAs

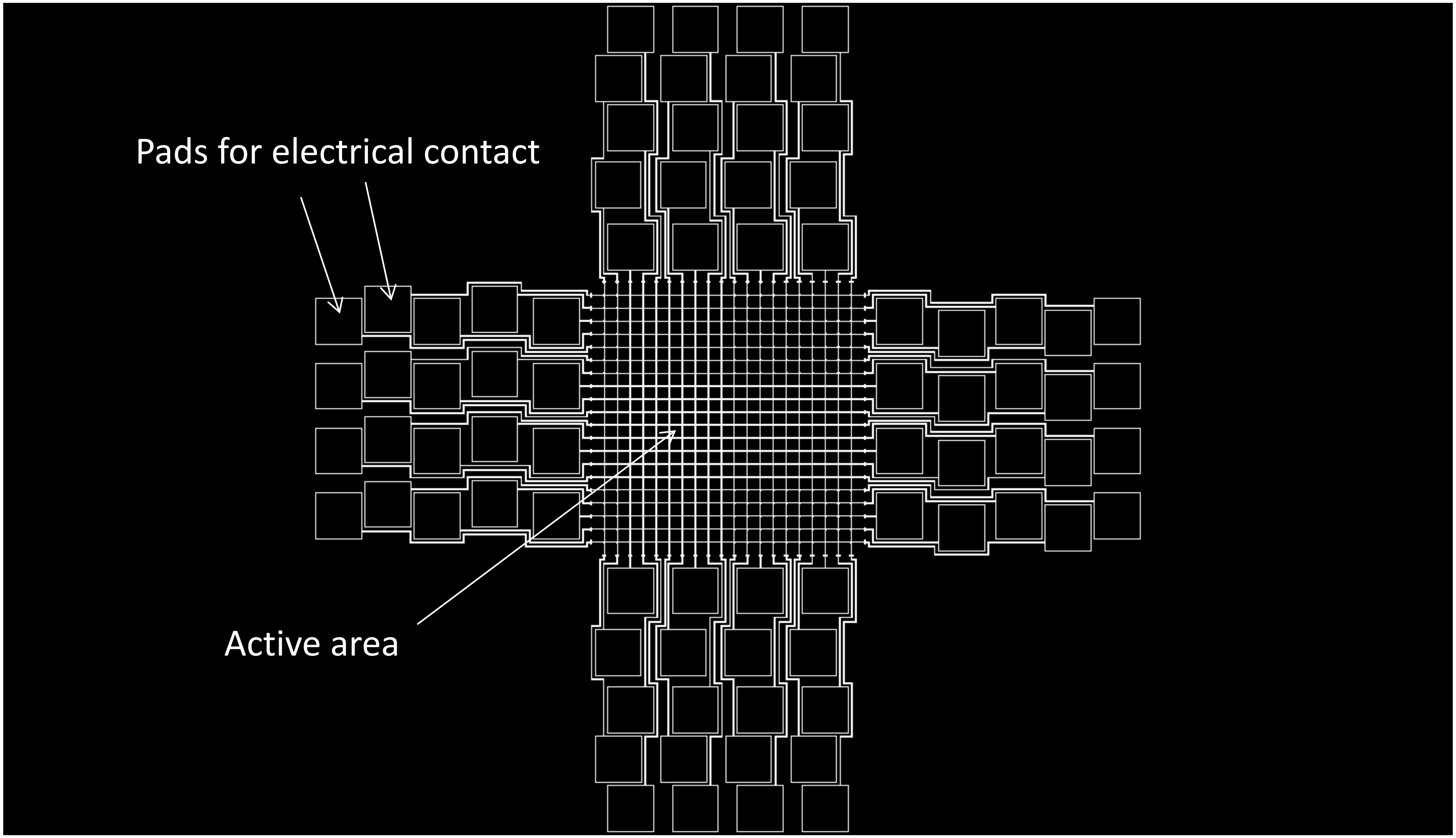

Multielement GaAs Detector Data (for a single element)

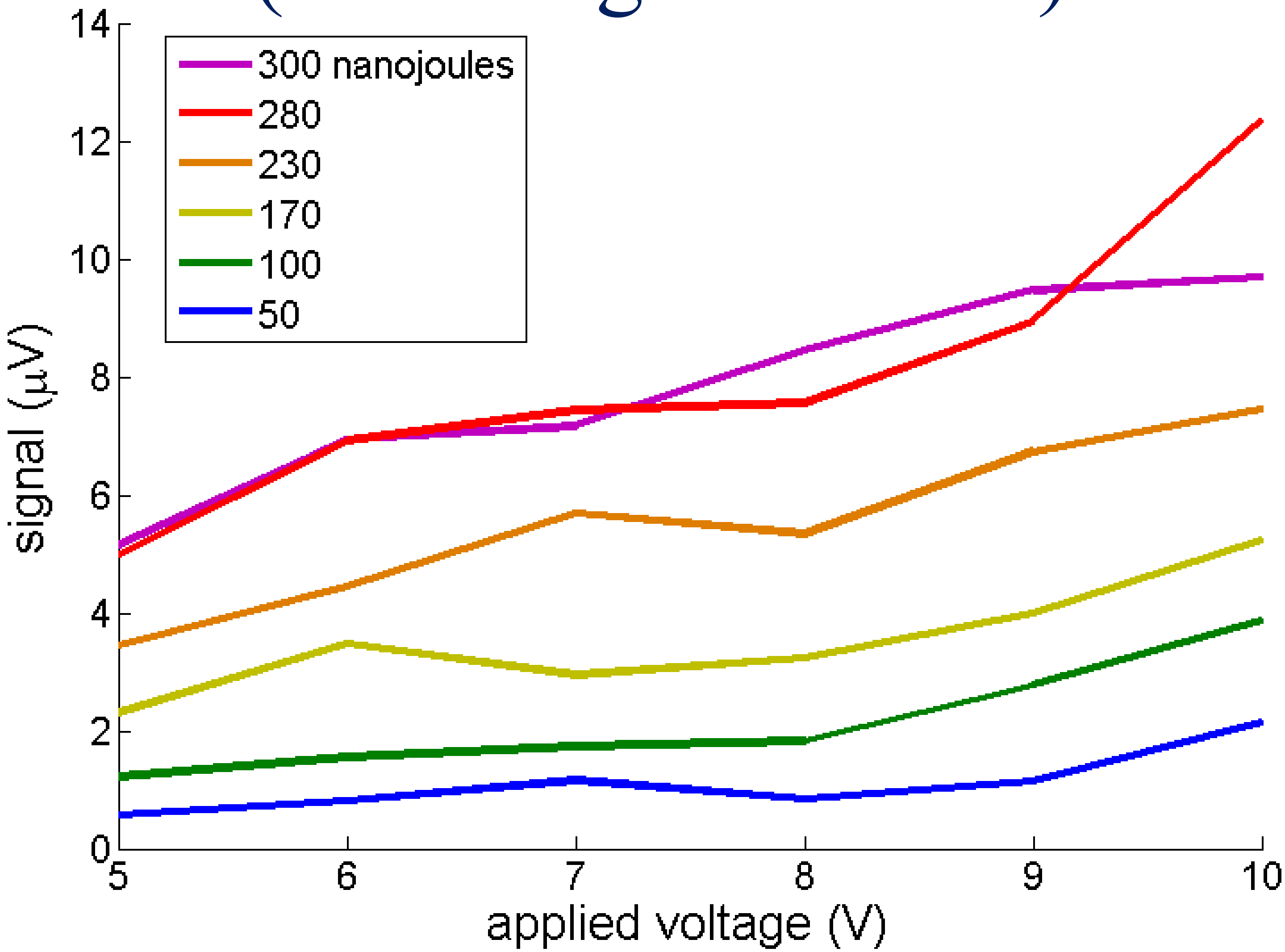

Multielement GaAs Detector Data (for a single element)

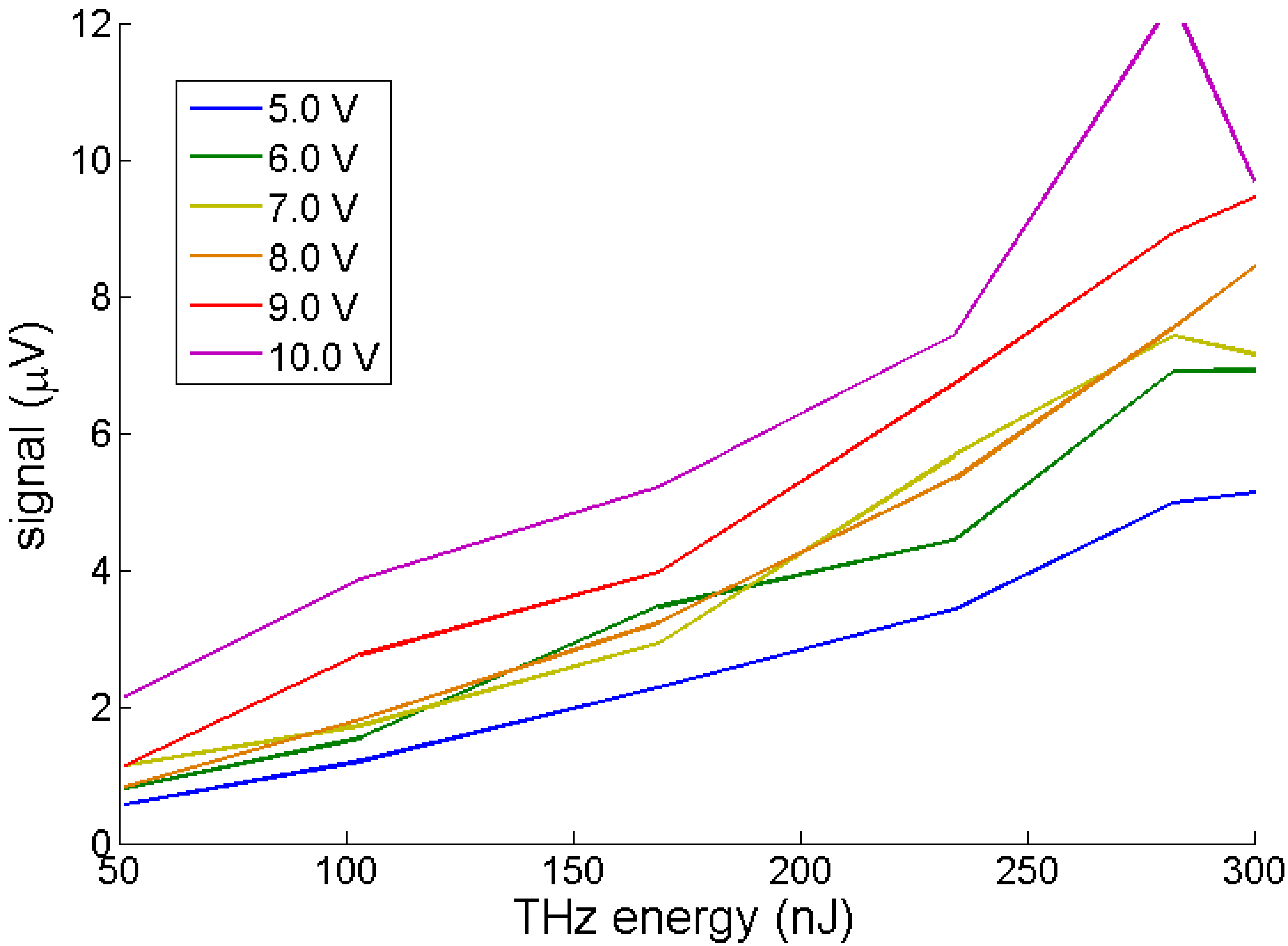

Multielement GaAs Detector Data (for a single element)

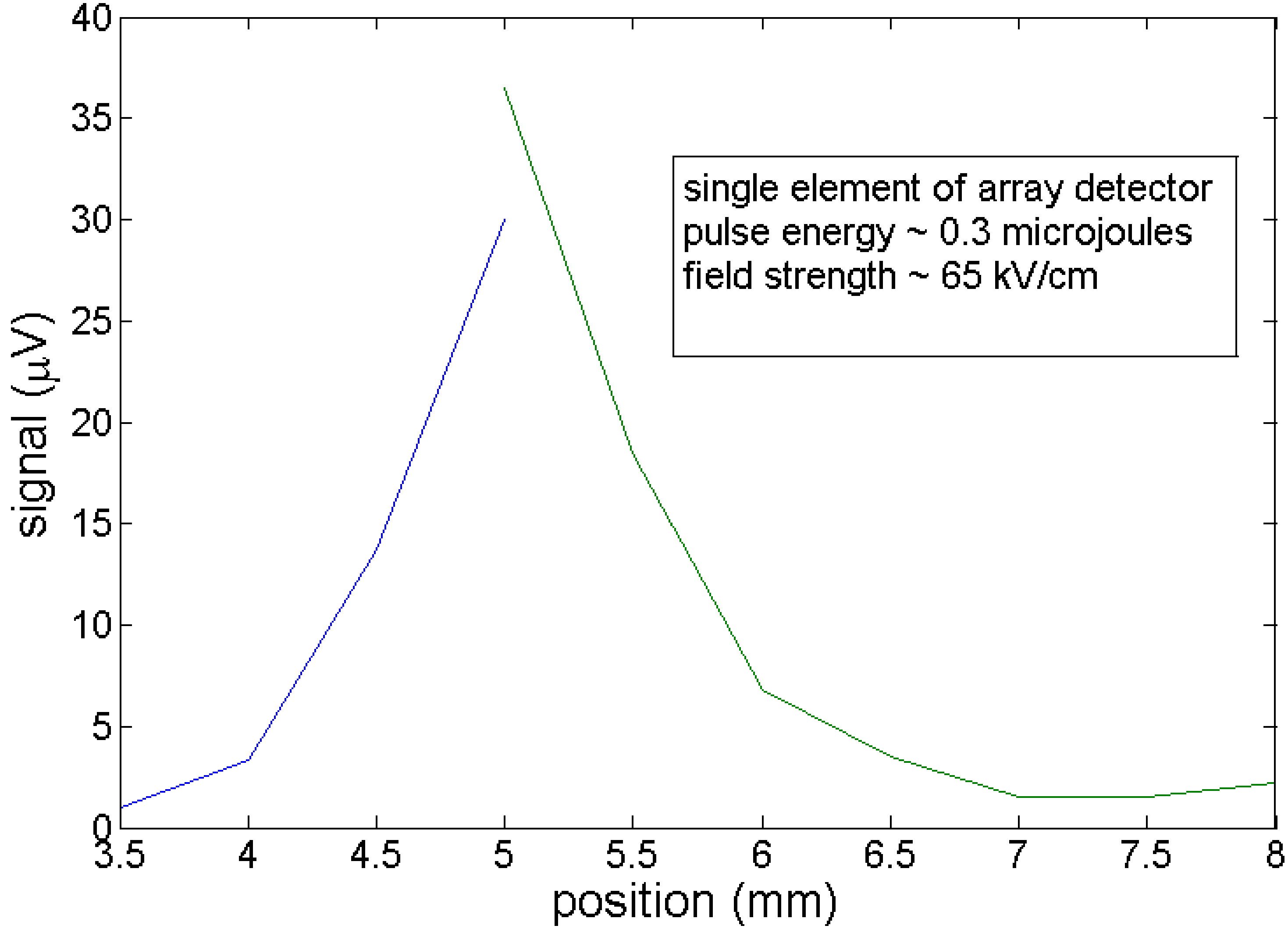

Multielement GaAs Detector Data (for a single element)

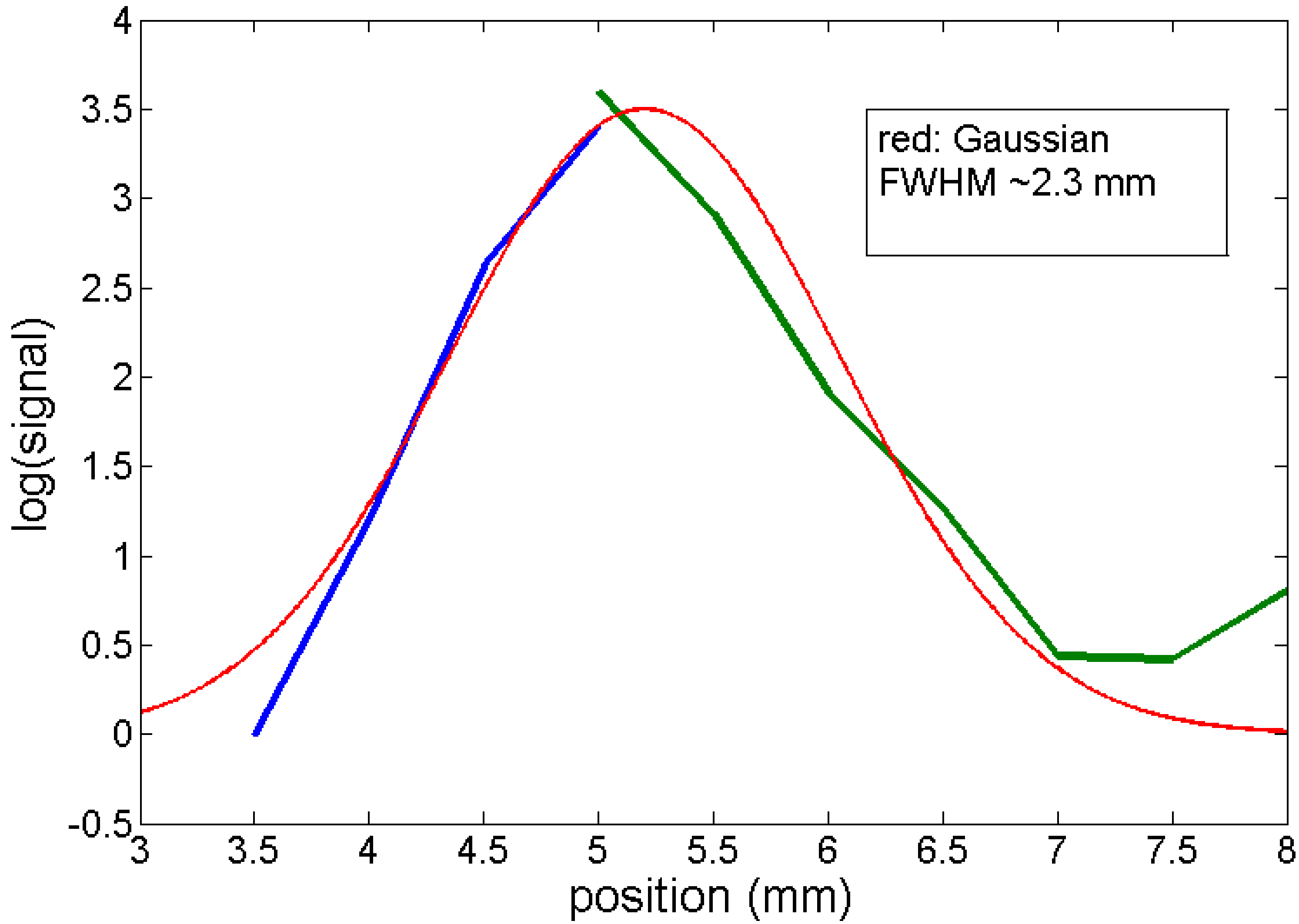

Vanadium Dioxide: Insulator to metal phase transition

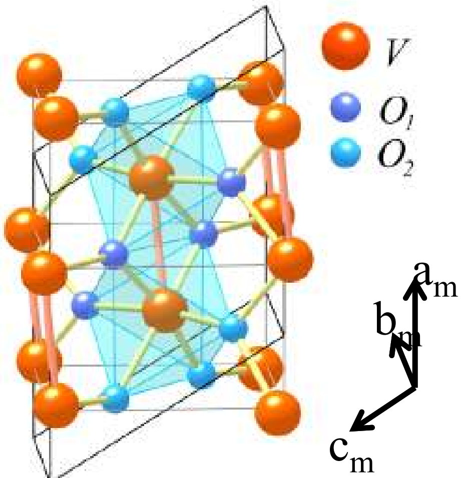

T_c=340K

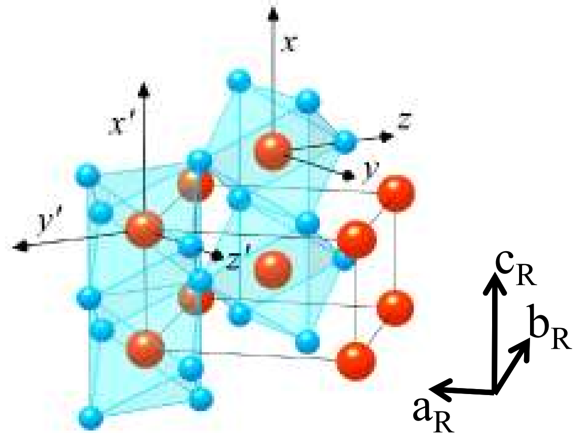

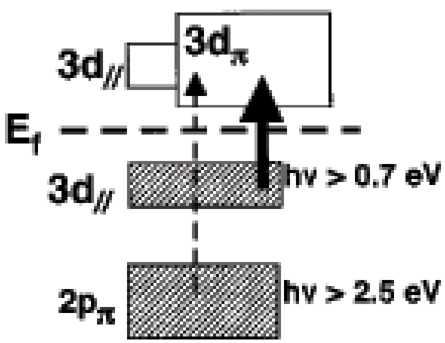

w/ Mengkun Liu & Rick Averitt,
Boston University

Nature **487**, 345–348
(11 July 2012)

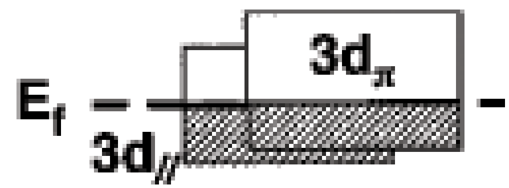

Low temperature
Monoclinic structure
Insulating: $\sigma < 10^{-2}(\Omega cm)^{-1}$

High temperature
Rutile structure
Metallic: $\sigma > 10^{3}(\Omega cm)^{-1}$

V. Eyert, *Ann. Phys. (Leipzig)* 11 650-702 (2002)
L.A. Ladd, W. Paul, *Solid State Commun.* 7 425-428 (1969)
M. M. Qazilbash et al., Phys. Rev. B 77, 115121 (2008),

VO_2 THz metamaterials
T-dependent insulator-metal transition

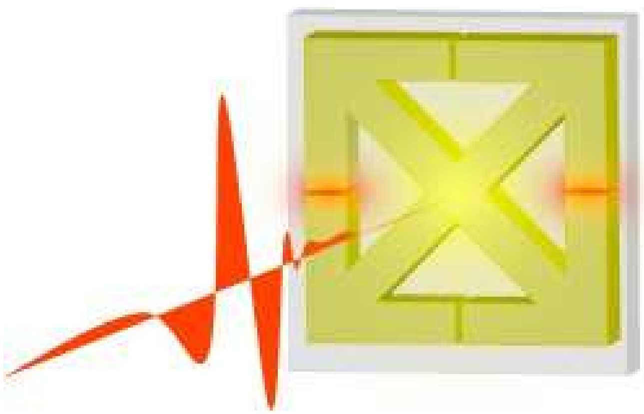

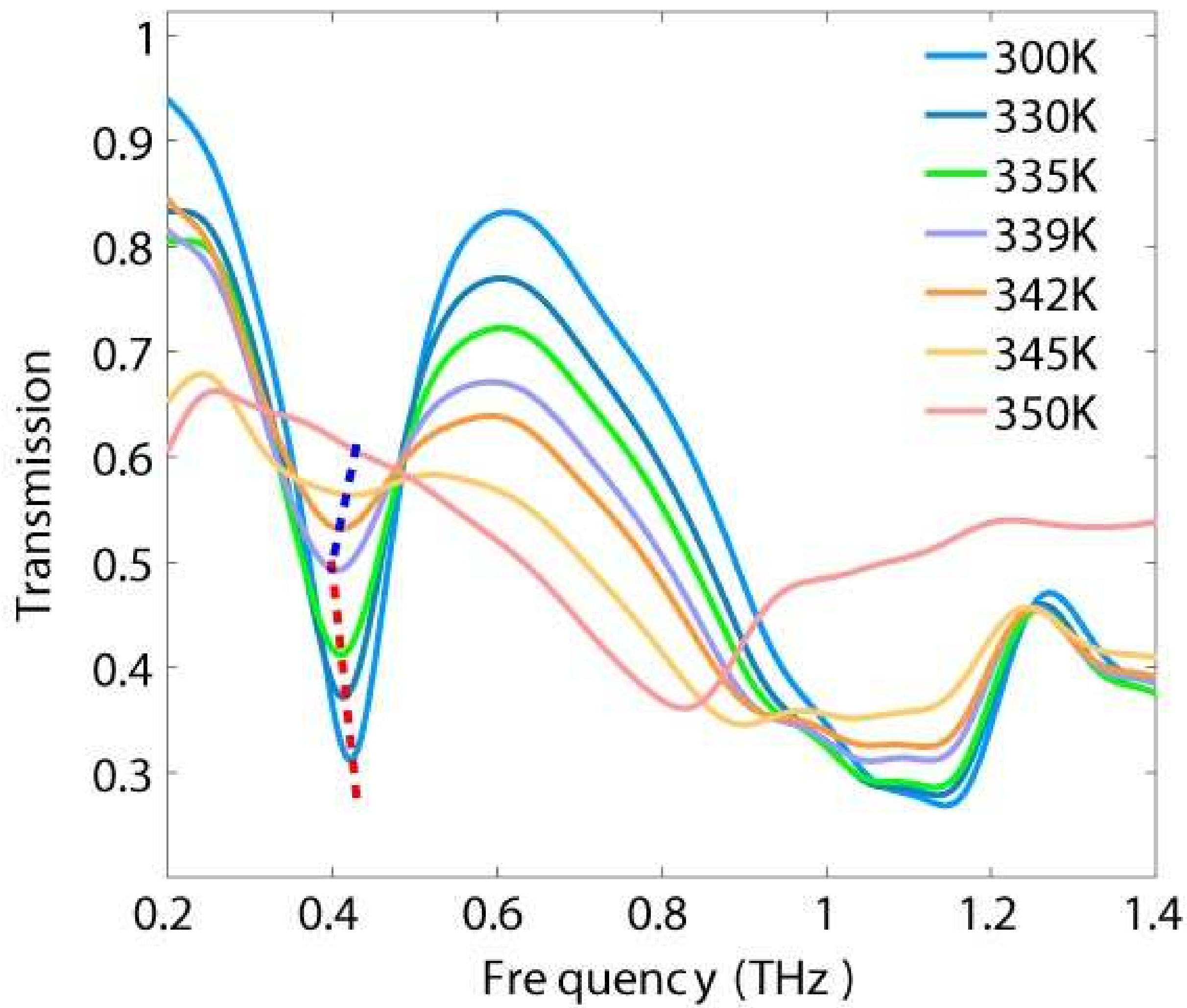

0.4 THz metamaterial resonance

Metallic VO_2 shorts gaps

THz resonance disappears at high T in metallic

VO_2 THz metamaterials
THz fluence dependence

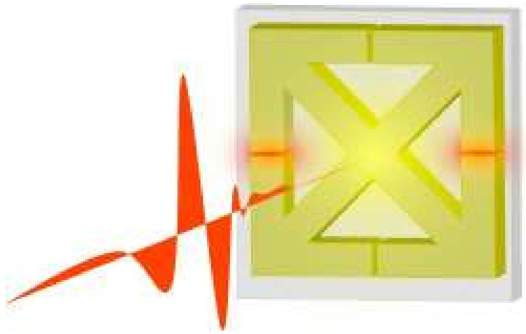

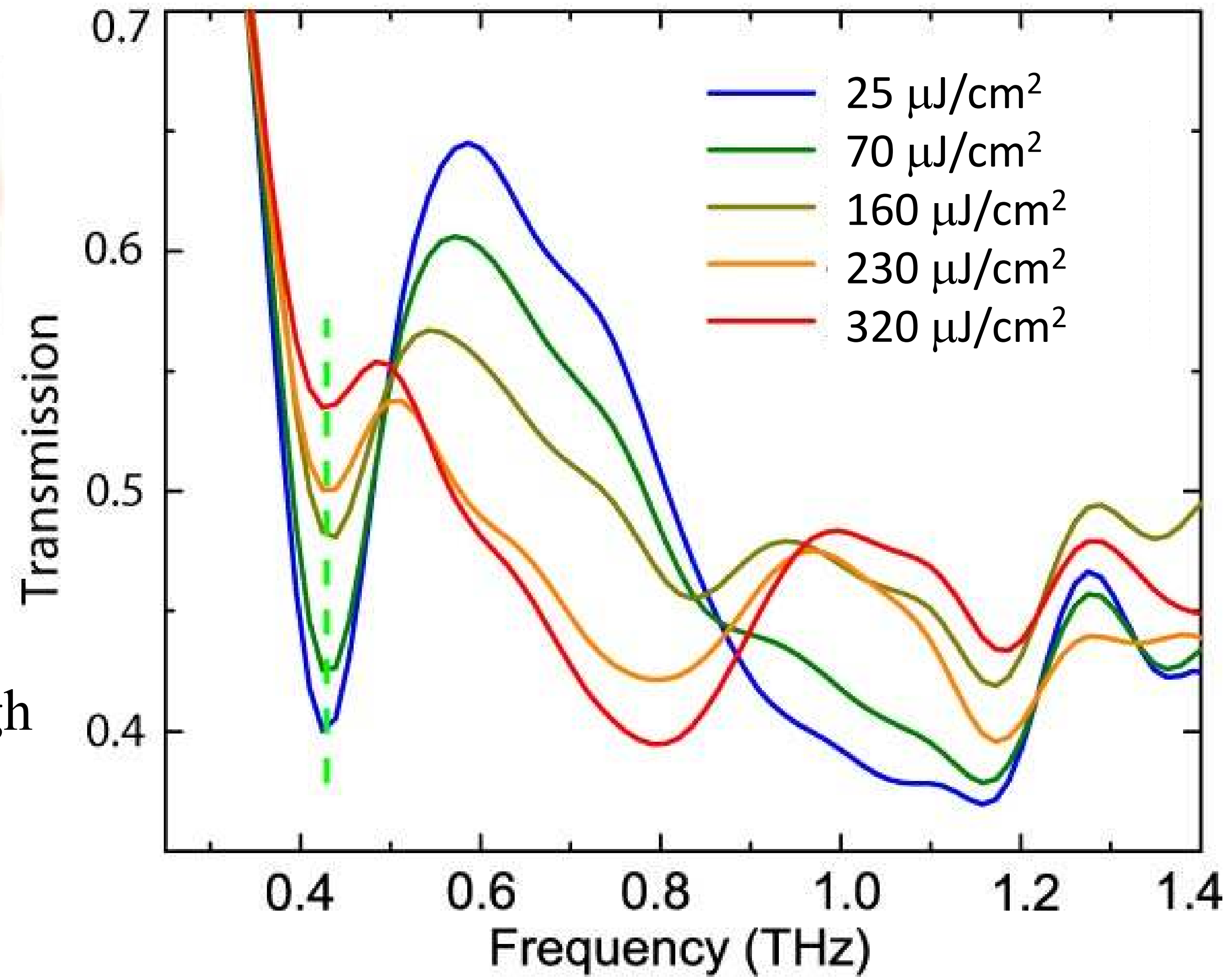

THz resonance disappears at high THz fluence

VO_2 THz metamaterials
THz fluence dependence

Measurement T = 325 K Simulation

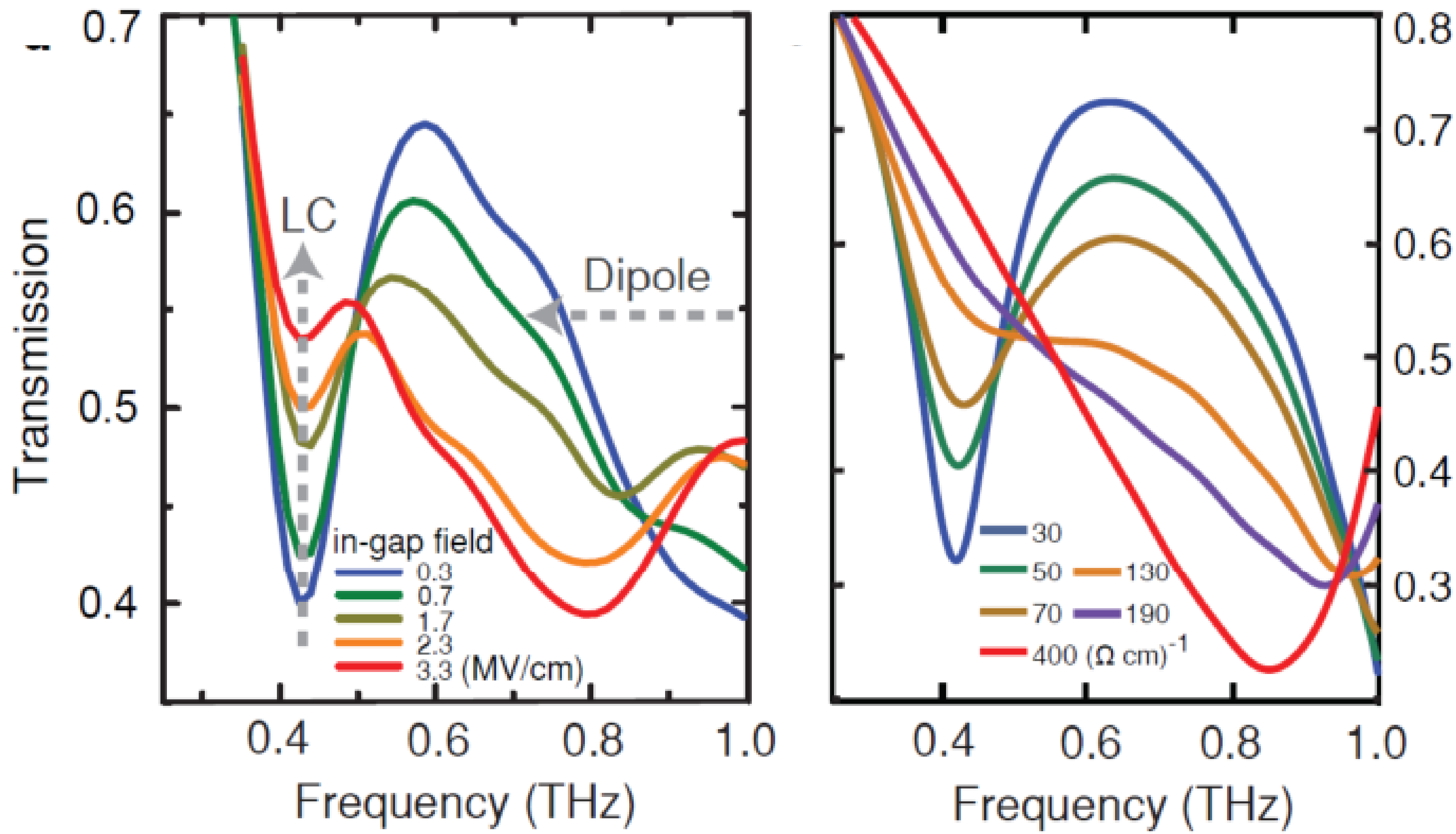

THz-induced IMT dynamics

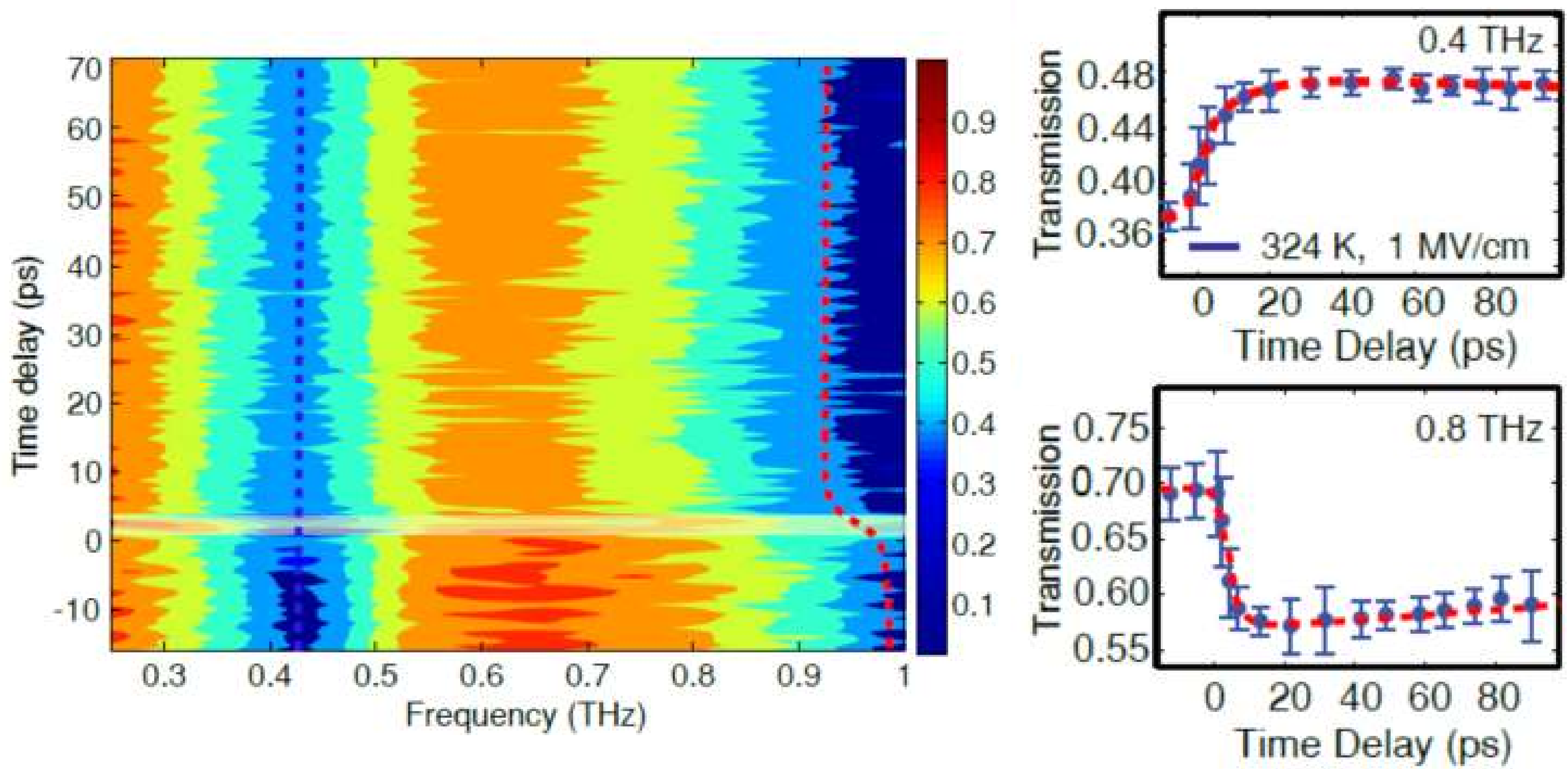

~ 5 ps for transition to occur

Poole-Frenkel ionization and carrier heating in VO_2
Two-temperature model

$$\sigma = \sigma_0 exp \frac{\sqrt{e^3|E(t)|/\pi\varepsilon}}{rk_BT}$$

$$C_e\frac{dT_e}{dt} = -G(T_e - T_i) + \sigma(t)E^2(t)$$

$$C_i\frac{dT_i}{dt} = +G(T_e - T_i)$$

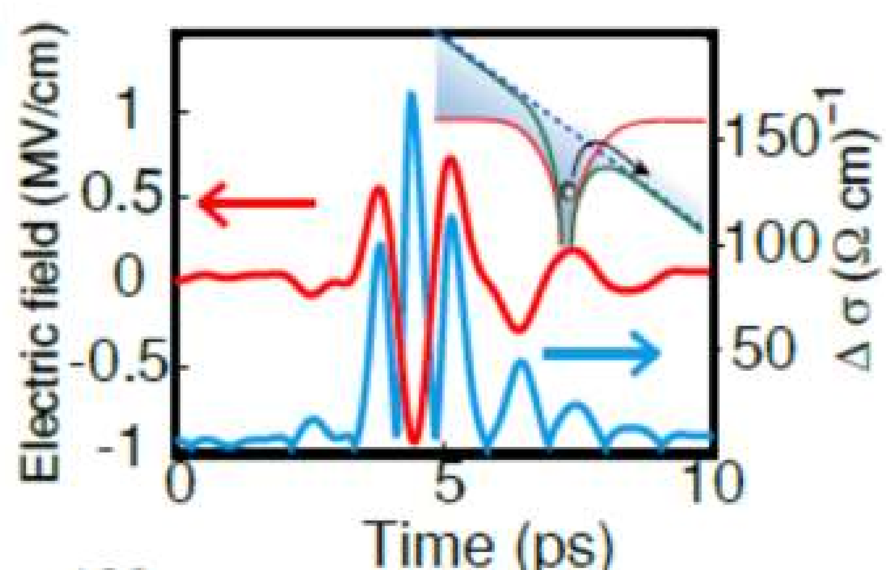

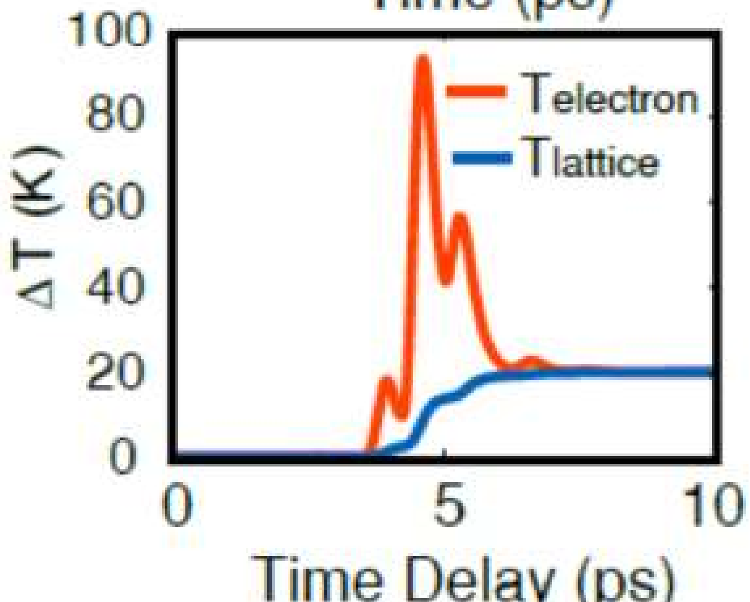

σ - conductivity
E - THz electric field
C_e, C_i – electron/lattice specific heat
T_e, T_i – electron/lattice temperature
G - electron-phonon coupling coefficient

- With P-F σ, ΔT ~ 20 K
- With σ_0 = 10 $(\Omega \cdot cm)^{-1}$, ΔT <1 K

THz-induced damage in VO_2: Damage patterns and the Poole-Frenkel mechanism

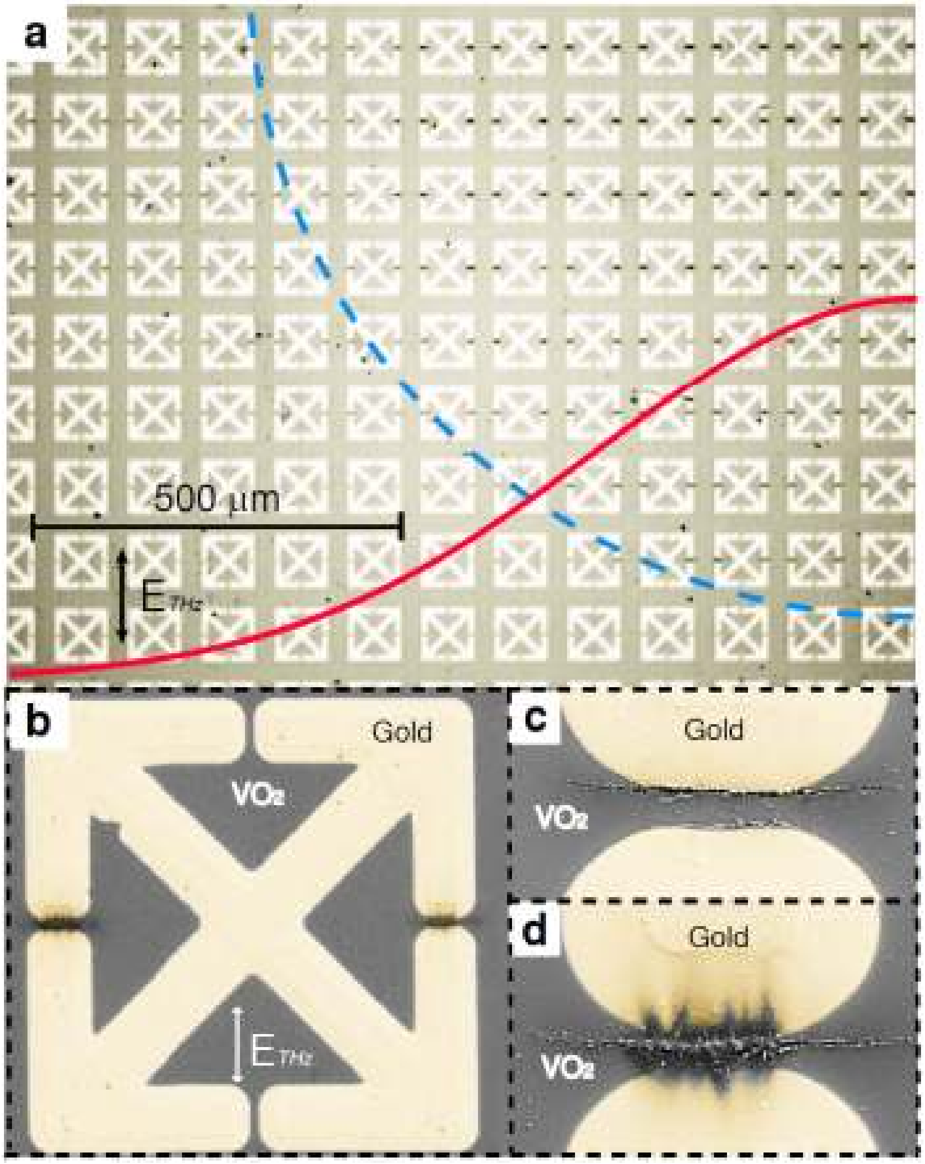

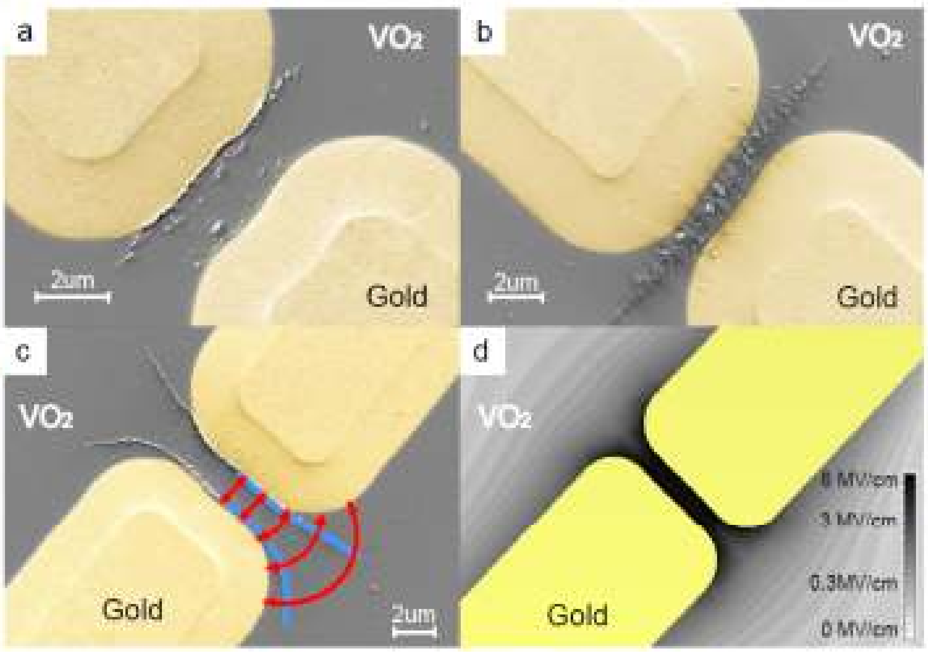

Damage along equipotential lines

Metamaterial-enhanced chemical decomposition

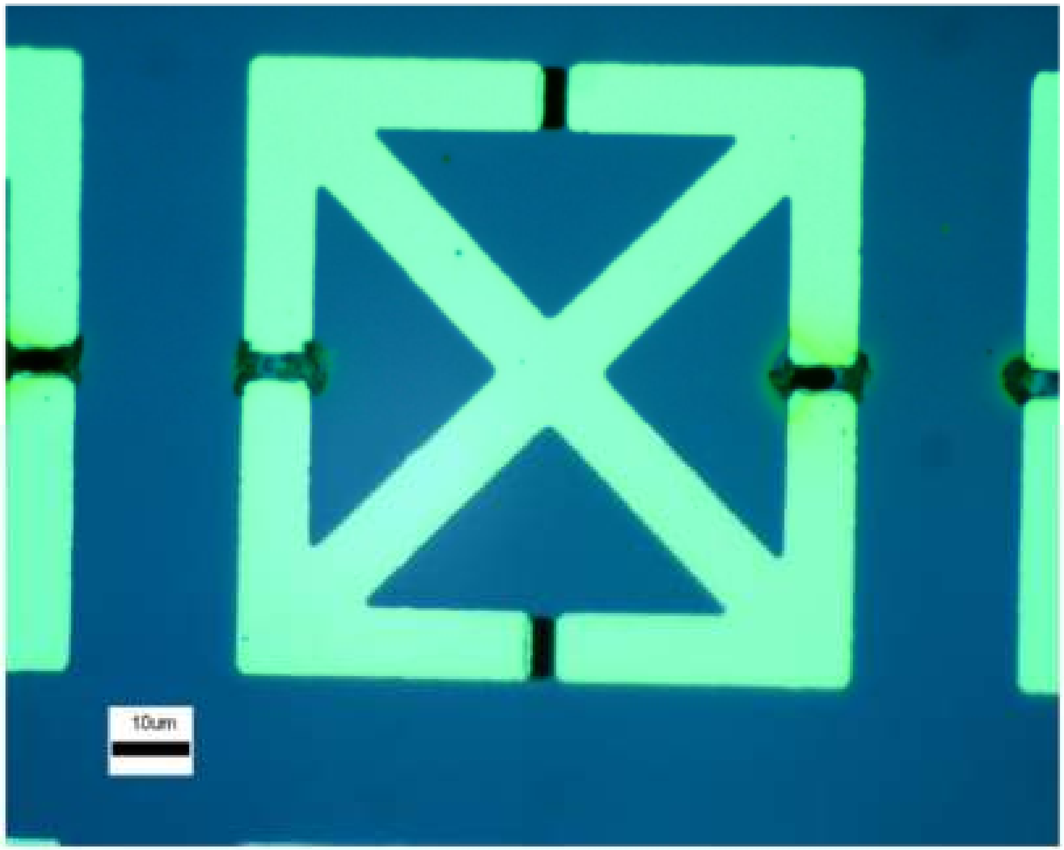

Partial decomposition of TNT!

THz Kerr effect in liquids & solids

THz pulse drives polarizability anisotropies, induces birefringence

$$n(t) = n_0 + \int_{-\infty}^{t} dt'\, R(t-t') \left|E\right|^2(t') \approx n_0 + n_2 I$$

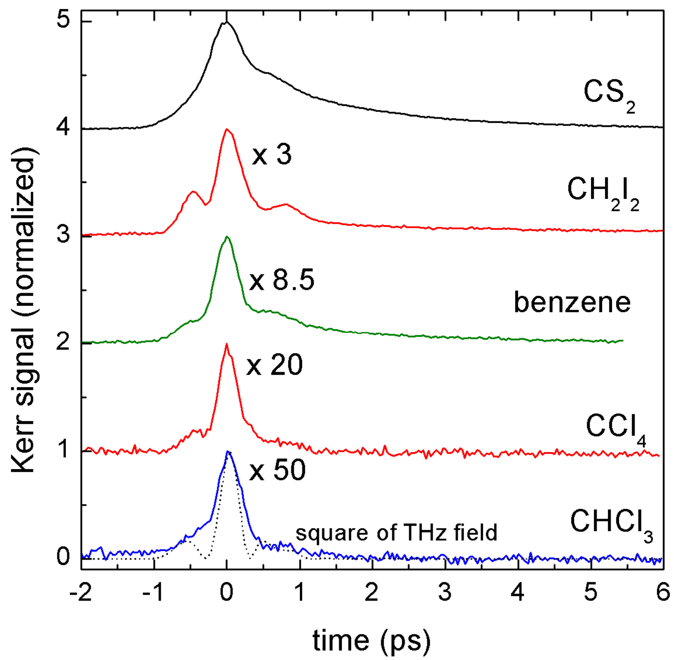

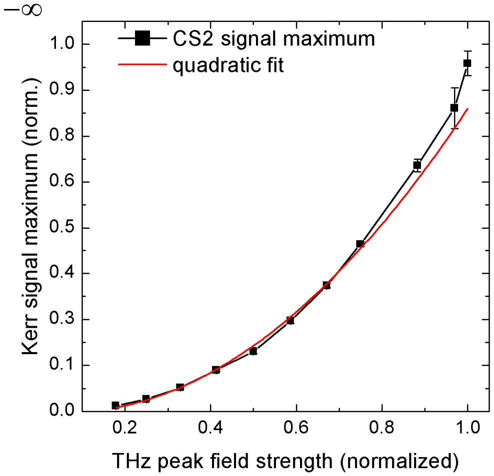

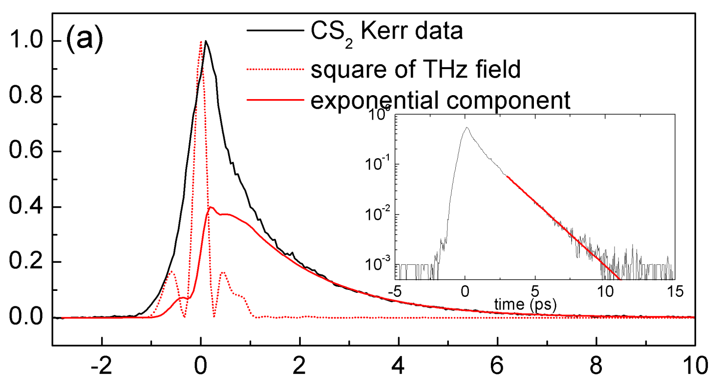

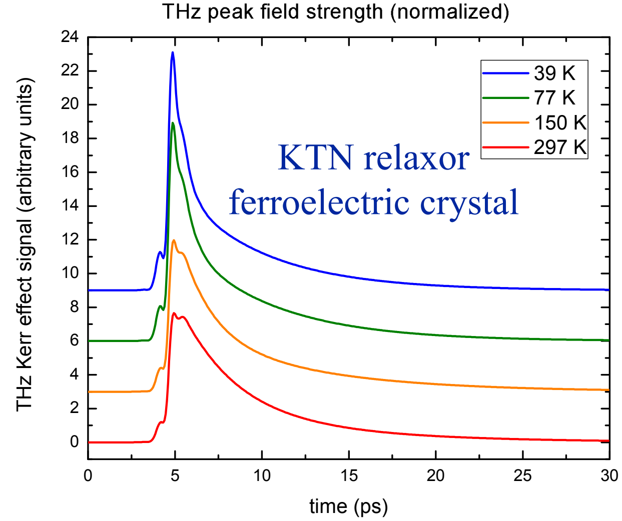

Hoffmann, *et. al.*, APL (2009)

Nonlinear Kerr response in air!

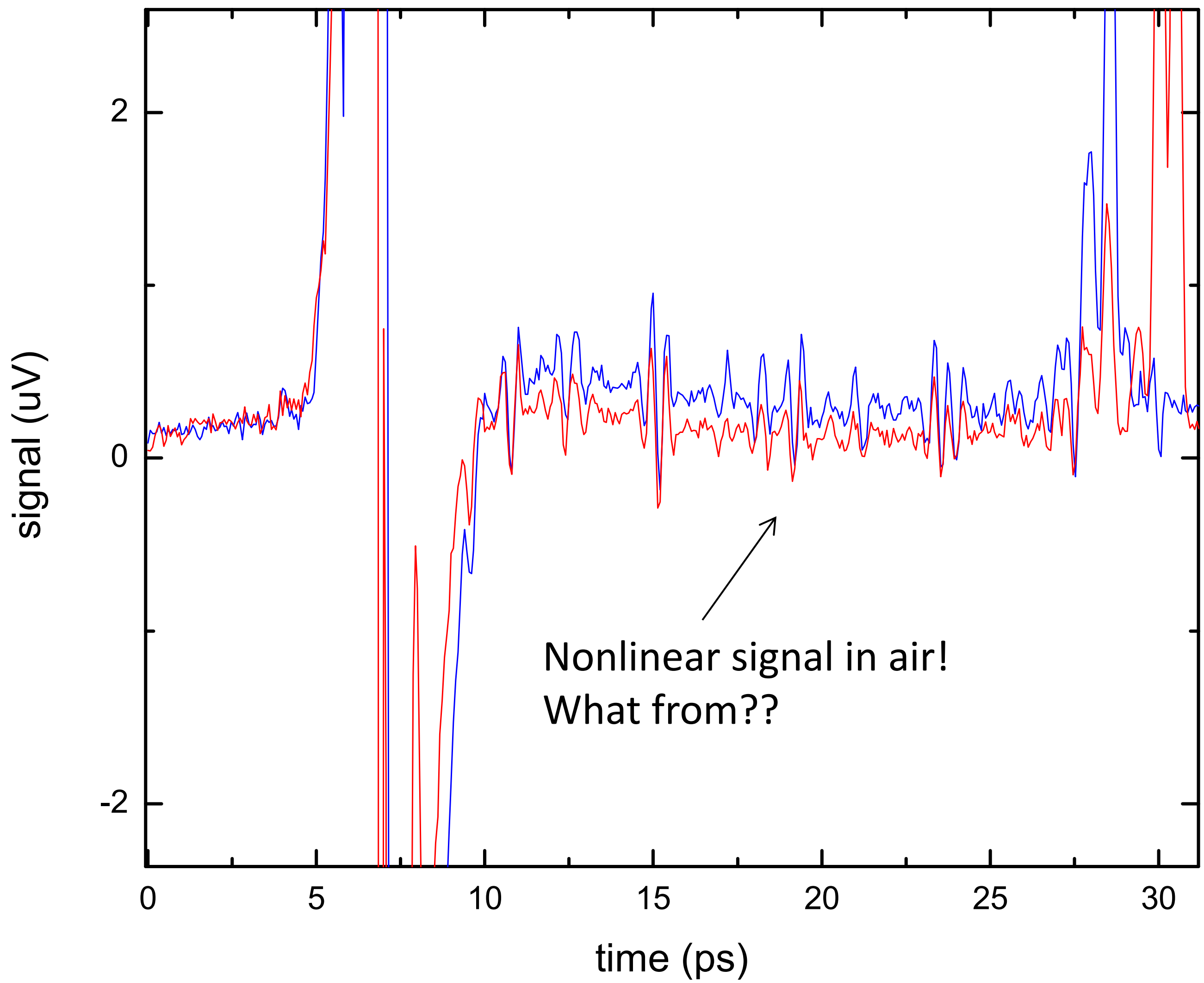

Orientation and Alignment of Gas Phase Molecules by Single Cycle THz Pulses

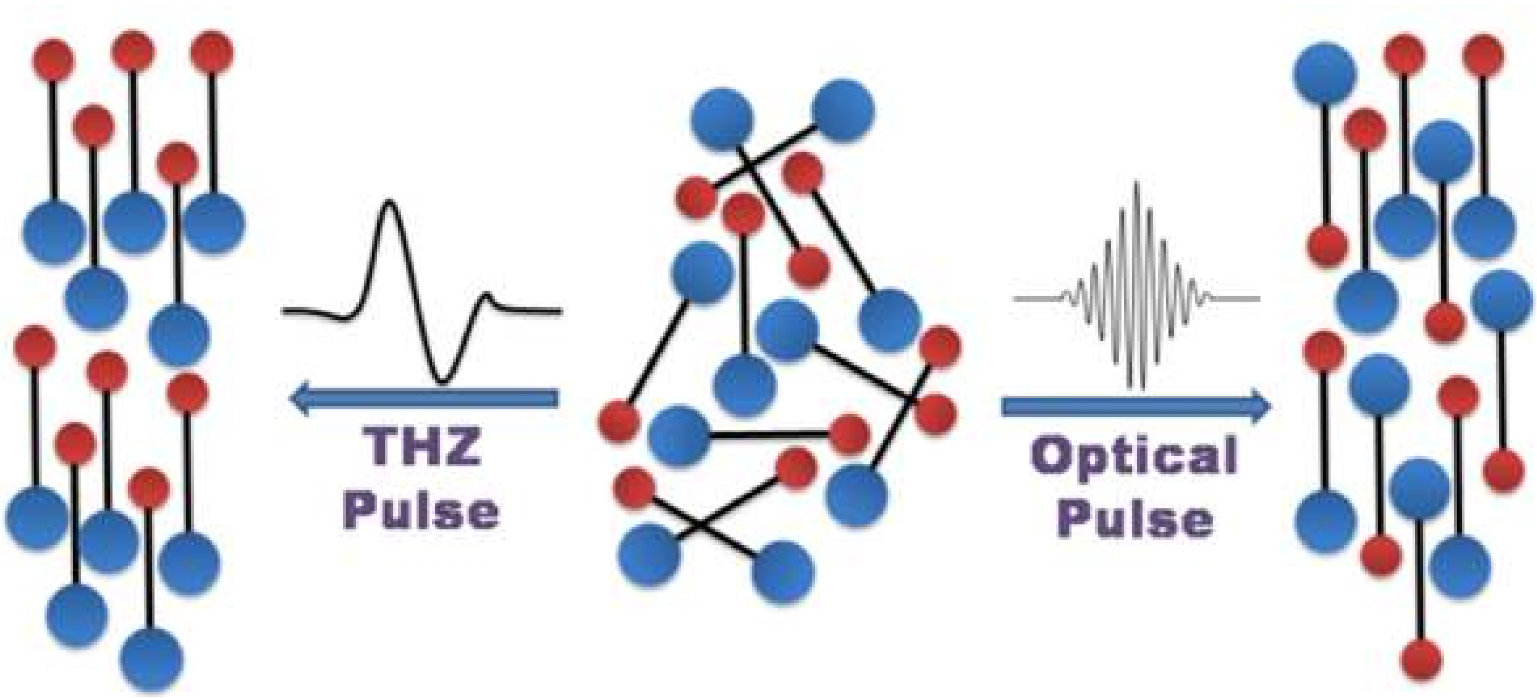

Sharly Fleischer
w/ Yan Zhou & Robert W. Field

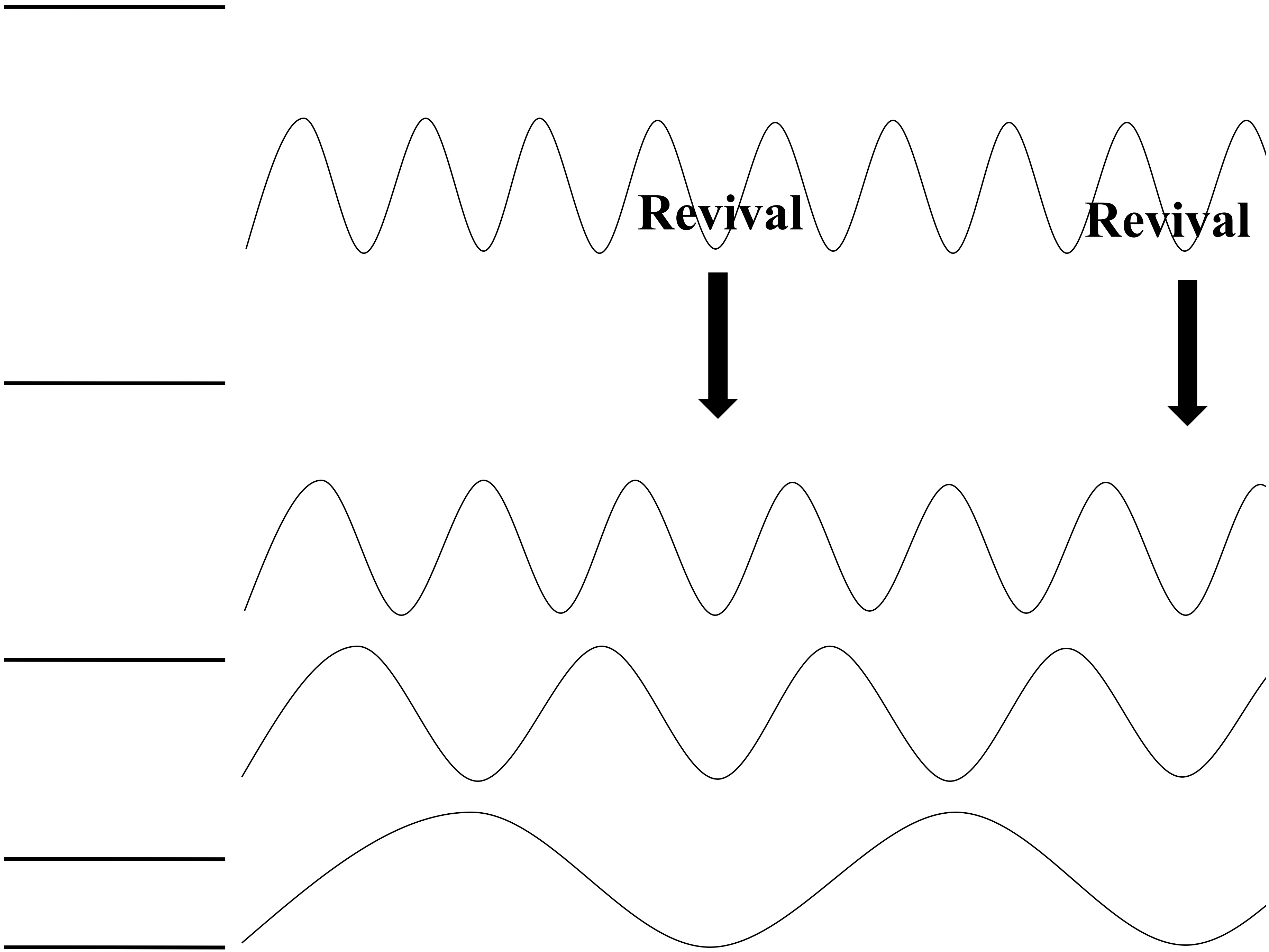
Revival
Revival

EO sampling, OCS 250torr

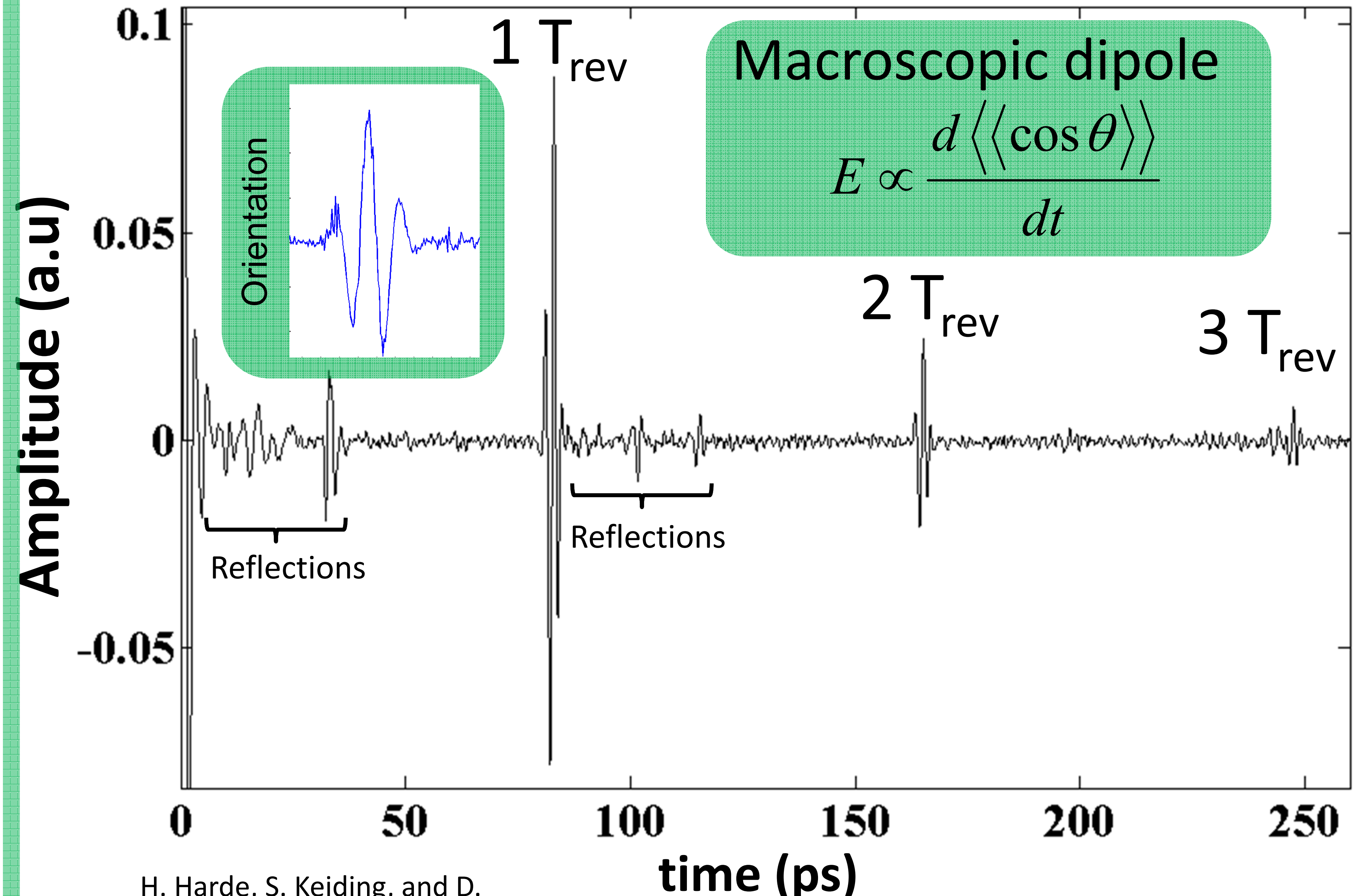

H. Harde, S. Keiding, and D. Grischkowsky, *PRL* **66**, 1834 (1991)

S. Fleischer et. al. *PRL* **107**, 163603 (2011)

Alignment of OCS, 350 torr, 300K

Measured through Kerr effect (optical birefringence)

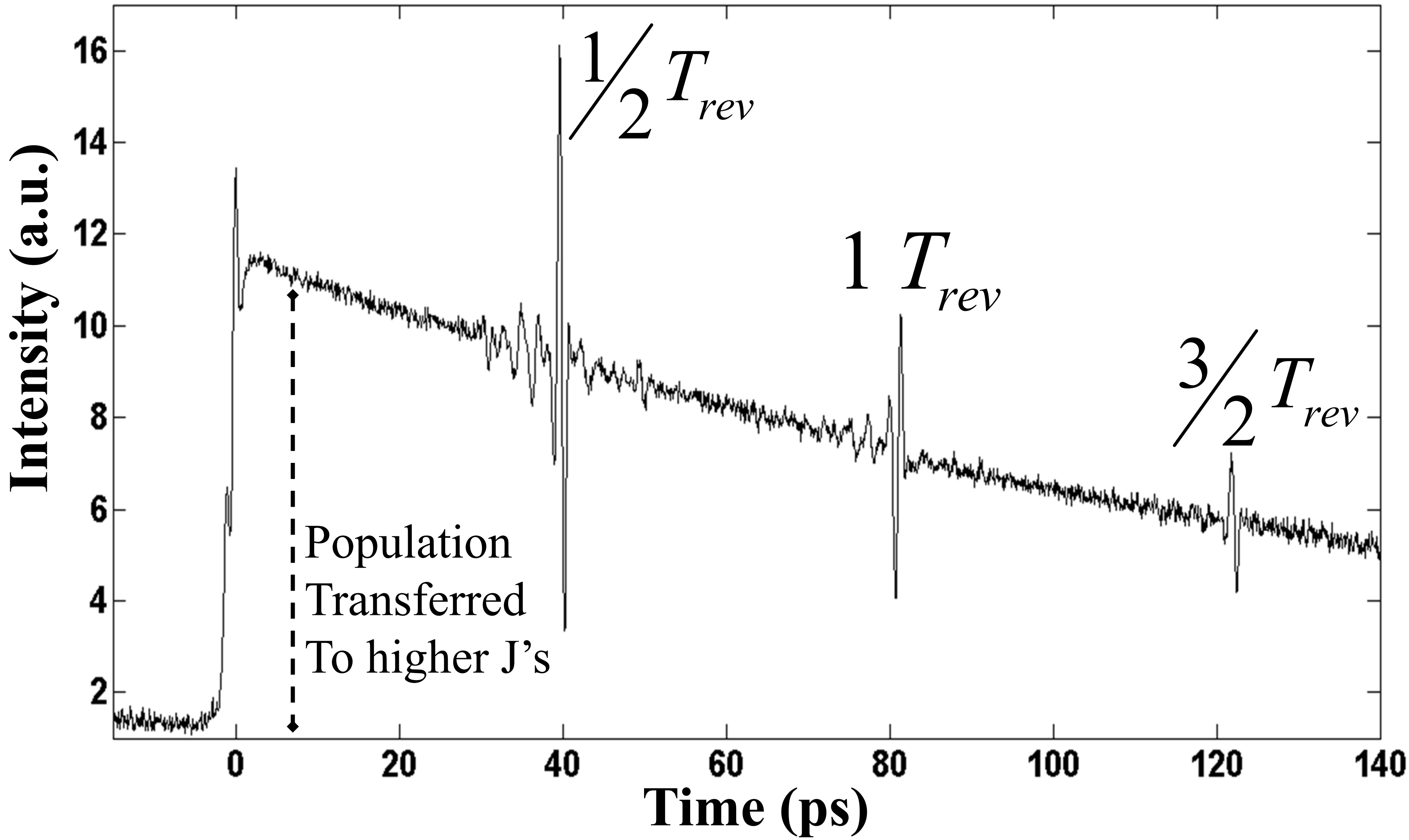

S. Fleischer, Y. Zhou, R.W. Field, KAN, *PRL* **107**, 163603 (2011)

Two delayed THz pulses   350 torr OCS

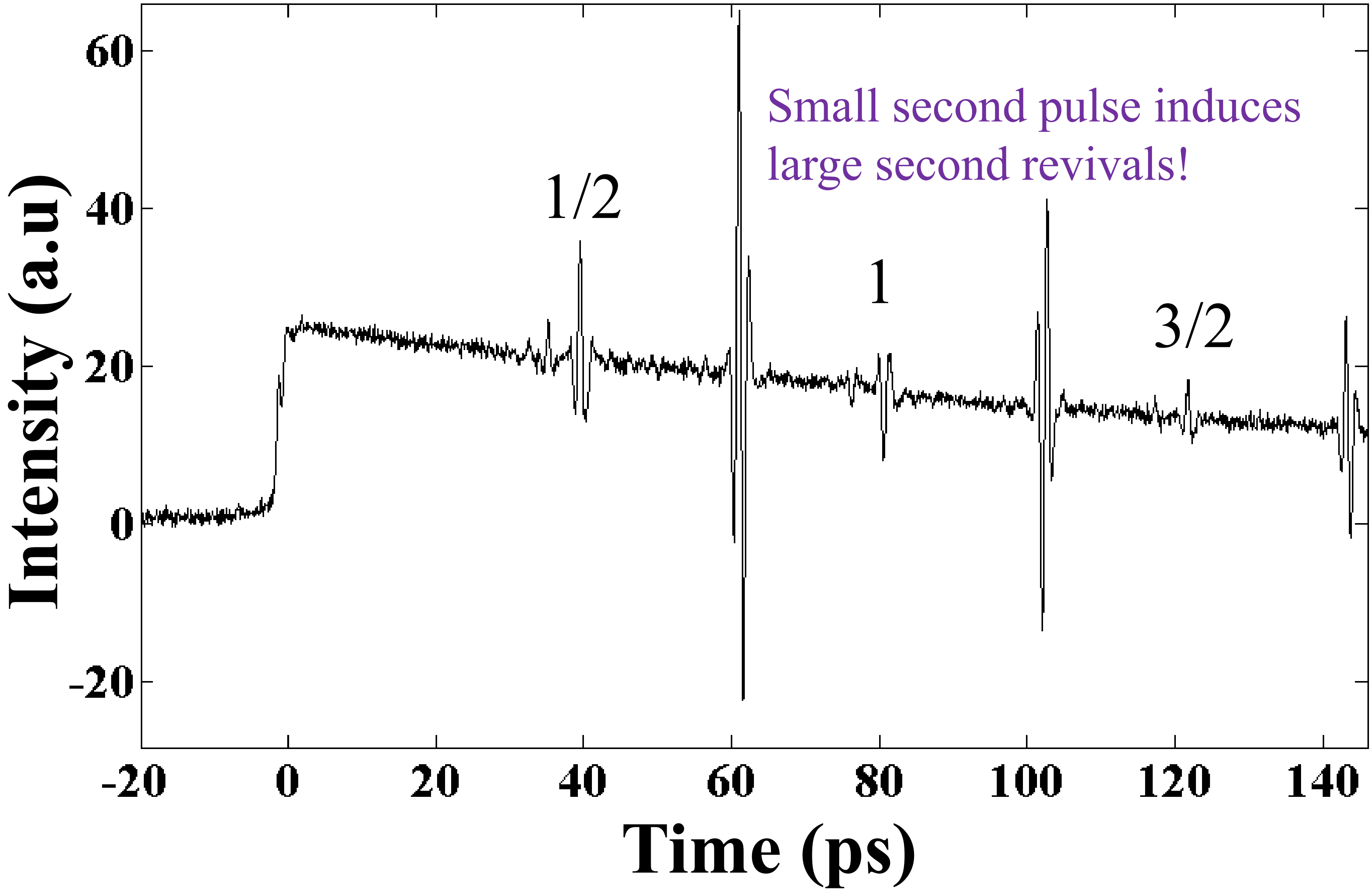

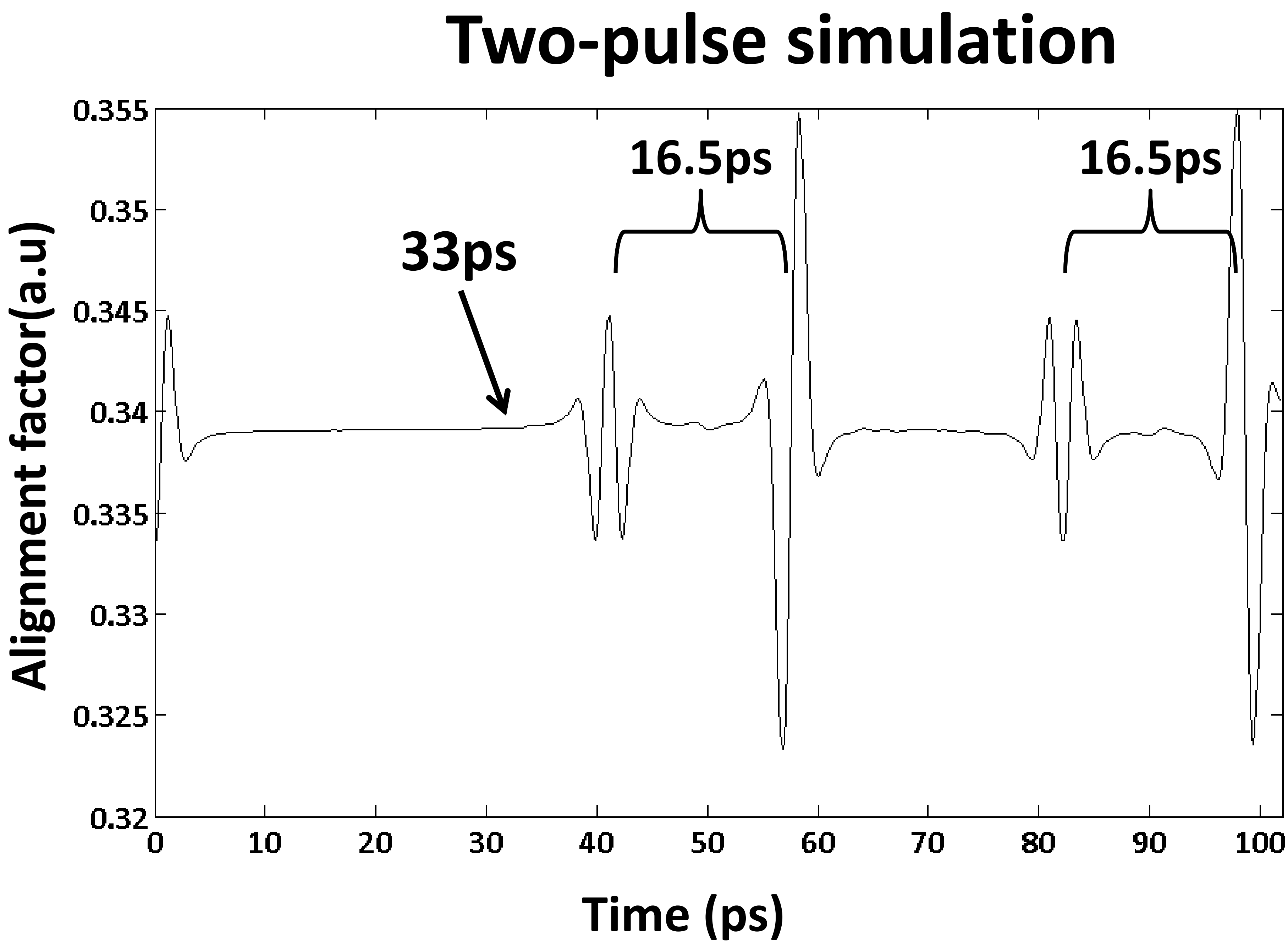
Two-pulse simulation
16.5ps
16.5ps
33ps
Alignment factor(a.u)
0.355
0.35
0.345
0.34
0.335
0.33
0.325
0.32
0
10
20
30
40
50
60
70
80
90
100
Time (ps)

Two-quantum coherences

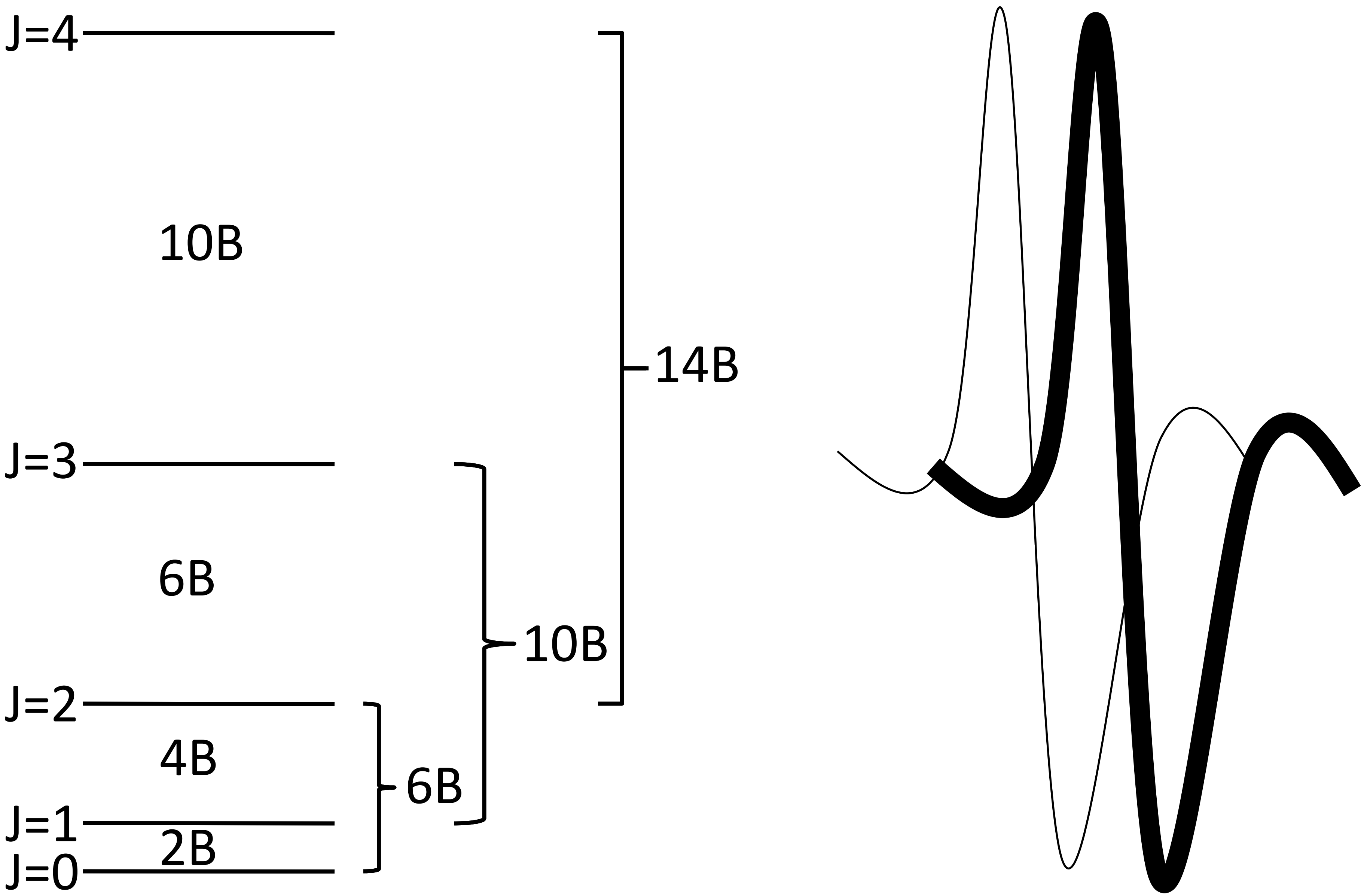

Density matrix

ρ_{11}	ρ_{12}	ρ_{13}	ρ_{14}	ρ_{15}
ρ_{21}	ρ_{22}	ρ_{23}	ρ_{24}	ρ_{25}
ρ_{31}	ρ_{32}	ρ_{33}	ρ_{34}	ρ_{35}
ρ_{41}	ρ_{42}	ρ_{43}	ρ_{44}	ρ_{45}
ρ_{51}	ρ_{52}	ρ_{53}	ρ_{54}	ρ_{55}

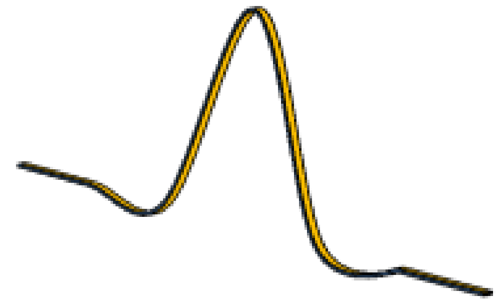

$J \leftrightarrow J \pm 1$

1Q coherences

Orientation $\langle \cos\theta \rangle$

$J \leftrightarrow J \pm 1 \leftrightarrow J \pm 2$

2Q coherences

Alignment $\langle \cos^2\theta \rangle$

Population transfer

Multiple-quantum coherences

Second pulse timing varied

Fully coherent 2D 2-quantum THz spectroscopy

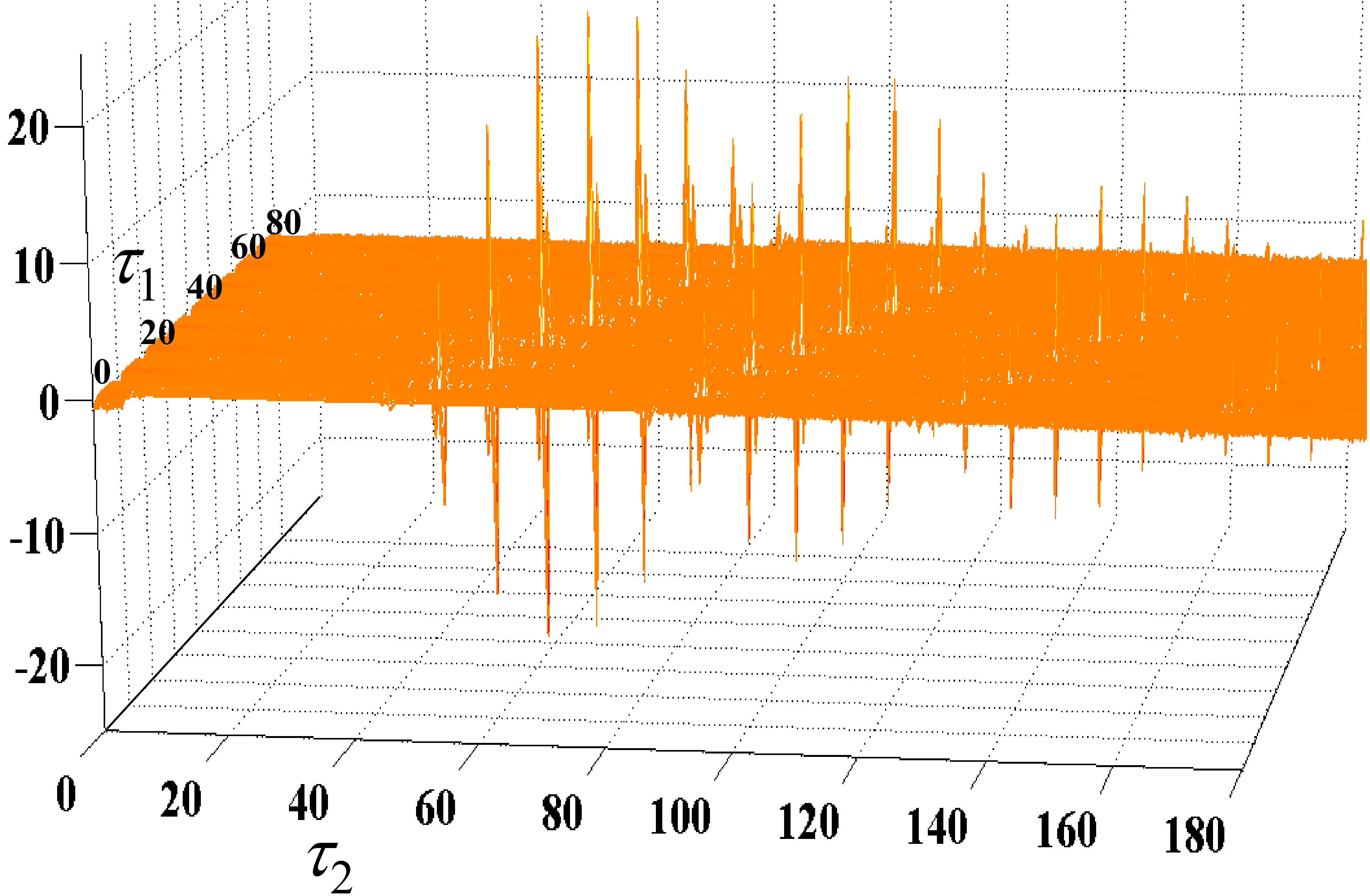

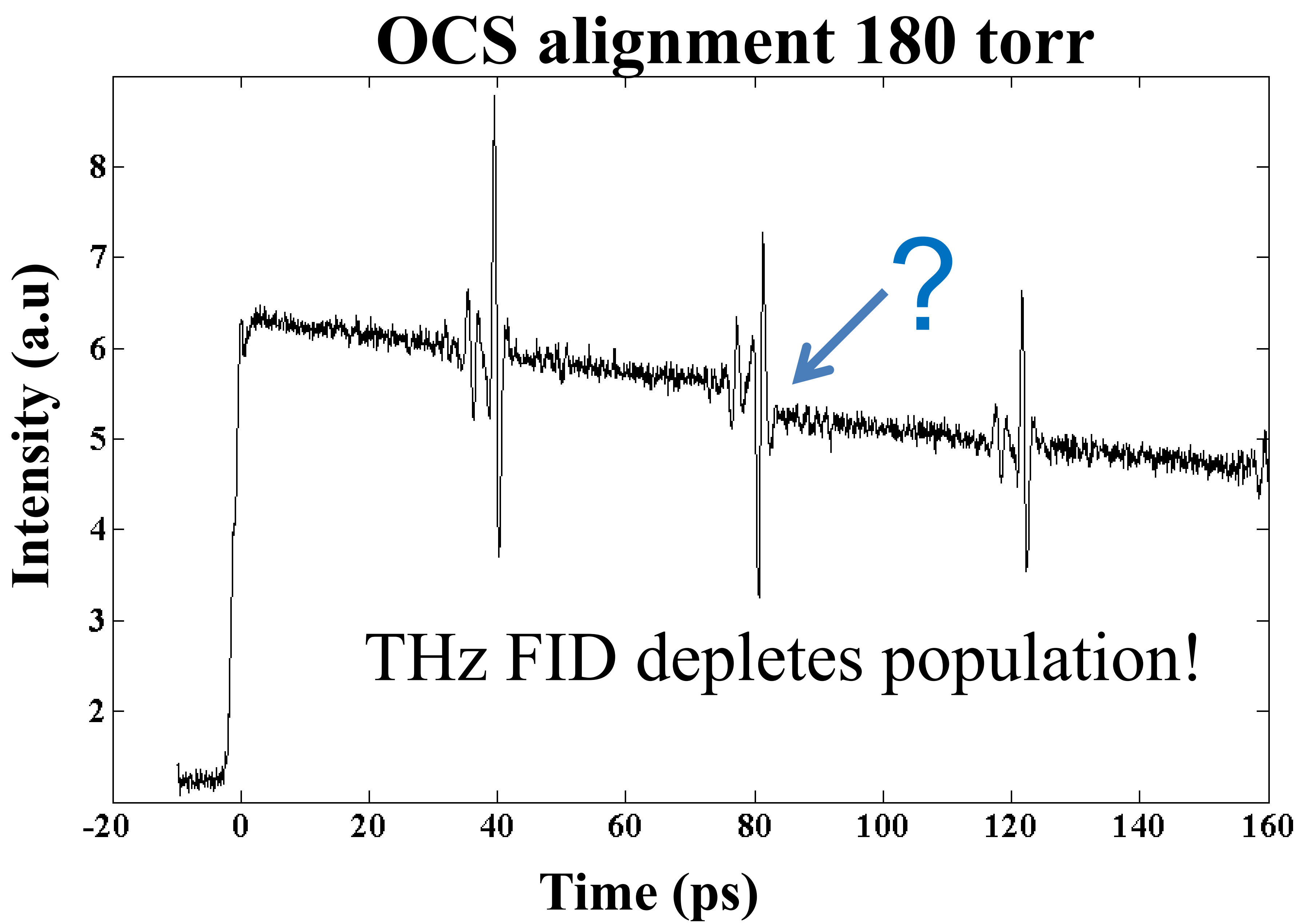
OCS alignment 180 torr
Intensity (a.u)
Time (ps)
?
THz FID depletes population!
8
7
6
5
4
3
2
-20
0
20
40
60
80
100
120
140
160

OCS alignment, no purge outside OCS cell

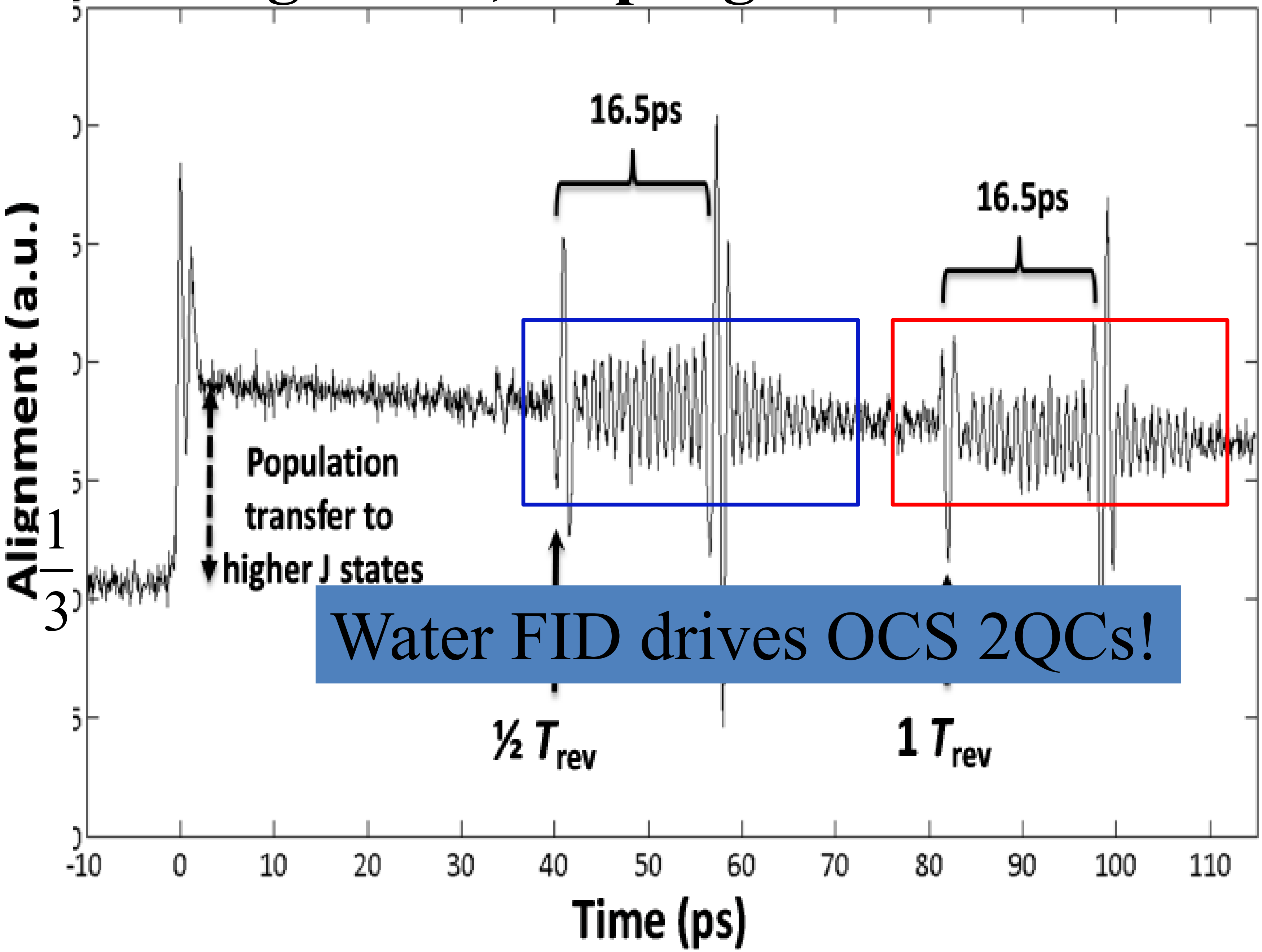

THz pulse can saturate rotational transitions!

Multiple-cycle waveform can be tuned to specific water lines

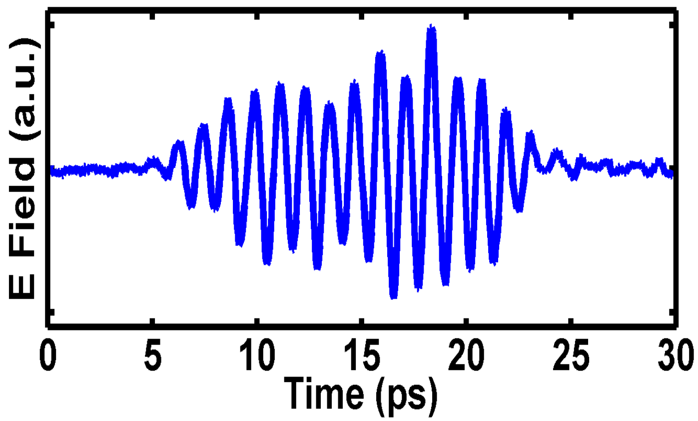

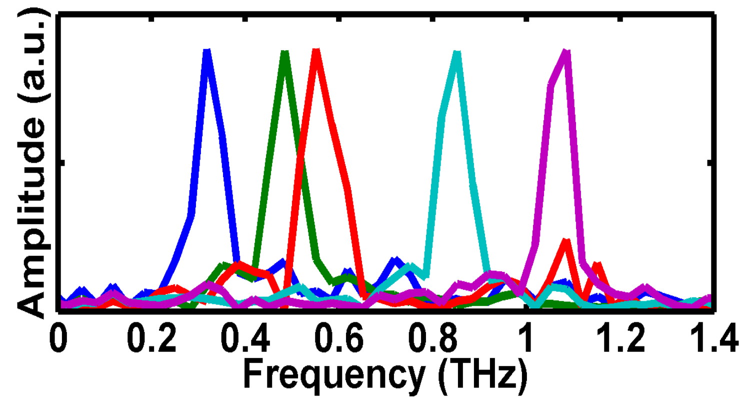

Waveform can be optimized for energetic material response

Can saturate water absorption lines

Simulation $\Rightarrow$ enhanced propagation in air!

Summary

Strong THz sources

Tabletop sources provide high THz pulse energies, high THz field amplitudes

Enable versatile nonlinear spectroscopy at low and high order

Nonlinear THz spectroscopy

Can be declared a subfield!

Nonlinear responses observed in solid, liquid, gas, plasma phases

Electronic, magnetic, vibrational, rotational responses

Collective structural and localized chemical rearrangements

Prospects

Nonlinear THz spectroscopy is just beginning

Multidimensional, high-order, multispectral spectroscopy

THz coherent control over molecular & collective responses

Credits

Thomas Feurer
Joshua Vaughan
Nikolay Stoyanov
David Ward
Eric Statz

Janos Hebling (Pecs U)
Mattias Hoffmann
Ka-Lo Yeh
Harold Hwang

Richard Averitt (Boston U)
Robert Field (MIT)

Christopher Werley
Nate Brandt
Qiang Wu (Tianjin U)
Kung-Hsuan Lin
Zhao Chen
Xibin Zhou
Bradford Perkins
Christopher Tait
Stephanie Teo

Thanks for slides from:

Andrei Tokmakoff, MIT
Gwyn Williams, Jefferson Lab
Antoinette Taylor, LANL
X.-C. Zhang, RPI
Koichiro Tanaka, Kyoto U
Aaron Lindenberg, Stanford
Christoph Hauri, Paul Scherer Inst